Hydrophilic Surface Modification of Upconversion Nanoparticles for LRET-based DNA Assays

By

Yingzhu Zhou

Institute for Biomedical Materials and Devices,

School of Mathematical and Physical Sciences,

Faculty of Science

Supervisor:

Prof. Dayong Jin

This thesis is presented for the degree of Master's by Research

September 2018

CERTIFICATE OF ORIGINAL AUTHORSHIP

I, Yingzhu Zhou declare that this thesis, submitted in fulfilment of the requirements for the award of master by research, in the Faculty of Science at the University of Technology Sydney.

This thesis is wholly my own work unless otherwise reference or acknowledged. In addition, I certify that all information sources and literature used are indicated in the thesis.

This document has not been submitted for qualifications at any other academic institution.

Signature: Production Note:
Signature removed prior to publication.

Date: Sep 20th , 2018

ACKNOWLEDGEMENTS

The completion of Master by Research thesis represents a start of my research journey. Through this meaningful and valuable period, lots of people helped and supported me to overcome difficulties. Here, I want to express my sincere appreciation to them.

First, my greatest appreciation goes to my principal supervisor, Prof. Dayong Jin. He is the one guided me into the science's word and provided me with an excellent research platform to achieve my goals. As an only and first master by research student in this group, Prof. Jin trained me with the patient to think independently and logically, and encouraged me to chase ideas, seek new knowledge and turn them into reality. Moreover, I benefited from his constructive suggestions and comments towards my experiments and papers. Without his support, I may not have an opportunity to explore the knowledge or meet my lovely group members.

Second, I acknowledge my bio-group members. Hao He helped me a lot to design and improve my first project and taught me how to do experiments step by step. Yinghui Chen helped me in adjusting details and analysing data. Wei Ren is an excellent researcher model for me in learning how to resolve problems and seek innovative directions logically. Jiayan Liao also kindly helped me in data collection. Also, Dr Maryam Parviz and Dr Gungun Lin kindly provided me with valuable comments on polishing and assisting my paper and thesis. Besides, I have to say Dr Fan Wang and Chao Mi established excellent optical systems as a cornerstone which benefited all group members.

Finally, particularly to my family and my boyfriend, thank you so much for your love and unlimited support, which equipped me with energy and courage to overcome upcoming challenges.

I admire all my senior group members, for their hardworking, optimistic attitude, and outstanding research ability. This is a memorable period with all of you, the time we discussed the projects, encouraged each other, celebrated together when we achieve the excited outputs, as well as the weekends we hung out together. I enjoyed the time studying in this great and beautiful country. I believe all of these delightful people will be my lifelong friends.

List of Publication

[1] Yinghui Chen, Hien T. T. Duong, Shihui Wen, Chao Mi, **Yingzhu Zhou**, Olga Shimoni, Stella M. Valenzuela, and Dayong Jin,'Exonuclease III-Assisted Upconversion Resonance Energy Transfer in a Wash-Free Suspension DNA Assay'，*Analytical Chemistry, 2018,90 (1), 663-668.*

[2] **Yingzhu Zhou**, Yinghui Chen, Hao He, Jiayan Liao, Hien T. T. Duong, Maryam Parviz, and Dayong Jin, 'A Homogeneous DNA Assay by Recovering Inhibited Emission of Rare Earth Ions-Doped Upconversion Nanoparticles', *Journal of Rare Earths.* Doi:10.1016/j.jre.2018.05.008.

[3] Wei Ren, **Yingzhu Zhou**, Shihui Wen, Hao He, Gungun Lin, Deming Liu and Dayong Jin, *Chem. Commun*.doi:10.1039/C8CC04200D

Abstract

Upconversion nanoparticles (UCNPs) are emerging as a new-generation optical nanomaterial that has drawn tremendous research interests. UCNPs can sequentially absorb two or more lower-energy photons in near-infrared (NIR) range to emit one higher energy photon, typically in the visible and ultraviolet range. This anti-Stokes' property offers a great deal of opportunities in biological and analytical applications, because NIR excites negligible amount of autofluorescence background in visible range that is an issue in conventional methods using UV or visible excitation. Furthermore, UCNPs are biocompatible, resistant to photobleaching and photoblinking, tunable in size, morphology, and composition. All these characteristics offer their potentials in diverse applications, including bioassays, chemical detections, bio-imaging, single-molecule tracking, thermometers, security inks, and photothermal therapy etc.

UCNPs are used in aqueous suspension, in particular, biomedical and analytical applications for targets recognition and detection, which requires a hydrophilic surface. However, UCNPs are synthesised in the organic solvent with the inherent hydrophobic surface. The key is to modify their surface from being hydrophobic into hydrophilic. Among a series of surface modification strategies, ligand exchange stands out because of its simplicity, and versatility for further conjugations with functional groups.

This thesis focuses on a systematic study of the hydrophilic surface modification methods to identify a one-step ligand exchange strategy for UCNPs. Based on this study, development of a robust homogenous assay, based on Luminescence Resonance Energy Transfer (LRET), is also demonstrated to achieve detection of DNA disease biomarkers. In this thesis, Chapter I covers the objectives, structure and organization; Chapter II gives the detailed literature review and the the introduction of UCNPs; followed by Chapter III, a systematical evaluation of the performance of four common polymers in transferring the surface of UCNPs from being hydrophobic to hydrophilic. Chapter IV reports the

development of a platform for DNA detection in homogeneous solutions based on LRET, which work has been published as a peer-reviewed article.

Keywords: Upconversion nanoparticles, surface modifications, ligand exchange, LRET, homogenous DNA detection

Contents

Figures

Tables

Chapter I. Introduction

1.1 Background

To overcome the limitations of traditional fluorescent materials, such as spectral overlaps of organic dyes(Resch-Genger et al. 2008), low stability of fluorescence proteins(Pollok and Heim 1999; Held 2012; Resch-Genger et al. 2008), intermittent emission of quantum dots(Clapp, Medintz, and Mattoussi 2006; Walling, Novak, and Shepard 2009), lanthanide-doped upconversion nanoparticles (UCNPs) has attracted some major efforts in the past decade and emerged as a new generation of luminescence nanomaterials. Breakthrough works include a variety of methods explored towards the controlled synthesis of UCNPs, in-depth characterizations of UCNPs to understand their upconversion mechanisms, strategies for tuning their optical properties, routes for surface modification and functionalization, and a range of demonstrations towards new applications of UCNPs.

The UCNPs synthesis methods have been developed, including coprecipitation, thermal decomposition, hydrothermal synthesis, sol-gel process, combustion synthesis, and flame synthesis, etc. (Zhang et al. 2010; B. Zhou et al. 2015). All of these synthesize methods can produce UCNPs with uniform size and good monodispersibility in the organic solvents. The unique property of UCNPs is that they can convert two or more lower-energy photons into one higher-energy photon to emit in the visible range. This anti-Stokes emission is induced either by excited state absorption (ESA), energy transfer upconversion (ETU), photo avalanche (PA), cooperative sensitization upconversion (CSU), or any combined mechanisms(J. Chen and Zhao 2012;Dong, Sun, and Yan 2013). Being such an unique optimal nanomaterial, UCNPs have many outstanding characteristics, such as good capability in resisting to photobleaching and photoblinking(L. Wang et al. 2005), achieving minimal background(Z. Song et al. 2012),

penetrating deeply inside biological tissues(Shen, Zhao, and Han 2013), and being tunable in size and morphology. However, due to the inherent hydrophobic surface of lab synthesised UCNPs, a hydrophilic surface modification is essential. To date, numerous strategies have been introduced for the water-soluble nanoparticle purpose, including surface ligand exchange, ligand oxidization, amphiphilic coating, layer-by-layer, silanization, and host-guest interactions(J. Zhou, Liu, and Li 2012). Recently, UCNPs have been widely employed in drug delivery(König et al. 2006), photodynamic therapy(Xie, Lee, and Chen 2010; G. Chen et al. 2014), bioimaging(Dong, Sun, and Yan 2015), security inks(Baride et al. 2015), biosensing and bioassays(J. Chen and Zhao 2012; C. Wang, Li, and Zhang 2016; Li et al. 2017).

Traditional DNA assays are delivered by quantitative real-time polymerase chain reaction (PCR) technique that is known for its sensitivity and high throughput(Git et al. 2010). However, it is limited by its high cost, tedious procedures, and trained operators' requirement for point-of-care applications. Fluorescence resonance energy transfer (FRET) is an alternative approach based on donor-acceptor pairs to sensitively response the analytes(Zadran et al. 2012). By taking advantages of its specificity and simplicity, FRET becomes a popular technique in bioassays(Held 2012; Zadran et al. 2012). However, FRET also appears to some problems that are their strict UV/Vis excitation sources requirement, which usually induces autofluorescence and scattering light from biomolecule. Besides, FRET donors suffer the spectral overlap between donors and acceptors, which is hard to resolve due to the intrinsic optical properties of most down-converting fluorophores. Therefore, as a derivative of FRET, luminescence resonance energy transfer (LRET) is introduced as a promising technique by employing upconverting fluorophores to break the bottleneck(K. Song et al. 2012). Such LRET-based platforms can report various analytes in a simple and robust design structure, and especially favoured in DNA assay platforms.

1.2 Objectives

The objectives of this thesis are to develop a practical DNA detection platform based on UCNPs. Before that, a systematic comparison of the hydrophilic surface modification of UCNPs by one-step ligand exchange will be investigated. This is aimed to provide a robust evaluation of the parameters, such as surface coating materials, buffers, and the operating environment where the water-soluble UCNPs could be well dispersed with long-term colloidal stability. Then, the hydrophilic UCNPs will be used along with the gold nanoparticles to form an energy donor-quencher pair for homogenous DNA assay. The designed bioassay platform will be optimized and tested to achieve high specificity, sensitive, simple, quick, and amplification/enzyme-free manner.

1.2 Thesis Organization

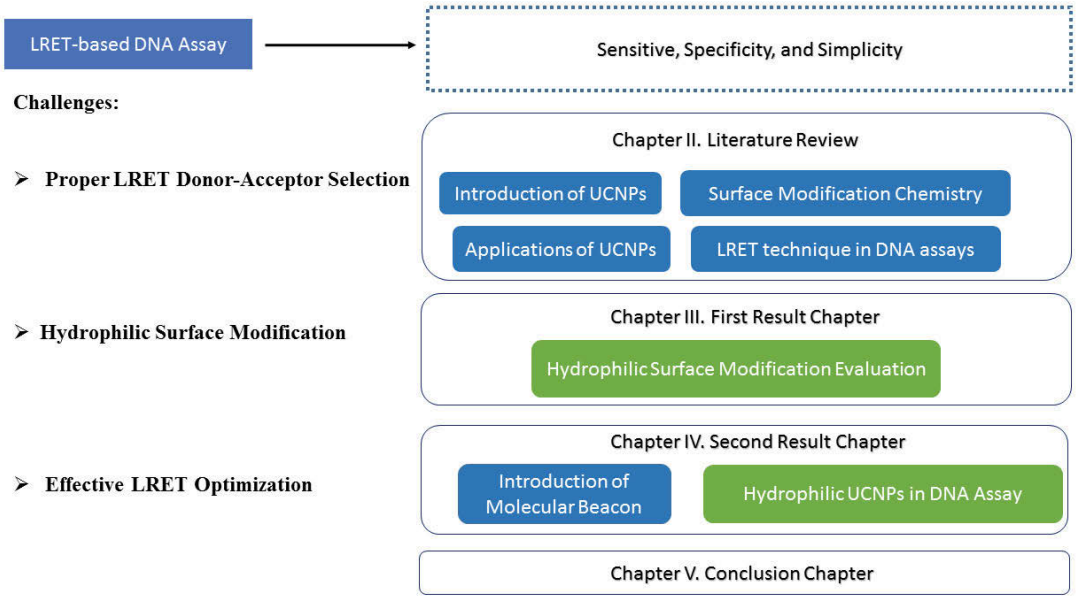

Figure I-1. Thesis structure organization.

This a conventional thesis composed of five chapters. The organization of this thesis is depicted in Figure I-1.

Specifically, chapter I introduces the background, research objectives, and the organization of this thesis.

Chapter II gives a detailed literature review, covering the basic material properties of UCNPs, representative upconverting mechanisms, commonly used synthesis methods, and their subsequent hydrophilic surface functionalization strategies for biological and analytical applications. The LRET-based DNA assay also introduced in this chapter.

Chapter III is the first result chapter that reports systematic comparison studies of hydrophilic surface modification of UCNPs using four different polymers.

Chapter IV reports a typical application of hydrophilic UCNPs for a DNA assay, based on homogenous LRET technique using UCNPs and gold nanoparticles as the energy donor and quencher respectively. Finally, chapter V concludes the remarkable output in this thesis and discusses future studies in related fields.

Chapter II. Literature Review

2.1 Introduction of UCNPs

François Auzel first discovered upconversion nanoparticles (UCNPs) in 1996(Auzel 2004). From then on, they have attracted an exposure of interests. Followed by decade's development, UCNPs have shown competitive strength among optical materials, such as low autofluorescence background interference, large anti-Stokes shifts, sharp emission bandwidths, excellent biocompatibility, high photobleaching resistance, low toxicity, and high penetration depth, etc. These advanced properties pave the way for UCNPs applied in various applications, both in biological, chemical and optical fields.

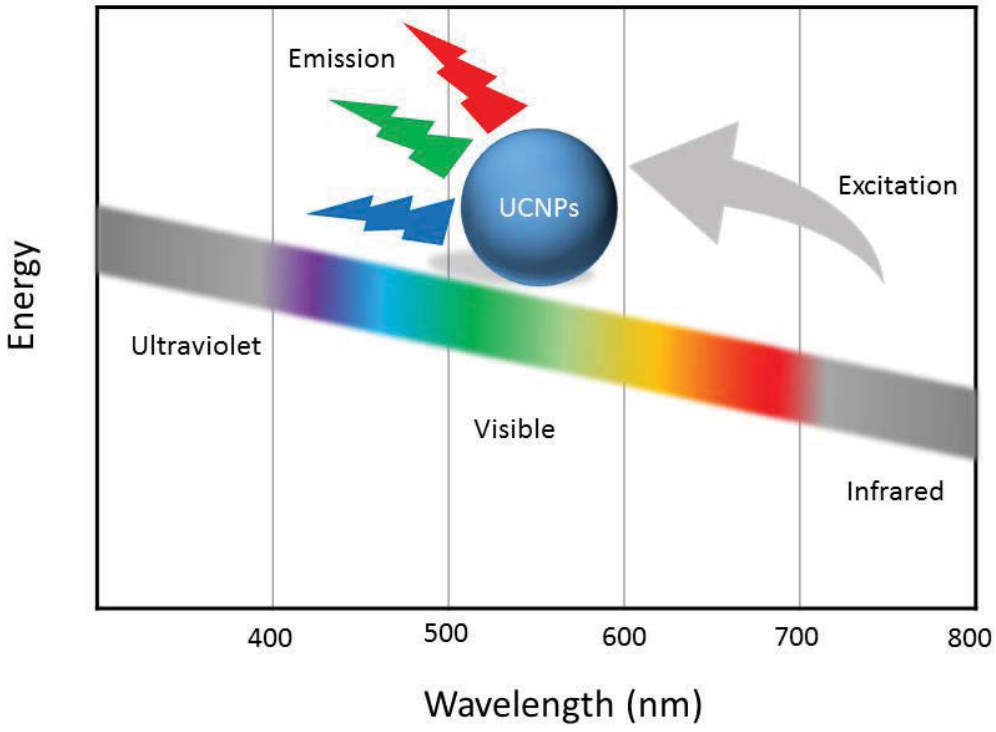

Figure II-1. Simplified principle of upconversion luminescence.

Figure II-1 illustrates the phenomenon of the UCNPs luminescence. This unique nanomaterial is excited in the near-infrared (NIR) range, in which the UCNPs can absorb two or more photons with lower-energy, and then emit the higher-energy photon with a shorter wavelength (ultraviolet or visible spectrum). This is a significant property that provides a NIR optical transmission window to allow deep tissue penetration in organs

and achieve negligible absorption or scattering as well. The UCNPs are adjustable in size, morphology (spherical, cubic, or rod-shaped), emission (UV-visible range), lifetime, power density, and other properties by merely replacing the combination of host and doping materials or concentration of doping ions. These properties enable UCNPs showing infinite formations with different characteristics.

Furthermore, unlike conventional fluorophores experience photobleaching and photoblinking, UCNPs bear permanent excitation and produce efficient light emission. Therefore, UCNPs adapt to diverse platforms: 1) they are ideal candidates as the smart nanocarriers for drug delivery and therapy, for the sake of the precise drug release control and minimal side effects; 2) UCNPs are powerful materials for targeting small tissues and organs with minimum background; 3) they can be utilized as background-free probes in analytical and clinical assays. To dates, UCNPs are also favoured in broader applications, such as 3D printing, security inks, microscopy, and thermometry, etc.

2.1.1 Architecture of UCNPs

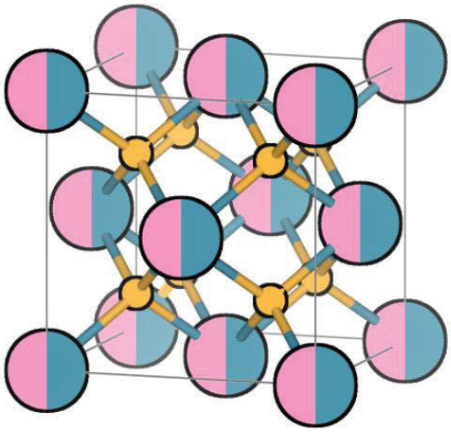

Figure II-2. A typical unit structure of cubic NaYF4: RE, where Na, rare earth, and F ions represented in teal, pink and yellow, respectively. (Ref. Wikipedia)

The size of UCNPs typically ranges from 1-100 nm. Each unit is consists of three essential components: host lattice, activator, and sensitizer ions(G. Chen et al. 2014). The host lattice serves as a medium for ions inside to perform energy transfer. Activator ions and sensitizer ions are neighbouring ions doped into host lattice shown in Figure II-2.

An appropriate host lattice owns the characteristics of low lattice photon energies, high chemical stability, and low symmetry. Low lattice photon energy can prevent the loss in conversion from excitation to phonon energy. High chemical stability is crucial since the conversion always take place in the chemical and photochemical environment. The low symmetry of lattice also can increase the f-f intermixing and thus promote upconversion efficiency. Typically, oxides and fluorides are suitable to provide both stability and low photon energies combinations. Therefore, $NaYF_4$:Yb/Er and $NaYF_4$:Yb/Tm become the most common and efficient UCNPs compositions.

In the selection of activators, the minimal energy differences between the ground to intermediate state and intermediates to excited emission state are preferable due to it can reduce non-radiative energy loss. The most frequently selected activators are rare-earth elements, such as Er^{3+}, Tm^{3+}, and Ho^{3+} ions, since their energy levels follow the "ladder" pattern to generate upconversion emission(J. Zhou et al. 2015). Moreover, lanthanide dopants can produce sharp f-f transition bands due to their characteristics and fill 5s and 5p shell and shield their 4f electrons simultaneously by their multiple 4f excitation levels. Since these transitions are Laporte forbidden, Ln^{3+} can generate longer excited state and allow longer time for numerous excitations required in upconversion process.

It is worth noting that the concentration of activator ions can profoundly affect the UCNPs behaviour. High level of activator may cause quick energy transfer and cross relaxation which results in low emission efficiency. Sensitizer ions are doped into UCNPs lattice to conduct electron transfer along with the activator ions. Yb^{3+} ion is the most popular candidate since it has a broad absorption cross-section for excited near infrared radiation. The typical doped concentration is approximately 20 mol% sensitizer and less than 2 mol% activator ions. These kinds of UCNPs own appropriate distance between activators and absorb enough excitation radiation by sensitizer while preventing cross-relaxation.

2.1.2 Upconverting Mechanisms

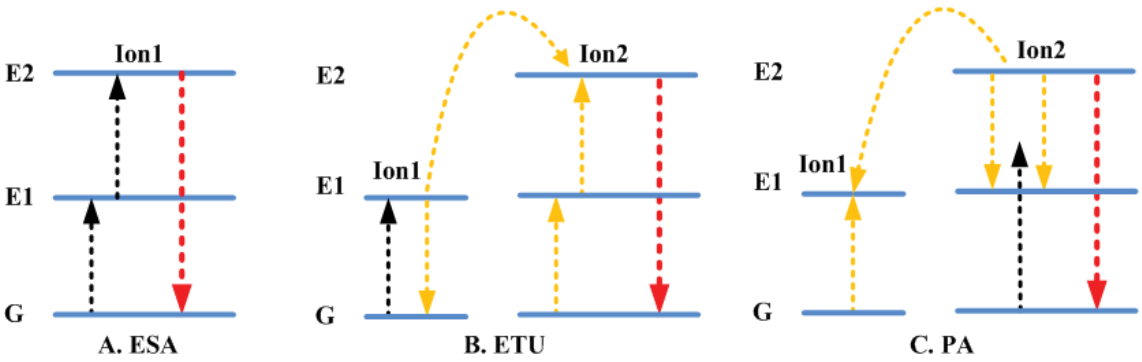

Figure II-3. Three common mechanisms for UNCPs emission

Three most common mechanisms for lanthanide-doped upconversion materials to achieve unique upconverting properties are excited state absorption (ESA), energy transfer upconversion (ETU), and photo avalanche (PA). More physical processes are also briefly explained below.

1. *Excited state absorption (ESA)*

Lanthanide-doped UCNPs can be modelled as a host-guest system. The lanthanide ions serve as the guest materials dispersed in a host lattice to produce emission under excitation. ESA appears most commonly especially when the unit has low dopant concentrations. It takes the pattern of sequentially absorbing two photons by one single ion and emit a photon with higher energy. The simplified mechanism process is illustrated in Figure II-3 (a). When an ion is excited from the ground state to E1, another photon acquires high possibility of pumping the ion from E1 to E2 energy level due to the long lifetime of E1 state, then upconverting emission occurs at E2 state. Although this emission mechanism is simple, it can only happen in units that are doped by few lanthanide ions, such as Er^{3+}, Ho^{3+}, Tm^{3+}, and Nd^{3+}(Auzel 2004), since only these few ions have a ladder-like arrangement of energy state to achieve sufficient ESA.

2. *Energy transfer upconversion (ETU)*

Different from ESA, ETU process involves two ions working together to achieve emission. In a typical ETU shown in Figure II-3 (b), the ion1 known as sensitizer, is first excited from ground state to E1 level; then partial of its energy is transfer back to the ground state G; the excited state E1 of ion2 known as activator, absorbing the energy of ion 1 and then exciting ion2 to its excited state E2, while sensitizer ion 1 relaxed to ground state twice. ETU efficiency is highly dependent on the distance between neighbouring ions, in other words, the doping concentrations. This mechanism is crucial since the most efficient UNCPs employ the ion pairs for enhanced excitation, such as Yb^{3+}/Tm^{3+}, Yb^{3+}/Er^{3+}, and Yb^{3+}/Ho^{3+}.

3. *Photon Avalanche (PA)*

Photon avalanche utilizes the thresholds of photon pump to control the luminescence intensity. It is a looping process involving ESA for excitation and CR for feedback which is sketched in Figure II-3(c). Therefore, the process has typically the highest upconversion efficiency as well as the strong emission.

4. *Other Mechanisms*

Cooperative sensitization upconversion (CSU), is existing in many structures. For example, as is shown in Figure II-3(c), this process involves the cooperative operation of three ions where ion 1 and ion 3 are generally the same type. Upon excitation, ion 1 and ion 3 are pumped to the excited state. The two sensitizers interact with ion 2 and transfer the energy to excite it to a higher state. Ion 2 will then reduce back to the ground state by emitting photons. Although CSU is a less efficient upconverting process then ESA and ETU, it still reported in systems such as Yb^{3+}/Tb^{3+}, Yb^{3+}/Eu^{3+} pairs. Cross-relaxation (CR) describes a process resulting from the ion-ion interaction. Ion 1 at already higher energy level transfers part of its energy to ion 2. CR is efficient in close ion, and it also causes the concentration quenching mechanism of emission.

2.1.3 UCNPs synthesis methods

The various methods are used to synthesize UCNPs including coprecipitation, thermal decomposition, hydro(solvo)thermal synthesis, sol-gel processing, combustion, and flame synthesis. Table II-1**Error! Reference source not found.** summarises the output and examples of each method(G. Chen et al. 2014).

Table II-1.Summary of Common UCNPs Synthesis Methods.

Method	Host Examples	Synthesis Output
Coprecipitation	LaF_3,$NaYF_4$ GdF_3, Y_2O_3 Lu_2O_3	▪ Simple protocols ▪ Facile and cheap procedure ▪ Require high-temperature treatment ▪ Poor size control
Thermal decomposition	LaF_3, $NaYF_4$ Y_2O_3, Gd_2O_3 LaOF	▪ High quality ▪ Well monodisperse ▪ Good size ▪ Costly procedure ▪ Toxic by-products
Hydro(solvo)thermal synthesis	LaF_3,$NaYF_4$ Y_2O_3, Gd_2O_3 GdF_3	▪ Good size and shape control ▪ Good dispensability ▪ Low amount of by-products ▪ Low reaction temperature
Sol-gel processing	TiO_2, Y_2O_3 Gd_2O_3	▪ Cheap raw materials ▪ Relatively long reaction time ▪ Tends to aggregate in aqueous solution
Combustion synthesis	TiO_2, Y_2O_3 Gd_2O_3, ZrO_2	▪ Sort reaction times ▪ High Temperature ▪ Tends to aggregate
Flame synthesis	Y_2O_3	▪ Short reaction time ▪ Readily scalable

Coprecipitation method is probably the most simple and cost-efficient approach to synthesize the nanocrystals with small size and narrow size distribution. In this procedure, the post-heat treatment is typically required. The well prepared LaF3 nanoparticles were synthesized by Chow's group (Yi and Chow 2005). They used ammonium di-n- octadecyl

dithiophosphate as the capping agent to control nanocrystal growth, and finally produced nanoparticles with uniform size at around 5nm. Figure II-4A shows the morphology of well-dispersed LaF_3 nanoparticles in the organic solvents.

Yan and co-workers (Mai et al. 2006) developed a thermal decomposition method to synthesize monodisperse nanocrystals with high quality. Figure II-4B displays the $NaYF_4$ products by using Na (CF_3COO) and $Y(CF_3COO)_3$ as the precursors. Followed by a series of delicate study, thermal decomposition method further expended as a standard route for high-quality UCNPs synthesis. For example, Capobianco and co-workers have produced almost monodisperse distributed NaYF4 UCNPs by thermal decomposition method (Boyer, Cuccia, and Capobianco 2007). They utilized trifluoroacetate and oleic acid as the precursor the capping ligand, respectively. The as-prepared UCNPs showed high colloidal stability and well dispensability in organic solvents. TEM image of NaYF4: Er^{3+}, $Yb3^{+}$ produced by thermal decomposition method is shown in Figure II-4C. Commonly, this protocol involves thermal decomposition of metal trifluoroacetate precursors in a high boiling organic solvent such as oleic acid and octadecane. During the manufacture procedure, carefully control of reaction temperature, metal precursors and their concentration, solvent nature, and reaction time are crucial to producing good quality of nanocrystals. However, it is worth mentioning that the toxic by-products limit its application in large-scale production.

Hydro (solvo) thermal approach utilizes the setup involving autoclave to produce good quality and dispensability of nanocrystals. The significant advantages of this method are that the nanocrystals can be synthesized with low toxic by-products and only relatively low temperature (<250℃) is required. By tuning the temperature, reaction time, solvent, and surfactant concentrations, one can easily control the dimension and morphology of nanocrystals. Figure II-4D shows a TEM image of typical example that $NaYF_4$: Eu^{3+} prepared with $NaF/Ln(NO_3)_3$ by solvothermal method(L. Wang and Li 2007).

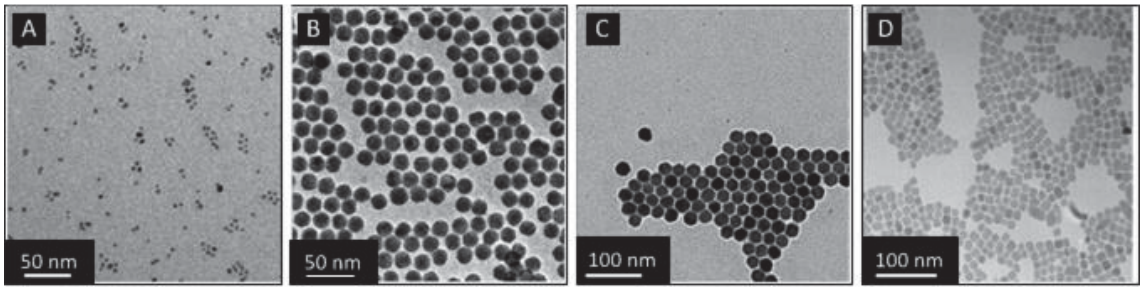

Figure II-4. TEM images of UCNPs. (A)LaF_3: Yb/Er nanoparticles synthesized by coprecipitation method proposed by Chow's group. (Yi and Chow 2005)*(B) $NaYF_4$ nanoparticles synthesized by thermal decomposition method proposed by Yan's group.(Mai et al. 2006) (C) $NaYF_4$: Er/Yb^{3+} nanoparticles synthesized by thermal decomposition method proposed by Capobianco's group. (Boyer, Cuccia, and Capobianco 2007) (D) $NaYF_4$: Eu^{3+} nanoparticles synthesized by a solvothermal method proposed by Li's group. (L. Wang and Li 2007).*

Metal alkoxide based precursors are treated by hydrolysis and polycondensation process in the sol-gel method. To improve the crystallinity and luminescence performance, further treatment at high temperature is always carried out. Moreover, the nanocrystals derived from this method is not suitable for the biological applications, as they tend to aggregate in aqueous solution.

In contrast of long reaction time that could up to days to finalize reaction in hydro (solvo) thermal and sol-gel methods, combustion synthesis method can complete reaction in few minutes. Usually, this method involves high exothermic process ranging from 500℃ to 3000℃ to form self-sustained manner that propagating through the materials.

Flame synthesis is another time-saving technique and generating the nanocrystals in a one-step process. Also, nanocrystals are readily scalable making this method stands out in other ways.

2.1.4 Characteristics of UCNPs

UCNPs, as a new generation of nanomaterial, has drawn growing attention and interests because of its unique properties. UCNPs are preferred materials compared with the traditional fluorophores and nanoparticles in many applications, especially in biological fields. The typical characteristics that drive the growth of needs are including zero auto-

fluorescence backgrounds, deep tissue penetration, tunable upconversion emission, and resistance to photobleaching. The following sections give the detailed explanations.

1. *Zero auto-fluorescence background*

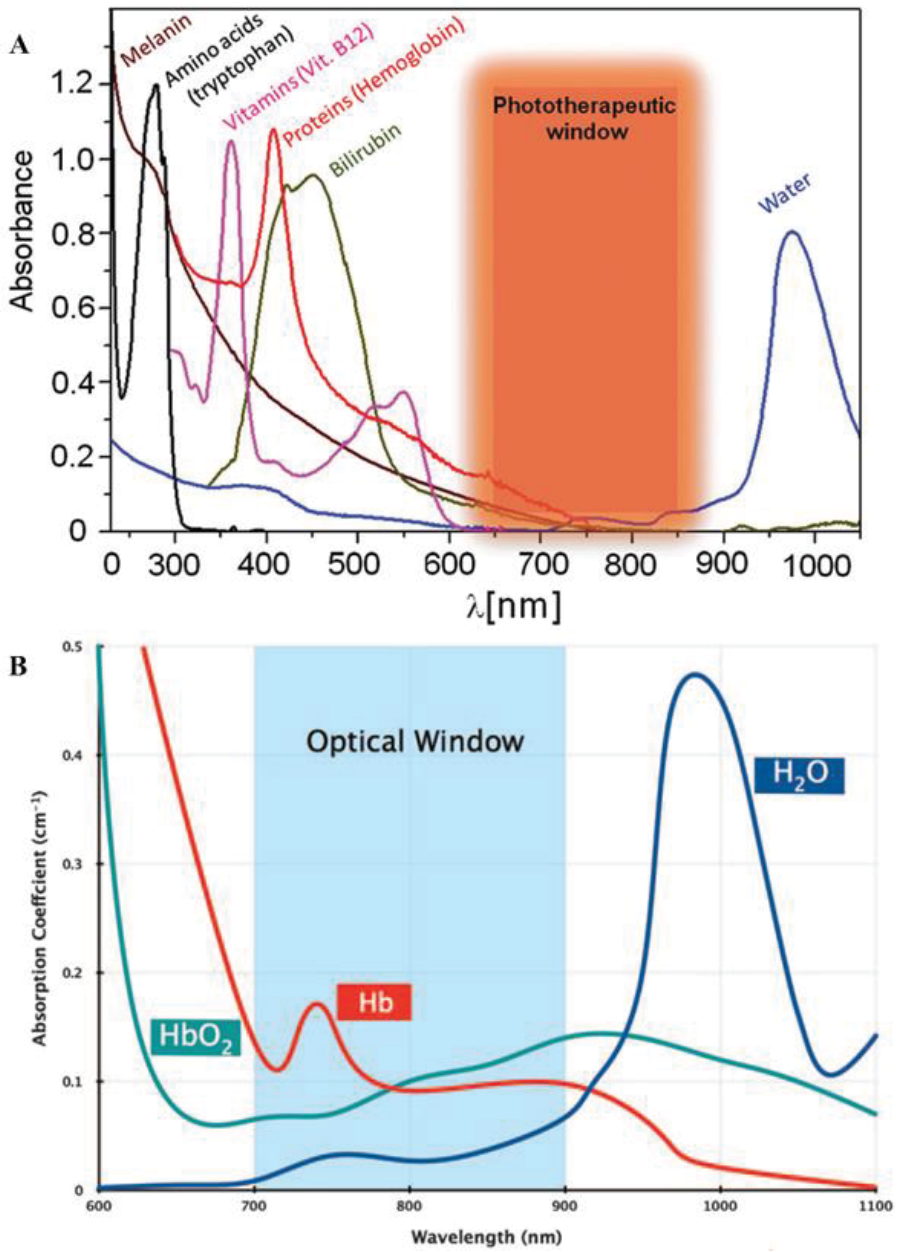

Figure II-5. (A) The absorption spectra of significant tissue light absorbers haemoglobin and water. (Ref. Phan and Bullen 2010)(B) Phototherapeutic window.(Ref. Dąbrowski and Arnaut 2015)

Luminescence nanomaterials are generated as new tools and technologies in life science for drug or gene delivery, phototherapeutic, and bio-imaging. Therefore, excitation and absorbance of water, the main component of biological tissue or important media,

becomes the main concern that would limit the efficiency of real applications of nanomaterials. Since traditional fluorescence probes, such as organic dyes and quantum dots, are exited under ultraviolet (UV) (100 nm – 400 nm) or visible range (390 nm – 700 nm) and detected in the visible spectral range as well. However, this is the range that biological tissues have strong light absorption and scattering (Figure II-5. (a)). Moreover, tissues expose to light in this range naturally generate emissions (terms "autofluorescence"), such as mitochondria and lysosome because of the presence of endogenous fluorophores (König et al. 2006). Although the spectra method can separate artificial and intrinsic biological tissue luminescence, multiple scattering of light induces unwanted signals to disturb the detection channels(Z. Song et al. 2012). Therefore, traditional fluorophores cause difficulties in obtaining adequate signals with high background noise and low practical efficiency.

To overcome these problems, advanced nanomaterials, UCNPs, are brought into applications. In the "optical window" (Figure II-5. (b)), from 700 nm – 900 nm, the water and haemoglobin as the main biological components have little light absorption(Phan and Bullen 2010), which can be considered optically transparent. Interestingly, UCNPs can be excited under 980 nm laser and provide emission at 798 nm, where its excitation achieve minimal bio-tissue autofluorescence and its luminescence emission band falls into transparent "optical window". Above property allows simple and efficient spectra separation of autofluorescence and UCNPs luminescence and contributes to ultrasensitive output in biological assays and advanced quality in bio-image.

2. *Deep tissue penetration*

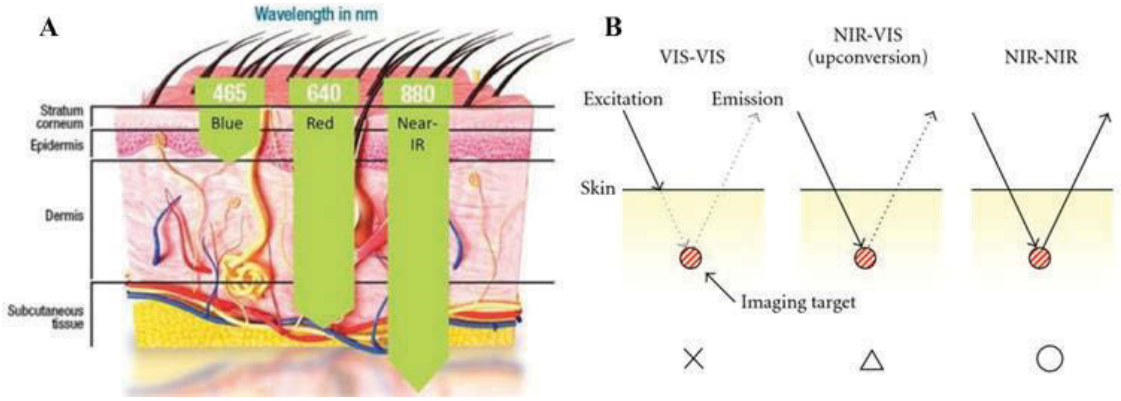

Figure II-6.UCNPs have deep tissue penetration property. (A)Light penetration depths in human tissues. (Ref: https://www.organicolivia.com/2016/12/why-at-home-infrared-light-therapy-is-a-cheap-easy-way-to-change-your-life/) (B)Different types of excitation and emission scenario(Zako et al. 2010).

Optical methods provide considerable potential for drug screening and phototherapeutic due to their non-invasiveness, high sensitivity and resolution(König et al. 2006). UV, visible and NIR lights are available excitation sources. However, NIR sources obtain strong advantages that can penetrate deep in human skin reaching down to the subcutaneous tissues (Figure II-6 (a)) because of their weaker scattering and absorption. Comparing with relatively expensive UV source, NIR is a mild excitation especially useful in therapeutic and bio-image purposes. Furthermore, according to simplified illustration of the imaging system (Figure II-6 (b)), conventional VIS-VIS image has a primary issue that it hardly penetrates the targets in tissues. Although NIR-VIS reach the targets in deep, it only generates weak visible light (Zako et al. 2010). Therefore, among many assaying nanoparticles practically used in vitro and in vivo, UCNP is a more advanced candidate than normal nanomaterials, since rare-earth doped nanoparticles are suitable in excitation/emission in NIR regions.

3. Tunable upconversion emission

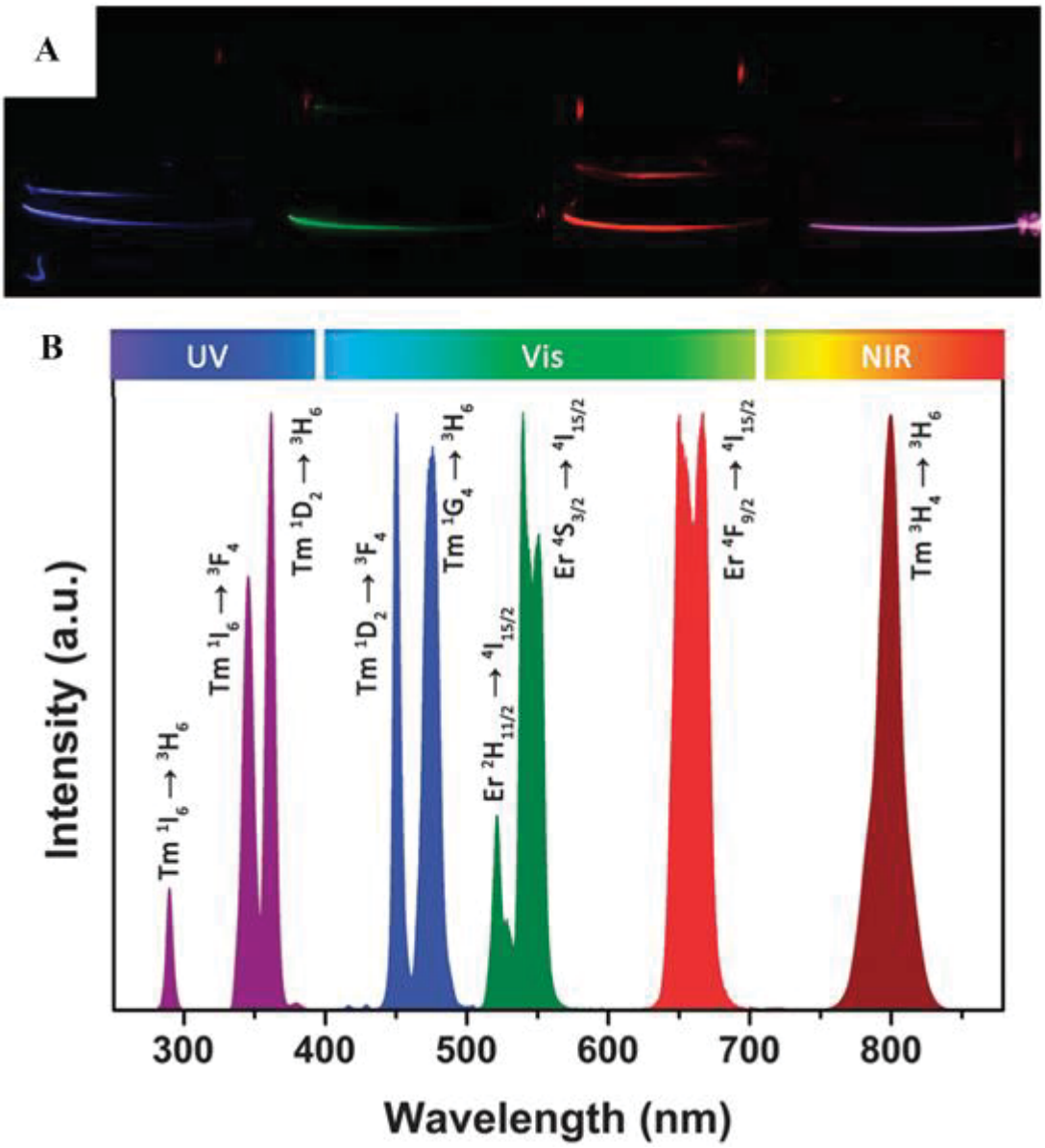

Figure II-7. (a) UC luminescence pictures of $NaYbF_4$: Tm, $NaYbF_4$: Ho, $NaYbF_4$: Er, and $NaYF_4$: Yb nanocrystals in chloroform solutions. These pictures were taken without the use of any colour filter. (Ref：Ehlert et al. 2007）(b) Typical UCNPs emissions, ranging from the UV to NIR regions, from Yb^{3+}–Er^{3+} and Yb^{3+}–Tm^{3+} co-doped UCNPs under 980 nm excitation. (Ref： Dong, Sun, and Yan 2015)

UCNPs can generate intrinsic various emission colours by different host/activator combinations and vary doping concentrations (Figure II-7 (a)). Many strategies are available to further tuning colour emission, which including energy transfer or migration pathway, control relaxation processes, adjust architecture (core/shell structure), synthesize different particles sizes or shapes, and even utilize the luminescence resonance

energy transfer (LRET) by conjugations with other nanoparticles(Dong, Sun, and Yan 2015). Colour tunability of UCNPs is a visualized consequence of emission shift in principle (Figure II-7 (b)). It is different from organic dyes and quantum dots, which have broad emission or absorption spectra, UCNPs have many sharp and narrow emission bandwidths, which eliminate the possibilities in spectrum overlap, especially in designing multi-channel detection platforms.

These unique properties of UCNPs with tunable luminescence colour and emission broaden the UCNPs applications in a multiplexed assay and multimodal image. Multiplexed assays develop resource friendly nanoplatforms that enable parallel detection of analytes. In this way, genotyping, DNA sequencing, and high throughput screening etc. can be combined in one single test. The multimodal image can real-track the multiple targets, such as proteins, DNA/RNA molecules and ions, which is essential for clinical, therapy and biological purposes.

4. Resistance to photobleaching

Photobleaching is main concerns when designing detection platforms based on fluorophore molecules. It is caused by cleaving of covalent bonds or nonspecific interactions between fluorophores and the surrounding environment. As a consequence, their fluorescence ability can be permanently damaged, which lead to unreliable and less efficient results in analysing signals. Therefore, UCNPs have efficient emission, and high resistance to photobleaching makes them a promising, reliable and robust candidate in broad chemical and biological applications.

2.2 Chemistry for UNCPs Surface Engineering

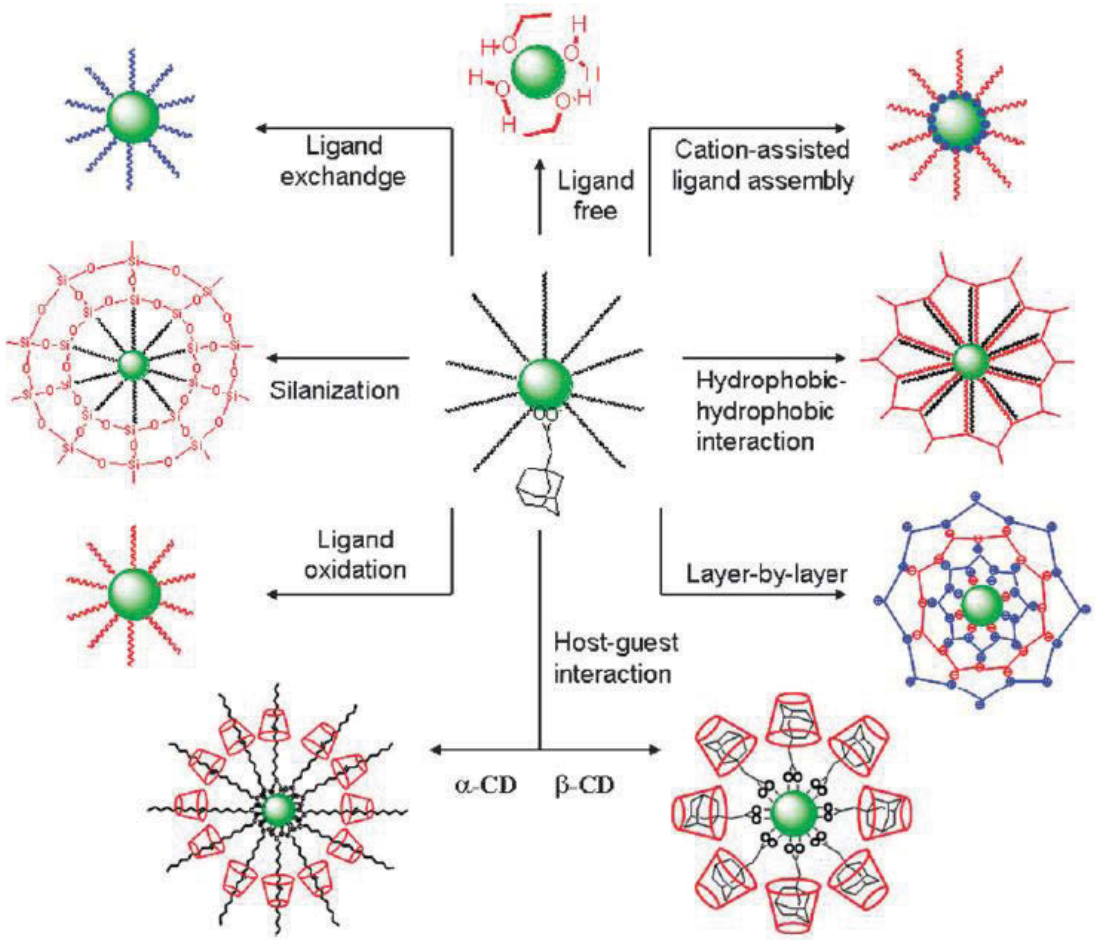

Figure II-8. Various schemes for hydrophilic surface modification of UCNPs.(J. Zhou, Liu, and Li 2012)

With increasing development in more advanced, facile and controllable UNCPs synthesis methods, it has drawn many interests of applying these nanoparticles in biological assays and bio-image study. However, the common lab prepared UCNPs are capped with surfactants, normally oleic acid or oleylamine, which has the polar head points towards the UCNPs surface while the hydrophobic head points outwards. Therefore, the hydrophobic surface of UCNPs becomes an ineligible limit in biological applications. Consequently, the desire for effective surface modification strategies that render a hydrophilic surface on UNCPs is increased. The most common and broadly used methods are sketched in Figure II-8, and the output of each strategy is summarized in Table II-2.

Table II-2. Summary of conventionally used methods for UNCPs surface modification.

Strategies	Advantages	Limitations
Ligand Exchange	simple and direct; the desire for further functional groups conjugation	Time-consuming
Ligand Oxidation	Simple and direct; Stalely conjugate with other molecules; Good water dispensability	Poor colloidal stability
Hydrophobic Interaction	Retain origin ligands; Aqueous dispersion and further bio-conjugation	Hard to control bilayer formation
Layer by Layer Assembly	Thickness controllable; High stability; Uniform layers	Repeated wash step required
Inorganic Shell	Biocompatibility; Cavities on the surface are benefited for drug loading	Tends to aggregate; Further surface modification required
Cation-assistant	Completely substitute original ligands	Strong acid requirement
Host-guest Interaction	Biocompatible, simple process	Produce nanoparticles with a relatively large size

2.2.1 Ligand Exchange

Ligand exchange is the most straightforward method to render UCNPs a hydrophilic surface. The basic strategy is using small hydrophilic molecules or polymers to replace the original capping agent, oleic acid or oleylamine ligand. In a typical one-step method, the additional more polar ligand is applied to substitute the native ligand to achieve water soluble purpose completely. The new ligands are designed to contain the functional group to coordinate the UCNP surface, such as –SH, $–NH_2$, –COOH, and $–PO_3H$. The commonly used hydrophilic molecules used are citrate, poly(acrylic acid)(PAA)(H. Chen et al. 2013), polyethyleneimine (PEI)(Y. Wang et al. 2012) (Hu et al. 2008), and

PEGylated (Tong et al. 2015) compounds. Although is the most simple method in principle, the conjugation process may need to continuous stirring from 4 hours to several days, and possibly to be aggregated during the ligand exchange process.

Two-step replacement protocols can also achieve ligand exchange method. Bogdan and co-workers proposed a method that using nitrosonium tetrafluoroborate ($NOBF_4$) or stronger acids are a reagent to produce bare UCNPs before new ligands introduce(Bogdan et al. 2011). In principle, after reaction of $NOBF_4$ and dispersion of UCNPs that BF^{4-} replace the original ligands of UCNPs, the secondary functionalization of various capping materials can be engineered. The advantages of two-step modification are that it can generate different types and varying size or shape of UCNPs. Also, the functionalized water-soluble UCNPs can be stabilized in polar media for years without significant aggregation or precipitation.

2.2.2 Ligand Oxidization

Another broadly used chemical method for UCNPs surface modification is achieved through ligand oxidization technique. In principle, the carbon-carbon double bond of oleate or oleylamine is oxidized and then forms a carboxyl or epoxy group. In this process, many oxidization agents are available, such as Lemieux−von Rudloff reagent (Z. Chen et al. 2008), ozone (H. P. Zhou et al. 2009), and 3-chloroper-oxy-benzoic acid (Hu et al. 2008). Such particles can be covalently attached to other species to reach for specific purposes (Dai et al. 2012). Besides, the formation of water-soluble groups can enhance the dispensability. After chemical modifications, nanoparticles can achieve subsequent bio-functionalized conjugation with other molecules through covalent bindings. However, oxidative surface displays poor colloidal stability and has a quite limited number of ligands can be generated, such as aldehydes, epoxides, and carboxylic acids.

2.2.3 Amphiphilic Coatings

In the above two chemical methods that generate the hydrophilic surface of nanoparticles all involves the new ligand formation after getting rid of native ligand. During this process,

bare UCNPs are exposed to strong acid or other reagents that can cause etching and surface defection. Therefore, the ligand attraction method is introduced to retain the original hydrophobic ligands via hydrophobic van der Waals interactions. The amphiphilic polymer is the key component that forms an additional layer on the top of oleic acid capped UCNPs. This polymer contains long alkyl chains can deposit between hydrophobic oleate molecules through hydrophobic attraction, and hydrophilic head groups are directed outwards. Therefore, successfully render nanocrystals a bilayer surface with adequate water solubility. Furthermore, the amphiphilic molecules can present functional groups allowing UCNPs attach with other molecules. However, the maximum length of the alkyl chain is limited by oleate capping itself. If the chain length exceeds the length of oleate, the interaction becomes too weak to stabilize the bilayer.

2.2.4 Layer-by-layer (LbL)

Instead of applying amphiphilic polymer for UCNPs hydrophilic surface modification, LbL technique utilizes oppositely charged polyions to engineer a water-soluble surface(L. Wang et al. 2005). The major advantages of LbL are that this approach permits the preparation of coated nanoparticles with precisely controllable size with uniform layers. Moreover, the high stability of biocompatibility coating layers make the water-soluble UCNPs attractive materials for a wide range of biological applications.

2.2.5 Silanization Treatment

The deposit of silica shell on UCNPs is an alternative approach for the hydrophilic and bio-conjugation purpose. A uniform layer of silica coating is based on a reverse microemulsion method(Lu et al. 2004), which involves the polymerization and silicate precursors. Tetraethyl Orthosilicate (TEOS) and non-ionic surfactant Igepal CO-520 are most commonly used precursors. During the coating process, a small amount of ammonia is important in keeping the concentration of silicic acid higher than nucleation concentration, which is a key step in controlling the growth of uniform silica shell. UCNPs encapsulated with silica are disperse in water and readily uptake by the cells. Therefore, UCNPs@SiO_2 becomes a powerful material in biological and cell image study.

Also, the porous silica coating on UCNPs provides many cavities that can be designed as drug carriers and explore the applications in drug delivery areas. However, the colloidal stability of silica coated UCNPs in aqueous solution is relatively poor and tends to aggregate in a short time. Therefore, subsequently, an introduction of charged functional groups are required for stability purpose.

2.2.6 Cation-assistant Ligands Assembly

The cation-assistant ligands assembly method is a facile approach to produce UCNPs a water-soluble surface. In a standard process, the original grafted ligands on the surface of UCNPs is cleaved, which exposes the positive charges on nanoparticle's surface. Then the negatively charged ligands are favoured to assemble new hydrophilic surface on UCNPs by electrostatic interactions.

2.2.7 Host-guest Interaction

The host-guest method mediates a self-assembly interaction between hydrophobic UCNPs and hydrophilic molecules, which serve as the "host" and "guest" role, respectively. The typical guest molecules are macromolecular, such as cyclodextrin(Ni et al. 2015) and Cucurbituril(Sun et al. 2018). These molecules have a hydrophilic outside and hydrophobic inside. Through a simply stirring and shaking process, they can be easily assembled onto hydrophobic ligands of UCNPs. Therefore enable UCNPs a stable hydrophilic outer shell.

2.3 Applications of UCNPs

With the past decade's effort, UCNPs have developed into a bright new era. The improvement in UCNPs synthesis, more and more facile and robust surface modification strategies, and varies nanoplatforms available provide UCNPs good opportunities in real applications, especially in drug delivery and therapy(Bagheri et al. 2016), bio-imaging(J. Zhou, Liu, and Li 2012), and bio-sensing and bioassays areas(Dong, Sun, and Yan 2015; J. Chen and Zhao 2012) where tremendous examples have been well demonstrated. UCNPs have become such a popular material due to its unique photophysical and chemical properties. First of all, controllable UCNPs size can be easily adapted with

different types of biological entities. Second, UCNPs have a large surface area, which enables large possibilities to functionalize nanoparticle surface with varies ligands for better cell interactions or uptake. Besides, its metallic core benefit in imaging fields(Mejia-Ariza et al. 2017). Importantly, evaluation of cellular morphology and mitochondrial function have shown that UCNPs have shown non-/low-toxicity to broad cell lines(J. Chen and Zhao 2012).

2.3.1 Drug delivery

Drug delivery therapy system based on nanoparticles have many advantages over the traditional medical treatment, including the efficient pharmaceutical loadings, better solubility, stability, and targeted distribution(G. Chen et al. 2014). Several types of nanoparticles employed in a drug delivery system have been demonstrated well in literature, such as iron oxide nanoparticle, quantum dot, gold nanoparticle, carbon nanotube, and silica nanoparticle. UCNPs emerging as a new alternative to building up more advanced drug delivery systems attribute to its special features. Three common drug loading strategies for UCNPs based system are briefly summarized below.

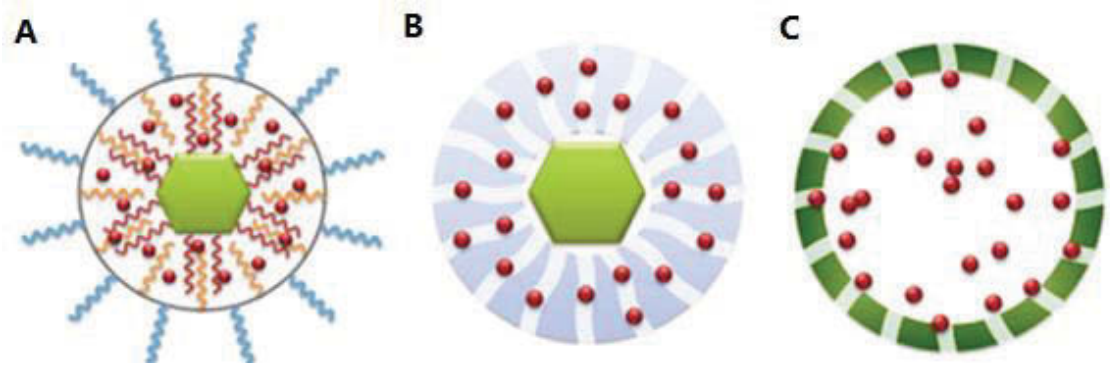

Figure II-9. Schematic representation of current approaches to constructing UCNPs based drug delivery systems: a) hydrophobic pockets, b) mesoporous silica shells, and c) hollow mesoporous-coated spheres. (Shen, Zhao, and Han 2013)

1. *Hydrophobic pockets*

Hydrophobic pockets represent the hydrophobic-hydrophobic interaction between the hydrophobic ligands on particle surface and drugs. A schematic representation is shown in Figure II-9(a). Typically, OA-capped UCNPs are modified with the amphiphilic

polymer, which creates a hydrophobic pocket for anticancer drugs molecules, doxorubicin (DOX), encapsulated. The loading and release of DOX can be controlled by varying pH of the environment, which has been observed that the acidic environment increases the DOX dissociation rate. Thus this strategy is favourable in tumour cells (Shen, Zhao, and Han 2013).

2. *Mesoporous silica shells*

In this method, drugs are encapsulated in pores of mesoporous silica shell which has been deposited on UCNPs surface. Figure II-9(b) shows a simple schematic of a typical example. The mesoporous silica shell is fabricated by electrospinning process. The mesoporous provide high specific area and large pore volume making the silica-coated UCNPs suitable for the efficient and stable drug loadings. The drug-loaded can quench the luminescence of UNCPs via energy transfer while the drug release process can be monitored by emission recovery.

3. *Hollow spheres with mesoporous surface*

Hollow spheres with mesoporous surface provide an alternative way for drug loading (Figure II-9(c)). In this case, drugs are encapsulated in a hollow sphere with higher loading capacity while still maintains the upconverting imaging ability. Based on this concept, a multifunctional mesoporous nanostructure is proposed with both upconverting luminescence and magnetic properties. The nanostructure has a rare earth doped UCNPs shell and inner magnetic nanoparticles. Anticancer drugs are loaded into the hollow sphere by porous UCNP layer.

2.3.2 Upconversion-Guided Therapy

Nowadays, photothermal therapy (PTT) has emerged as a strong candidate to classical cancer therapies. It employs photo-absorbers to generate heat from heat absorption and provide thermal ablation. Although UCNPs have the less efficient capacity to convert light directly to heat due to its intrinsic low excitation coefficient, it is still active in PTT application. Since mentioned before, UCNPs can be easily coupled with various

nanoparticles which possess strong excitation coefficient. These nanosystems can achieve upconverting luminescence, magnetic properties, and PTT function in a single modified platform.

Photodynamic therapy (PDT) is a clinical treatment that utilizes the photosensitizers to produce single oxygen ($^1O_2$) which is toxic to tumour cells. In a typical PDT process, the photosensitizers are excited under a specific light and then jumped from the single ground state to a single excited state, which undergoes an intersystem crossing to a longer-lived triplet state then react with the surrounding oxygen to produce $^1O_2$. UCNPs have the advantages to overcome the limitation of low penetration depth caused by traditional PDT, since UCNPs can be excited by NIR light and penetrate significantly deeper in tissues. Moreover, visible light can be efficiently generated from NIR light by UCNPs to provide a light source for photosensitizers to produce $^1O_2$. Therefore, paving the avenue of UCNPs in PDT area.

2.3.3 Bio-image applications

Lanthanide-doped UCNPs have become increasingly favourable in biological and medical imaging, since they utilize less expensive NIR (980 nm or 808 nm) diode laser as the excitation source, and have significant penetration depth which makes the deep tissue image available. With the more advanced synthesised methods introduced, a large scale of UCNPs with good dispensability, low cytotoxicity and stable luminescence capacity enable them used in multifunction applications. Indeed, UCNPs based nanoprobes have been successfully demonstrated in multiple cell lines imaging, such as prostate cancer cells, Hela cells, breast cancer cells, and ovarian cancer cells, etc.

2.3.4 Bio-sensing and Bioassays

The most popular applications of UCNPs are in bio-sensing and bioassay fields, which employ the UCNPs as the nanoprobes or reporters. Numerous biological and chemical assays have been proposed in recent decades, such as DNA hybridization assays, early diseases detections, immunoassays, affinity assays etc. Among them, a DNA assay based

on UCNPs is one of the most popular applications as it has great importance in point-of-care theranostics. Ultrasensitive detection of disease biomarkers makes the early diagnosis possible. The biggest advantage of UCNPs as the biosensors attributes to its superior signal-to-noise ratio, which largely enhances the detection sensitivity and the detection limit compared to classical luminescence materials. So far, the majority of UNCPs based bioassay platforms are taking advantages of the luminescence resonance energy transfer (LRET) process.

Homogeneous DNA assays based on UCNPs already gain a lot of mature experience. In recent years, many groups have demonstrated their work in developing simple and sensitive platforms(Alonso-Cristobal et al. 2015a; Yinghui Chen et al. 2018). What's more, thanks to the effort has been devoted, more advanced DNA detection can be transferred from a homogenous system to a paper-based platform, which brings the opportunity for Point-of-Care development. For instance, Zhou and coworkers developed gene fragment detection on cellulose paper(F. Zhou, Noor, and Krull 2014). The developed UCNPs based DNA assay could achieve high sensitivity, selectivity and fast response, which may be suited for rapid diagnostic applications.

2.4 Introduction of Luminescence Resonance Energy Transfer (LRET) Based Bioassays

Förster resonance energy transfer (FRET) was firstly introduced over 60 years ago(Forster 1946). It describes a physical process of non-radiation energy transfer between two chromophores. This process can be delivered in molecular proximity up to 10-100 Å (Sekar and Periasamy 2003). Over decades' development, FRET has been used as a powerful technique to study tremendous biological or chemical phenomena which induce the proximity changes. However, FRER only appears based on the following requirements:

1) Donor and acceptor are placed in proximity, typically between the 1-10 nm.

2) The donor's fluorescence emission spectrum overlaps the acceptor's absorbance or excitation spectrum.
3) The dipole orientations of donor and acceptor must be approximately parallel.

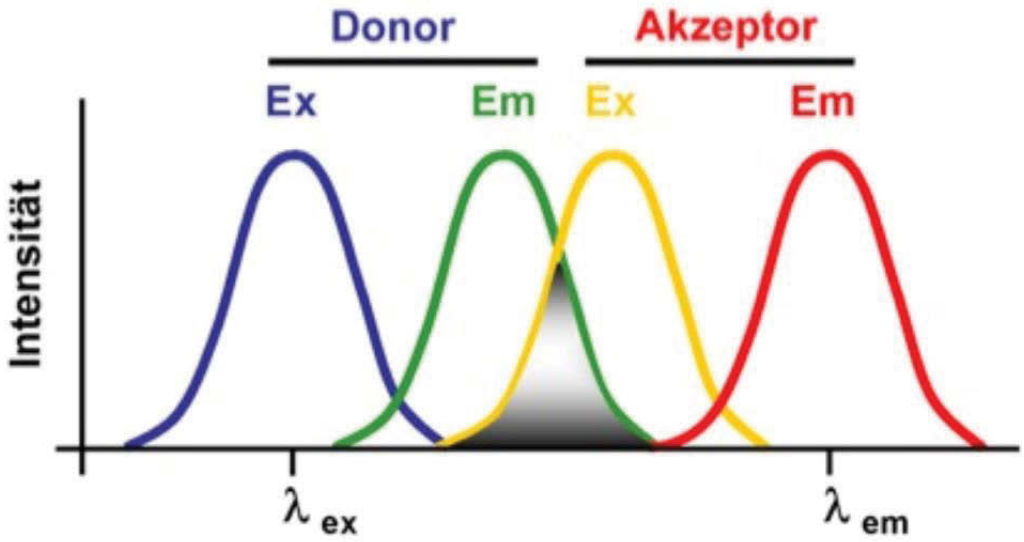

Figure II-10. FRET mechanisms between donor and acceptor. (Ref. https://bitesizebio.com/23012/you-may-not-know-theodor-forster-but-you-know-his-work-fret/)

When the FRET occurs, it finally leads to fluorescence quench of energy donor or acceptor emission increase. Figure II-10 illustrates the FRET mechanism. The donor has been excited under a certain wavelength, it emits the emission that overlaps with the excitation wavelength of the acceptor, and thus excite the acceptor to produce or enhance the emission. FRET is a distance-dependent process. Therefore, the efficiency of FRET process (E) is relevant of the inverse sixth power of the distance between the donor and acceptor R, as the following equation shows (Forster 1946; Zadran et al. 2012):

$$E = \frac{1}{(1 + \left(\frac{R}{R_0}\right)^6)}$$

Where R_0 represents Förster radius, defining the distance between the fluorophores at which half of the excitation energy is transferred to acceptor; and R is the real distance between the fluorophores. The R_0 magnitude depends on donor and acceptors' spectrum properties, such as the fluorescence quantum yields, the refractive index of the solvent,

dipole angular orientations, and the integral of spectral overlaps. The value of R_0 ranging from 20 to 90 Å is comparable to the thickness of the organism membranes and diameters of many proteins, and therefore, FRET gains powerful applications in biology (Held 2012). Overall, in many well-established bioassays, biophysics, and biochemistry, FRET is broadly used to study protein-protein interactions, protein-DNA interactions, and protein conformation change by monitoring the molecule interactions with high sensitivity.

2.4.1 Selection of energy donor-acceptor pairs in FRET

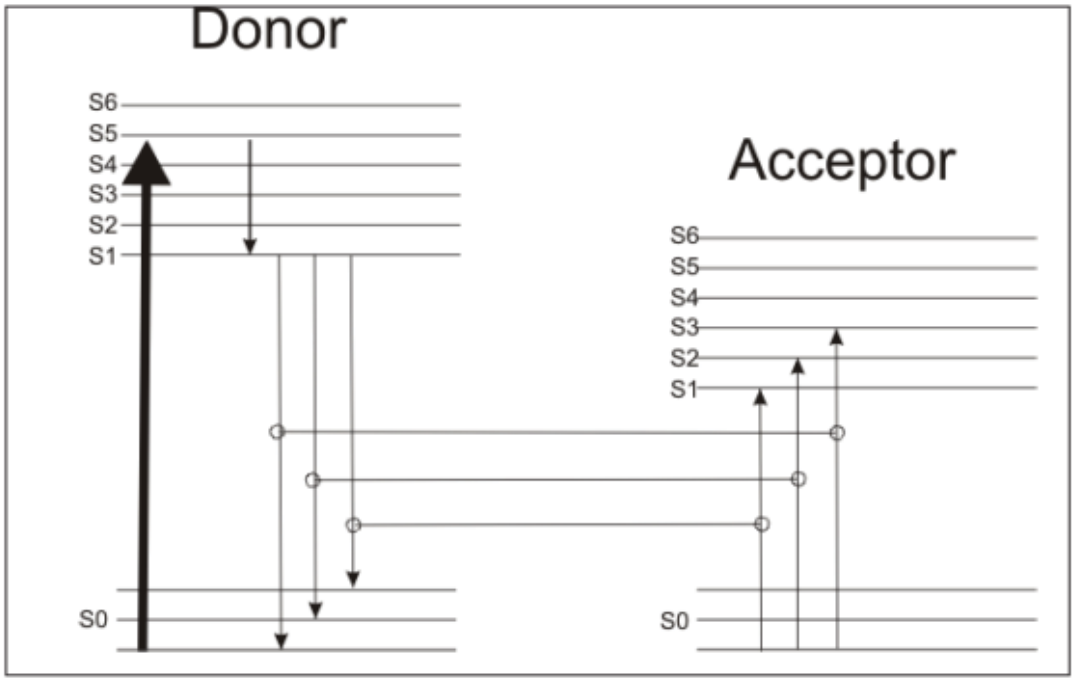

Figure II-11. Schematic diagram of electron transfer in typical FRET process (Ref. Held 2012).

FRET is a non-radiation energy transmission process from donors to acceptors. Figure II-11 illustrates the electron vibrational energy states occurring in a typical FRET process. Specifically, the electrons in the donor fluorophore jump from the ground state (S_0) to the higher energy levels under appropriate excitation. Then it quickly decays toS_1, the lowest energy level. In normal processes, the electron will finally decay back to the original ground state, while when FRET between two molecules, the process of electron decay from S_1 to S_0 compete with the process of energy transfer from donor to acceptor.

As a consequence, the electrons in acceptors are excited to higher energy states and eventually return to the ground state (Meyer and Teruel 2003).

To achieve higher efficient FRET and to be accurately detected, the energy donor and acceptor are usually designed to be different, for the sake of more obvious luminescence change. Quenching in donor or luminescence appearance or enhances are common results in a typical FRET process. As one of the main components required in the FRET, energy donor can be understood as a fluorescence molecule which transfers the energy to nearby acceptor via a non-radiative dipole-dipole coupling. The common options in donor selection are listed in Table II-3. Most common types of FRET donors

Table II-3. Most common types of FRET donors

Types of donors	Highlights	Limitations
Organic dyes	small size, large detectable optical signal, varies optical color, and simple covalent coupling strategies	Significant emission overlaps, difficult to achieve "multichannel" , mainly excited by ultraviolet light
Autofluorescent proteins	easier for intracellular loading, manipulation, and expression in live tissues	Low quantum yields and broad emission and absorbance spectra
Quantum dots (QDs)	size controllable, broad tunable absorption spectra, narrow symmetric PL spectra, high quantum yields, high photobleaching thresholds, resistance to photo and chemical degradation, and large effective "Stokes shift"	Potential cytotoxicity, intermittent emission, excited by ultraviolet light

Carbon dots	convenient synthesis, prominent biocompatibility, colorful photoluminescence, and low cost	UV excitations required
Upconversion nanoparticles (UCNPs)	photostability, low toxicity, low background interference and biocompatibility	Relatively low luminescence emission

Organic Dye

The organic dye is a type of traditional energy donor to generate FRET. Its special advantages, such as small size, large detectable optical signals, varies optical colors, and simple covalent strategies make it an excellent candidate to achieve highly efficient energy transfer (Clapp et al. 2004) due to the inherent of organic dye that it usually display narrow absorption spectra, broad emission and low photobleaching thresholds, it is difficult to apply in the multichannel platform. Specifically, when there are more than two fluorophores co-exist in the system, organic dyes tend to show significant spectra overlaps and cause problems in distinguishing the individual behaviour by donor or acceptors.

Autofluorescent Proteins

Genetically encoded fluorescent proteins have occupied a space in FRET applications. Green fluorescent proteins (GFP) is the most well-known type of this family(Pollok and Heim 1999). Their intrinsic properties of easier for intracellular loading, manipulation, and expression in living tissues guarantee the broad applications in biological related FRET assays. However, proteins usually have relatively low quantum yields, broad emission, and absorbance spectra, which limit their potential in more sensitive platforms development.

Quantum Dots (QDs)

Quantum dots are one of the new generations of luminescence materials. Colloidal QDs are synthesized through the high-temperature solution. As the lab synthesis technique getting matured, it has been more frequently employed in diversity assays attribute to its excellent performance and properties. For example, QDs are size controllable within the range of 2-10 nm, making them suitable for lots of platforms(Walling, Novak, and Shepard 2009). Also, it also possess the advantages of broad tuneable absorption spectra, large molar extinction coefficient, narrow symmetric PL spectra, high quantum yields, high photobleaching thresholds, resistance to photo and chemical degradation, and large effective "stoke shift" etc. (Murray, Norris, and Bawendi 1993; Hines and Guyot-Sionnest 1996; Clapp et al. 2004). All these properties make it a promising FRET donor candidate and broaden its applications in bioassays, such as the nanoparticles-based platforms to detect protein or DNA conformation change. For instance, Shasimsipur attached the QDs on DNA to detect the human papillomavirus 18 and achieved high sensitivity up to the nanomolar amount(Shamsipur et al. 2017). QDs can also be designed for environmental assays purpose. Abolhasani's group established a system based on QDs to quantitatively determine the copper and nickel contamination is well and dam water(Abolhasani et al. 2015). In short, the proposed detection platforms took the advantages of the QDs to use it as a FRET energy donor, and the targets can be detected by fluorescence intensity change. However, QDs are potentially cytotoxicity, photoblinking, and ultraviolet light (UV) excited, which limit their further applications in vivo, since the risks to creatures and environment are still unclear. Besides, UV as an excitation source also induces the autofluorescence and interferes the fluorescence from the analytes, which should also be considered when designing QDs based assay platforms (F. Wang et al. 2010).

Carbon Dots (Cdots)

Carbon dots or nano carbons compose the discrete, quasispherical particles with the size below 10 nm (Baker and Baker 2010), emerged as a new alternative to QDs. Cdots have

attracted explosion of interests due to its unique properties, including convenient synthesis, prominent biocompatibility, colourful photoluminescence, and relatively low cost, which enable Cdots being a strong competitor in sensing, bioimaging, nanomedicines, and energy storage. Recently, Yang's group reported a method of using Cdots to successfully establish a drug delivery system by connecting Cdots to a hairpin DNA, which loaded with doxorubicin and polyethylene glycol modified folic acid. Such a platform allowed drugs release to demand under the stimuli of targets, and fluorescence turned on by FRET relief between Cdots and doxorubicin (Yang et al. 2017). However, Cdots as the particular quantum dots-like nanoparticles, it possesses the similar drawbacks such as it requires continuous UV excitations that limit their potential applications.

Upconversion Nanoparticles (UCNPs)

Luminescence energy transfer (LRET), as a derivative of FRET, was firstly introduced by Selvin(Selvin, Rana, and Hearst 1994) to study the FRET of lanthanide chelated complexes. As it introduced before in Chapter II, UCNPs are unique luminescence materials with strengths of photostability, low toxicity and biocompatibility, minimal background interference, and controllable size, shape, and emission spectra. Till now, they have become the youngest substitution of conventional energy donor in FRET systems. In this section, some examples of UCNPs utilized in FRET will be shown here.

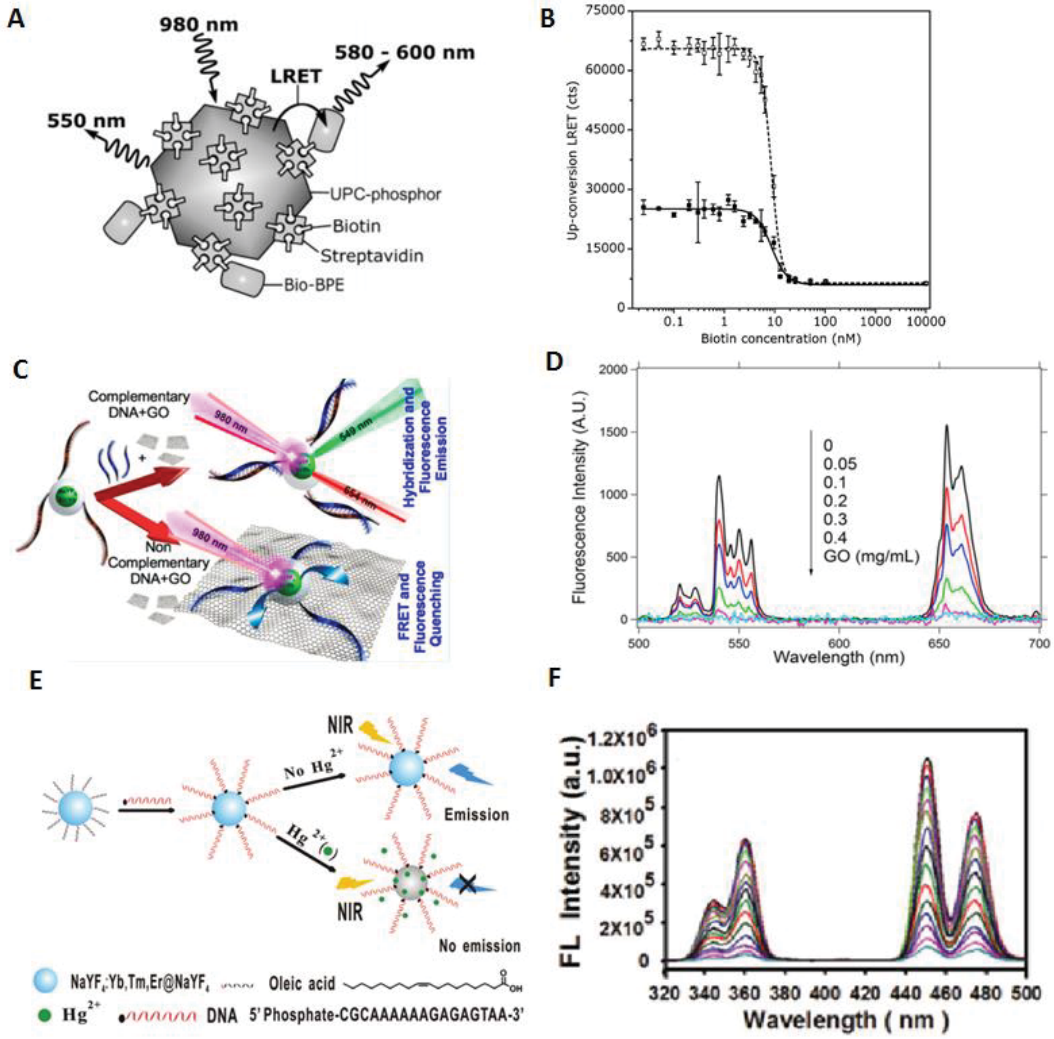

Figure II-12. Examples of LFET employing UCNPs as the energy donor in various assays.(A)(B) (Kuningas et al. 2005)(C)(D) (Alonso-Cristobal et al. 2015)(E)(F) (L.-J. Huang, Yu, and Chu 2015)

Figure II-12A shows the illustration of the mechanism of Kuningas' group innovative concept of applying UCNPs in LRET (Kuningas et al. 2005). They employed streptavidin-conjugated UCNPs as LRET donors and biotinylated phycobiliprotein as the acceptor to successfully detect the biotin. Figure II-12B gives the results obtained based on their detection system. Detection platforms based on UCNPs can also achieve DNA, protein, and metal ions detection. For instance, Alonso's team reported a target DNA detection by UCNPs and graphene oxide system (Figure II-12C). The target presence can be reported by fluorescence quenched due to energy transfer. As their results show in Figure II-12D, higher concentrations of GO result in reduced upconversion intensity

(Alonso-Cristobal et al. 2015b). Also, a sensitive, rapid and selective detection of Hg^{2+} was achieved by UCNPs based biosensor (Figure II-12E), which has high FRET efficiency and quenches the luminescence of UCNP when Hg^{2+} ions exist(Figure II-12F)(L.-J. Huang, Yu, and Chu 2015). Though UCNPs are popular in biological detection platforms, it can be even improved regarding of relatively low upconversion emission efficiency. The strategies to overcome these drawback are proposed, such as synthesize the core-shell structure, conduct surface modifications, and introduce the metal to increase the luminescence intensity.

Distinct from the donor who donates the energy, acceptor acts as the energy absorbance part which will eventually emit the photons. Just as there are numerous types of donors, there are many types of acceptors. In the LRET process, a limitation of fluorophores is that they have a relatively short lifetime, which limits the opportunities and accuracy of emission measurement. In this case, autofluorescence involves in emissions can even interfere with the results. Therefore, although emissive fluorophores can be used as donor or acceptors, the “dark” quenching dye is preferred and can only be designed as an acceptor. As demonstrated in the above section, fluorescent dyes and proteins can be designed as acceptor as long as they are in proximity with the donor and have adequate spectral overlaps for efficient energy transfer. The first “quencher” dye used in FRET is azobenzene, dabcyl. It has a broad absorbance centred at around 478 nm to quench the blue to green fluorescence region (Marras et al. 2002; Seidel, Schulz, and Sauer 1996).

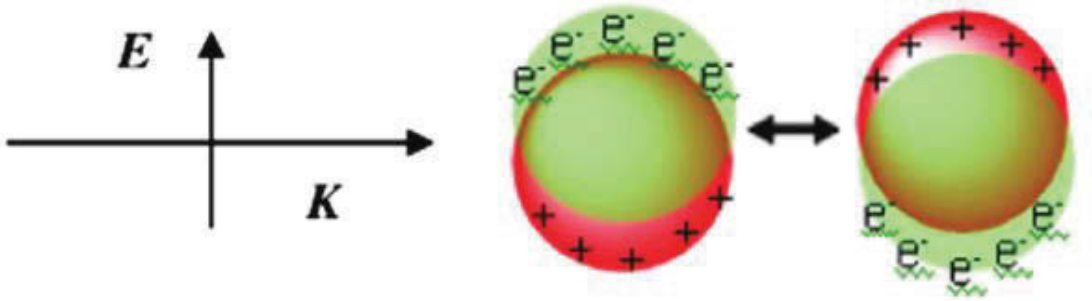

Figure II-13. Schematic illustration of AuNPs surface Plasmon resonance (SPR) (Ref： X. Huang and El-Sayed 2010).

Some metal nanoparticles can be included in consideration as well. For example, gold nanoparticles (AuNPs) has been broadly applied in FRET and play the role of acceptor attributed to its unique optical properties. The oscillation of free electrons on AuNPs surface induces a charge separation on the ionic lattice, producing a dipole oscillation under a specific light (Figure II-13). Light absorption and light scattering are two main contributions for total light extinction (X. Huang and El-Sayed 2010). Due to SPR oscillation, the absorption and scattering can be strongly enhanced by 5-6 order of magnitude compared with the other organic dye, and displays higher emission of most fluorescent molecules(Jain et al. 2006). Therefore, equipped with strongly enhanced radiative properties of adjacent molecules, and its biocompatibility, AuNPs are extremely helpful in optical and biological applications, such as cell imaging and proper therapies.

2.4.2 Design strategies for UCNPs based LRET detections

Multiple ways are available to monitor the interactions and distance change between two complexes in LRET system. The design principle is based on the different energy transfer efficiencies of luminescence nanocrystals before and after the targets.

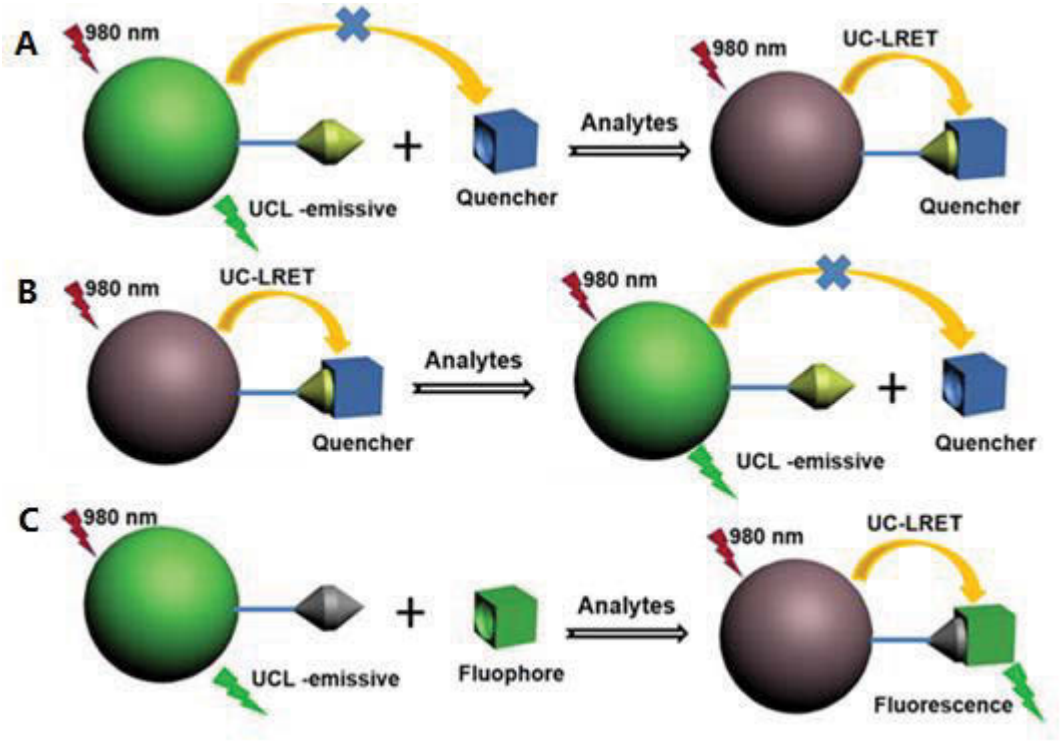

Figure II-14. Schematic illustration of LRET system based on distance change between donor-acceptor pairs. (Ref: J. Zhou et al., 2015)

As mentioned previously, adequate proximity and spectrum overlap between two complexed is a priority to achieve FRET. Same, LRET can only occur based on these two requirements. In UCNP LRET system, spectrum overlap can be controlled via selection of donor and acceptor, while LRET efficiency is largely dependent on distance. Therefore, distance change between donor and acceptor is utilized to construct an LRET detection platform. Usually, a linker bond to energy donor is used to respond to target stimuli, which will bring the change in distance, and achieve difference LRET efficiency change (Figure IV-1). Typically, LRET can be analysed through the frequently applied methods: intensity variations of the acceptor and donor emissions, photobleaching rate of the donor in presence and absence of targets, and fluorescence-lifetime change as well.

Chapter III. Systematic Hydrophilic Surface Modification of UCNPs

3.1 Introduction

The macromolecule is large molecule created by polymerization of smaller monomers. The well-known examples of macromolecules in biopolymers are nucleic acids, proteins, and lipids. The polymer is a type of macromolecules constituted of repeated subunits. Both natures existed, or synthesized polymers are produced by polymerization of small molecules and therefore possess sizeable molecular mass. Importantly, polymers naturally exhibit or can be modified with multiple anchoring ligands, such as hydroxyl, amine, carboxylic, phosphate, and thiol groups etc. Therefore, varies polymers have been used in UCNPs surface modification to render them a hydrophilic surface.

Some commercially available polymers are used during the UCNPs synthesis process to directly produce hydrophilic UNCPs. For instance, polyethylenimine (PEI), poly(acrylic acid) (PAA), and polyvinylpyrrolidone (PVP). However, water-soluble UCNPs synthesised by this method suffers poor stability and tends to aggregate(M. Wang et al. 2009). In contrast, the ligand exchange and amphiphilic coating strategies can create much more stable and monodispersed UCNPs in aqueous solution. Although a lot of polymers have been successfully applied in functionalized nanocrystals, a systematic study of four common polymers will be demonstrated here with a simple one-step ligand exchange strategy to provide a comparison regarding dispersity, luminescence ability, and colloidal stability of lab-synthesized UCNPs. Therefore, this study can be useful in choosing the most appropriate polymer to functionalize nanocrystals for a specific purpose. In this section, the most popular and widely used polymers have been examined, including PEI, PAA, PVP, and POEGA-b-PMAEP(PEG).

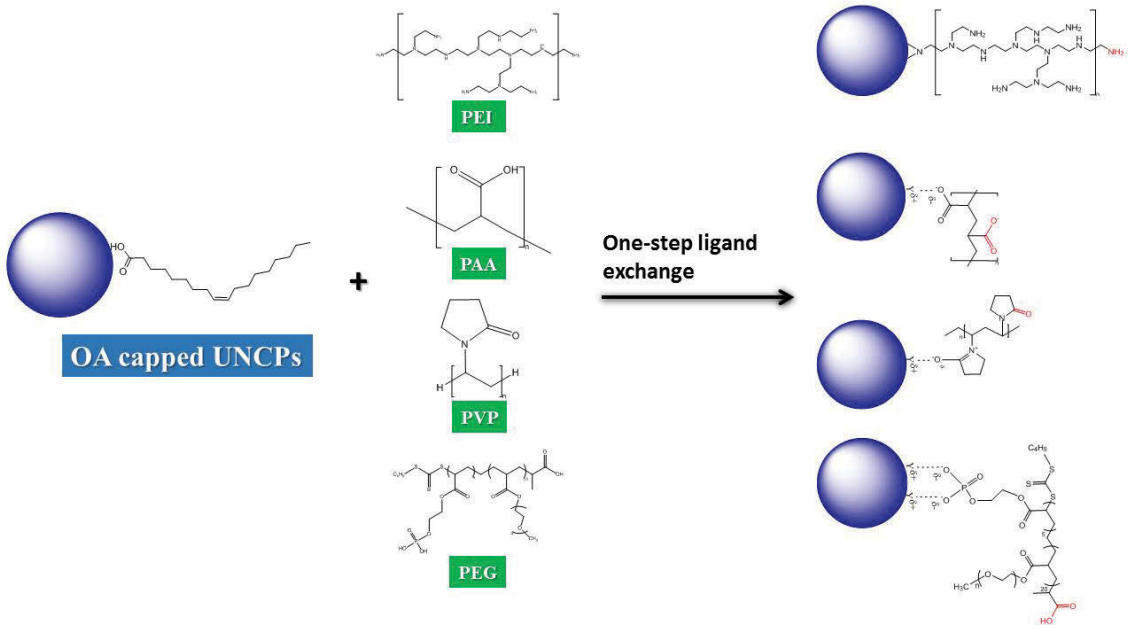

Figure III-1. Reaction mechanisms of four typical polymers used in UCNPs ligand exchange.

Polymers employed in UCNPs surface modification via one-step ligand exchange have two main groups: bonding groups and functional groups. Since original UCNPs are usually capped by oleic acid, bonding groups that possess higher binding affinity than oleic acid are essential to substitute the original ligands on UCNPs surface and render the nanocrystal hydrophilic ligands. Functional groups, such as NH_2, COOH, SH, and N_3 etc., guarantee the ability that hydrophilic UCNPs can be subsequently conjugated to other molecules for diverse application purposes. PEI used in this section is branched type, which contains primary, secondary and tertiary amino groups. It has many applications in biology, attachment, water treatment, and cosmetic etc. PAA is a high molecular weight polymer with the monomer of acrylic acid. It displays negative charge in neutral solution, and ideally used as surfactants due to the ability to form hydrogen-bonded complexed in low pH environment, and its –COOH groups are useful in bio-applications. PVP is polymerized from its monomer N-vinylpyrrolidone. It has been widely used in pharmaceutical, cosmetics, blood compatibilizer, and surface modification agent due to its good compatibility with numerous chemicals. PEG polymer is synthesized by RAFT polymerization. It contains a binding group, a phosphate group, which have strong binding affinity to rare earth ions. Besides, UCNPs, after coated by PEG possess a layer

of polymer with –COOH group facing outward, which offers an opportunity for as-synthesized UCNPs broadly used in subsequent attachment to proteins, DNA, and bioactive molecules.

3.2 Experimental

Materials and Chemicals

All the chemicals were obtained from Sigma Aldrich (Sydney) with reagent grade or higher. Branched PEI, PAA and PVP with an average molecular weight of 25,000 g mol^{-1} by LS, 1800 g mol^{-1}, and 40,000g mol^{-1}, respectively, were used as received. All materials, cyclohexane, chloroform, ethanol and tetrahydrofuran (THF) were used as received without further purification, except 2, 2'azobisisbutyronitrile for PEG polymer synthesis, which was purified through recrystallization from methanol.

Instrumentation and Apparatus

The synthesized UCNPs were characterized by D8 Discover diffractometer (Bruker Corporation) Powder X-ray diffraction (XRD) and FEI-Tecnai T20 instrument to analyze the size and morphology of nanoparticles. Fourier-transform infrared spectroscopy (FTIR) spectra tests were carried out using a Nicolet 6700 FT-IR spectrometer (Thermo Scientific) to determine the surface ligands. Dynamic light scattering (DLS) was run using Zetasizer nano series (Malvern Instrument) to test the hydrodynamic size of nanoparticles. Thermogravimetric analysis (TGA) was carried out on a Simultaneous TG-DTA instrument S600 with a heating program consisting of a heating rate of 10 K/min from 373.15K to 923.15 K under N_2. Upconversion luminescence intensity spectra were measured by an iHR550 spectrometer (HORIBA Scientific Instruments Inc.) with a modified external 980nm laser. The excitation irradiance value was up to 1.36×10^6 W cm^{-2}.

Synthesis of $NaYF_4$: Yb, Er UCNPs

UCNPs used in this project were doped by 20% Yb and 2% Er by traditional co-precipitation method [2]. Specifically, 1 *mmol* $LnCl_3$ (Ln=Y, Yb, Er) with the molar ratio of 78:20:2 were reacted with 6 *mL* of oleic acid (OA) and 15 *mL* 1-octadecene. Then, the solution was heated up to 160 $℃$ under continuous argon gas for 30 *min*. The clear solution was obtained and cooled down to the room temperature, followed by the addition of 5 *mL* methanol solution of 4 mmol NH_4F and 2.5 *mmo*l NaOH. After continuous stirring for 30 *min*, methanol was evaporated under 100 $℃$ for 20 *min*, and water was removed under 120 $℃$ for another 20 *min*. The reaction was finalized by further heating the solution at 300 $℃$ for 90 *min*. The nanocrystals were precipitated by centrifuge at 13,000 *rpm* and washed with cyclohexane, ethanol, and methanol, respectively. The synthesized products, dispersed in cyclohexane, were well-monodispersed.

Surface modifications via one-step ligand exchange

To synthesize UCNPs@PAA, wash the UCNPs by chloroform and resuspended in chloroform. Then 1 mg UCNPs in chloroform were mixed with same volume of the 10 mg PAA dispersed in ethanol. The mixture was stirred overnight. Then centrifuged the mixture at 14680 *rpm* and disposed of the supernatant. Using water and ethanol mixed solution to wash the product three times, and then dispense the UCNPs@PAA in 1 mL water and stored in 4 ℃ fridges for further usage. The UCNPs@PEI and UCNPs@PVP were conducted with the same procedure.

To synthesize UCNPs@PEG, we prepared the PEG polymer according to the reported method(Duong et al. 2018). Specifically, the copolymer was synthesized by using poly(ethylene glycol) methyl ether acrylate as a macro-RAFT agent for chain development with mono(2-acryloyloxyethyl) phosphate (MAEP) to form a copolymer, POEGA-b-PMAEP, or PEG in short. Then, the amphiphilic solvent THF was used as the processing solvent for preparing UCNPs@PEG. Specifically, 10 mg UCNPs were

centrifuged at 14680 *rpm* to get rid of the cyclohexane. Then mixed 5 mg PEG and 10 mg UCNPs in THF and stirring overnight. THF and water mixture was used to wash the sample three times to remove the excess unreacted PEG. The final product, UCNPs@PEG were dispensed in 1 mL water with the concentration of 10 mg/mL and stored in 4 ℃ fridges for further usage.

3.3 Results and Discussion

Many surface modifications are essential and important to render a hydrophilic surface for UCNPs in terms of the colloidal stability and a specific functional surface purposes. In this section, we employed the four popular polymers to do surface modification via a simple one-step ligand exchange process. Figure III-1 simply illustrated the four polymers utilized to replace the original OA capped UCNPs. To evaluate the behaviour of these modified water-soluble UCNPs, various techniques were carried out to compare the stability, dispensability, and binding strengths of polymers, which provided a useful guideline for polymers coated UCNPs in a large range of bio-applications.

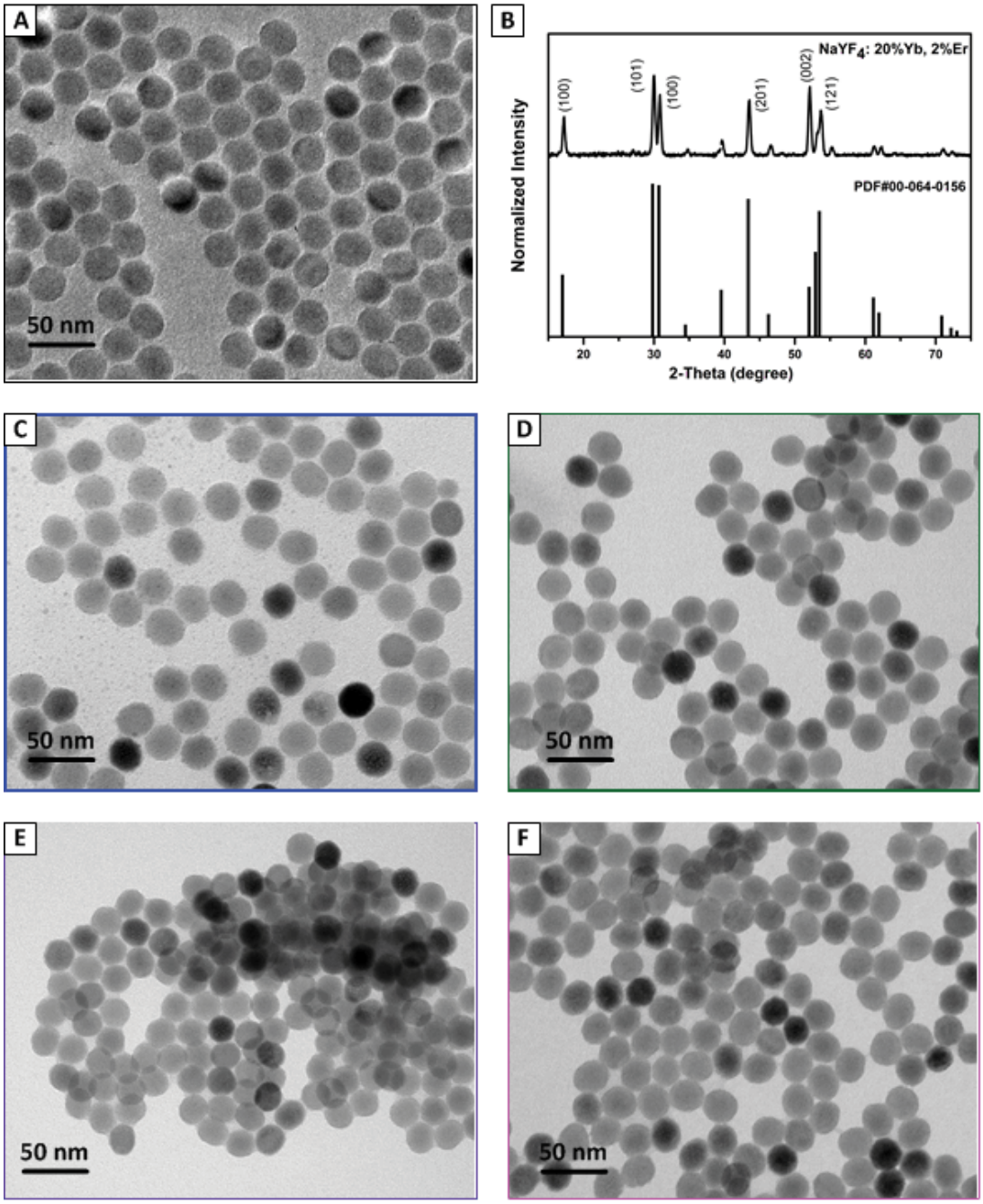

Figure III-2. TEM images of OA-capped UCNPs and four polymers anchored UCNPs and XRD of $NaYF_4$: Yb/Er. A)UCNPs@OA; B) XRD of UCNPs; C) UCNPs@PEG; D) UCNPs@PEI; E)UCNPs@PAA;F)UCNPs@PVP.

$NaYF_4$: Yb/Er nanoparticles capped by oleic acid (UCNP@OA) used in this work were synthesized via a user-friendly method. Oleic acid was used as a capping agent to control the growth of nanoparticles and prevent the aggregation. The XRD result (Figure III-2. b) of UCNPs revealed a $\beta-$ phase of as-prepared UCNPs. TEM images of UCNP@OA showed a monodispersed nanoparticles in cyclohexane with a uniform size of around 25

nm (Figure III-2.a). Figure III-2(c-f) are TEM images of UCNPs grafted by four different polymers in water after proposed ligand exchange method. The results proved that the ligand exchange process does not affect the UCNPs morphology and still maintains good dispensability, except the UCNPs@PAA had a slight aggregation due to the comparably large surface charge.

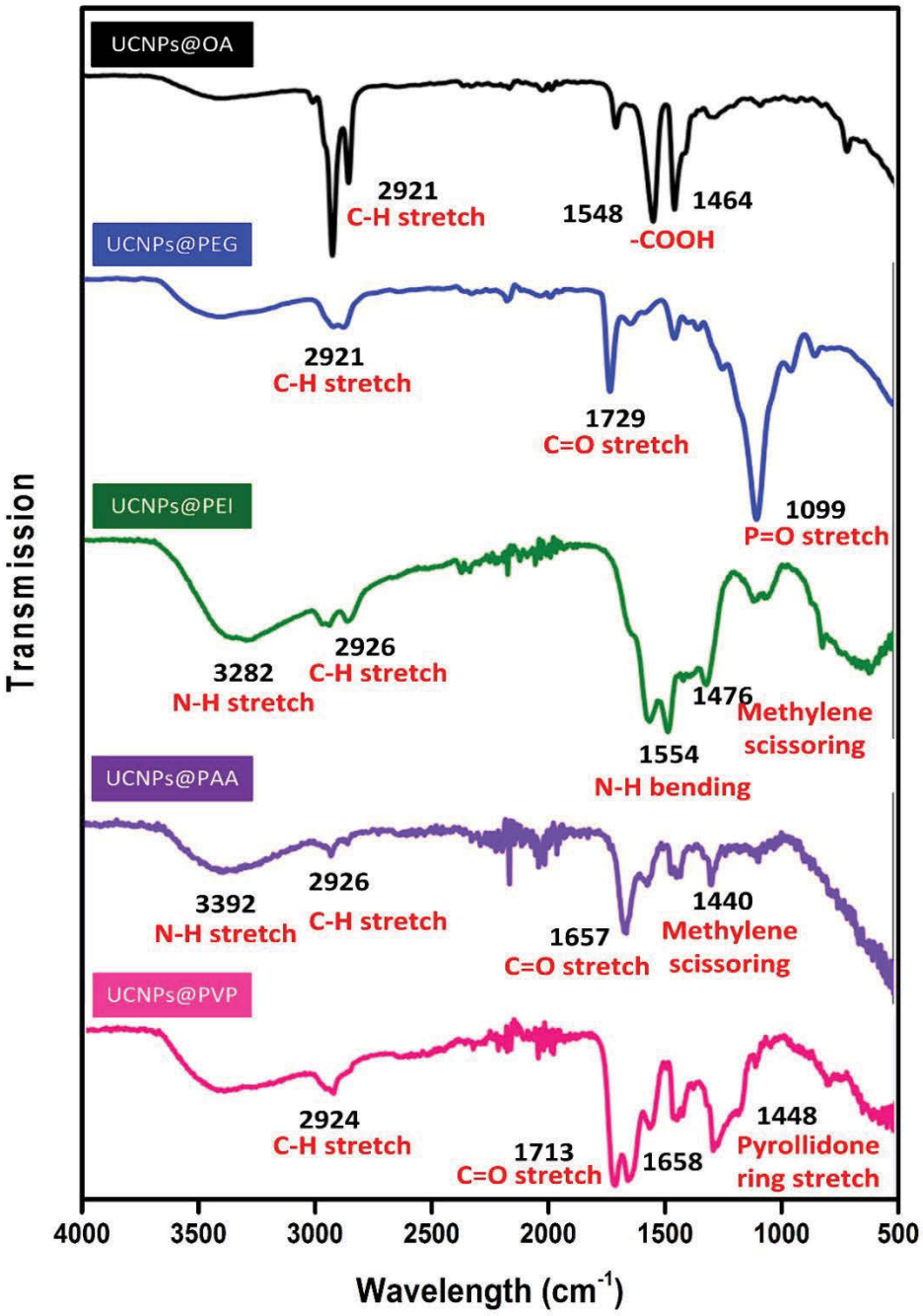

Figure III-3. FTIR spectra of UCNPs@OA and UCNPs@polymers.

Figure III-3, The as-prepared UCNPs were originally capped by OA, which exhibit strong transmission bands at 2921 cm^{-1} and 2854 cm^{-1} which corresponding to the asymmetric and symmetric stretching of methylene($-CH_2$), respectively, caused by long-chain alkyl from OA. The bands appear at 1548 cm^{-1} , and 1464 cm^{-1} are assigned to the carboxylic group (-COO-). These results proved that the lab synthesized UCNPs were capped in OA molecules and surface modification is required prior to further bio-applications. After

ligand exchange by PEG, new peaks at 1729 cm^{-1} and 1099 cm^{-1} shown up correspond to C=O and P=O vibration stretches; After ligand exchange PEI, the new bands centered at around 1554 cm^{-1} and 1476 cm^{-1} could be assigned to amine N-H stretching and methylene scissoring; After PAA coating, the bands at around 1657 $cm^{-1}$and 1440cm^{-1} suggested appearances of C=O stretching and methylene scissoring; And after PVP ligand exchange, typical bands of 1658cm^{-1} and 1448cm^{-1} represented the increasing quantities of C=O and pyrollidone stretching; Furthermore, all UCNPs@polymers had an inconspicuous peaks of around 2926cm^{-1} compared with UNCPs@OA, which indicated that the polymers had replaced of OA molecules and attached to UCNPs surface.

Table III-1. TGA results for UCNPs@OA and UCNPs@polymer

	Weight loss (wt%)	Grafting density (molecules/nm^2)
UNCPs@OA	23.20%	5.13
UCNPs@PEG	12.23%	0.12
UCNPs@PEI	22.03%	0.71
UCNPs@PAA	9.43%	0.74
UCNPs@PVP	8.25%	0.04

To quantitatively confirm the substitution of polymers on UCNPs surface, thermogravimetric analysis (TGA) was performed. The weight loss percentage and grafting density are shown in Table III-1. Grafting density was calculated by assuming a spherical UCNPs with a diameter of 24 nm and bulk density is 4.2 g cm^{-3}. The grafting density of polymer coated densities was less than original ligand capped UCNPs. This is a predictable result as the OA molecules are 30 times lower than polymers in terms of

molecular weight. The higher weight loss of PEI grafted UCNPs may due to the water consisted of nature. And compared with UCNPs@PEG, UCNPs@PAA and UCNPs@PVP also exhibited higher weight loss, this could be attributed to the remaining OA due to incomplete ligand exchange. Moreover, as shown in Figure III-4, most of weight loss of UCNPs@OA was before 400℃, while after ligand exchange with polymers, UCNPs@PEG, UCNPs@PAA, and UCNPs@PVP not experienced similar weight loss before 400℃ and exhibited a stable state after 500℃. This is a clue that the OA has been substituted and new ligands are presented. UCNPs@PEI experienced a dramatically weight loss in the whole heating process, this is due to the branched PEI polymers are gel-like substance and rich in water molecules. Table III-1. TGA results for UCNPs@OA and UCNPs@polymer.

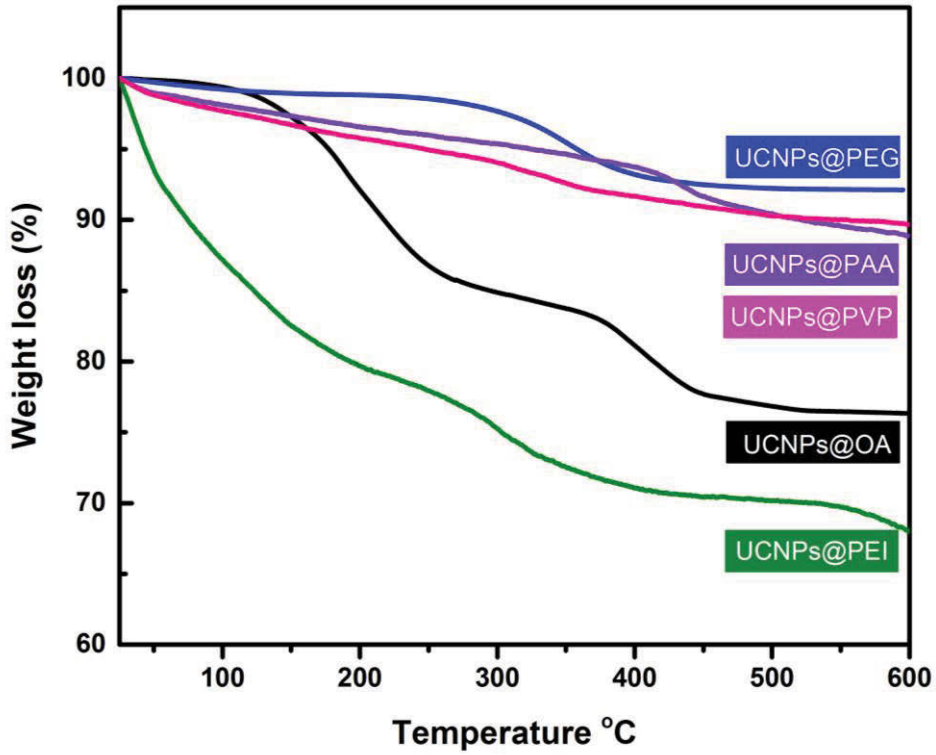

Figure III-4.TGA results for UCNPs@OA and UCNPs@polymers.

DLS data were collected to test the hydraulic diameter of each nanoparticle. The UCNPs@OA has a narrow size distribution of 28.21 nm in cyclohexane. After polymer surface modifications, the UCNPs@ polymers show a little bit sizes increase in water ($pH = 5.4$) to 50.39 nm, 46.02 nm, and 50.04 nm of PEG, PEI, PAA, and PVP coatings,

respectively. Polydispersity Index (PDI) < 0.3 for all results. However, some aggregates of UCNPs@PAA also occurs in water due to the largest standard deviation, but just not shown in the fitting curve. In this case, the results obtained by TEM and DLS are in agreement.

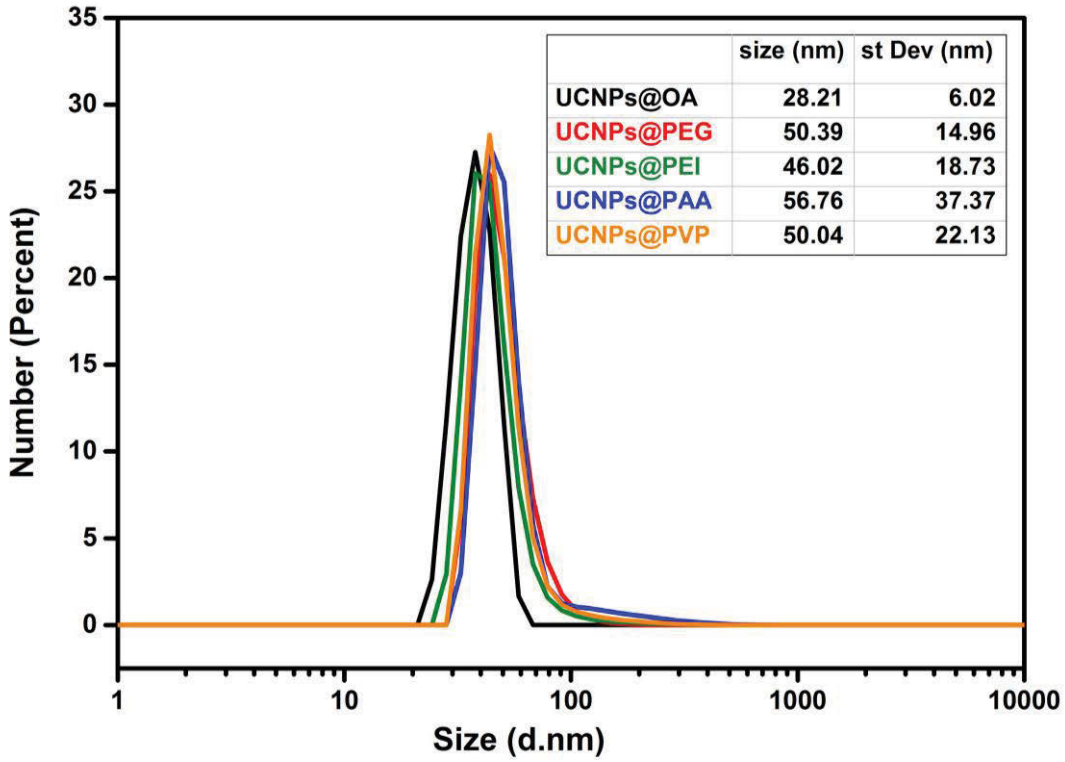

Figure III-5.DLS data of OA capped UCNPs and four polymers coated UCNPs in water by one-step ligand exchange.

To investigate the long-term colloidal stability of UCNPs@polymers, continuous DLS data were collected over one week period. Referring to Figure III-6, UCNPs@PEG exhibits a uniform size over one week time without significant changes. In comparison, UCNPs@PEI, UCNPs@PAA, and UCNPs@PVP have different degrees of aggregation with longer time storing.

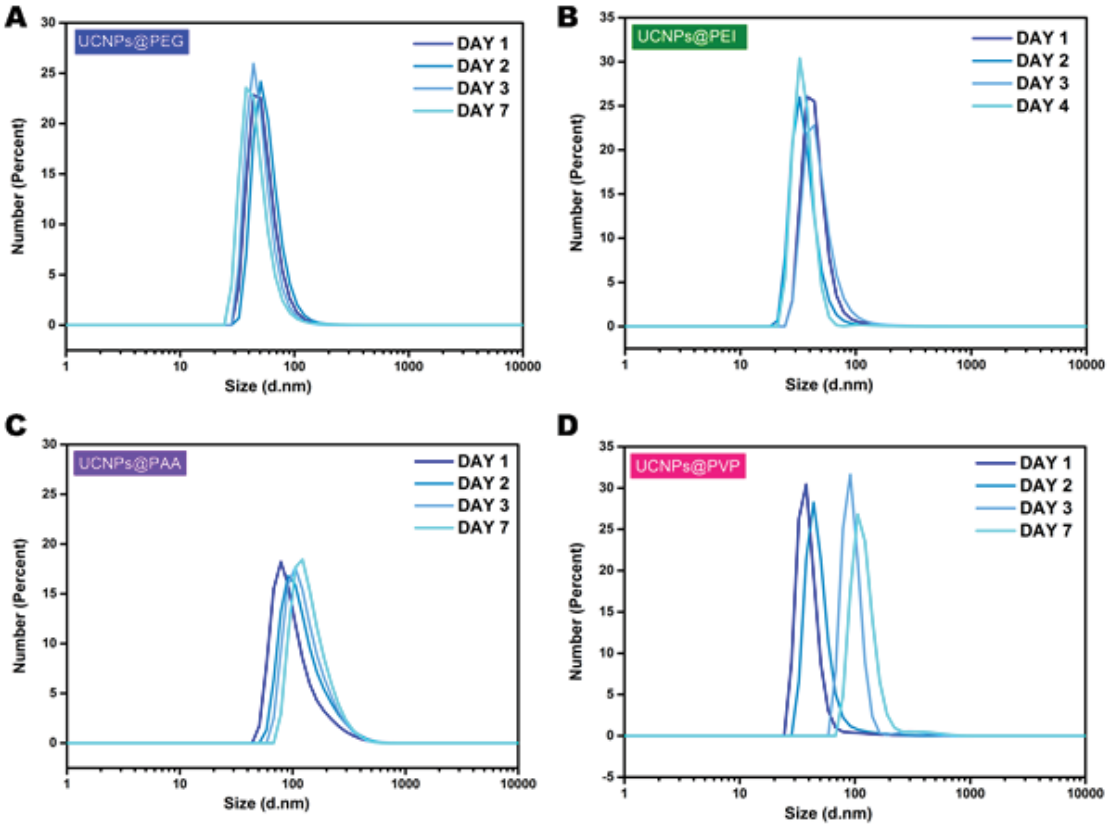

Figure III-6.Colloidal stability of (A)UCNPs@PEG, (B)UCNPs@PEI, (C) UCNPs@PAA, and (D)UCNPs@PVP over one-week storage measured by DLS.

Buffers selection is a preliminary step in many biological and chemical assays, which plays an essential role throughout the experiment and homogeneous system. Various buffers are available with different pH for specific experiment purposes. For example, MES is a conventional buffer broadly used in biochemistry with the merits of minimal salt effects, chemically stable, and minimal absorption under visible or UV spectra(Ferguson et al. 1980). HEPES buffer is another buffering agent widely used in cell culturing attribute to its better ability to maintain physiological pH, as well as the enzyme structure, which do not change much with temperature(Baicu and Taylor 2002). Therefore, a systematic comparative study of UCNPs@polymers stability in four different common buffers (MES buffer, HEPES buffer, SSC buffer, and Tris Buffer with the pH value of 5.1, 5.6, 7.0, and 7.6, respectively) was carried out for a potential guideline in surface modifications and buffer selections.

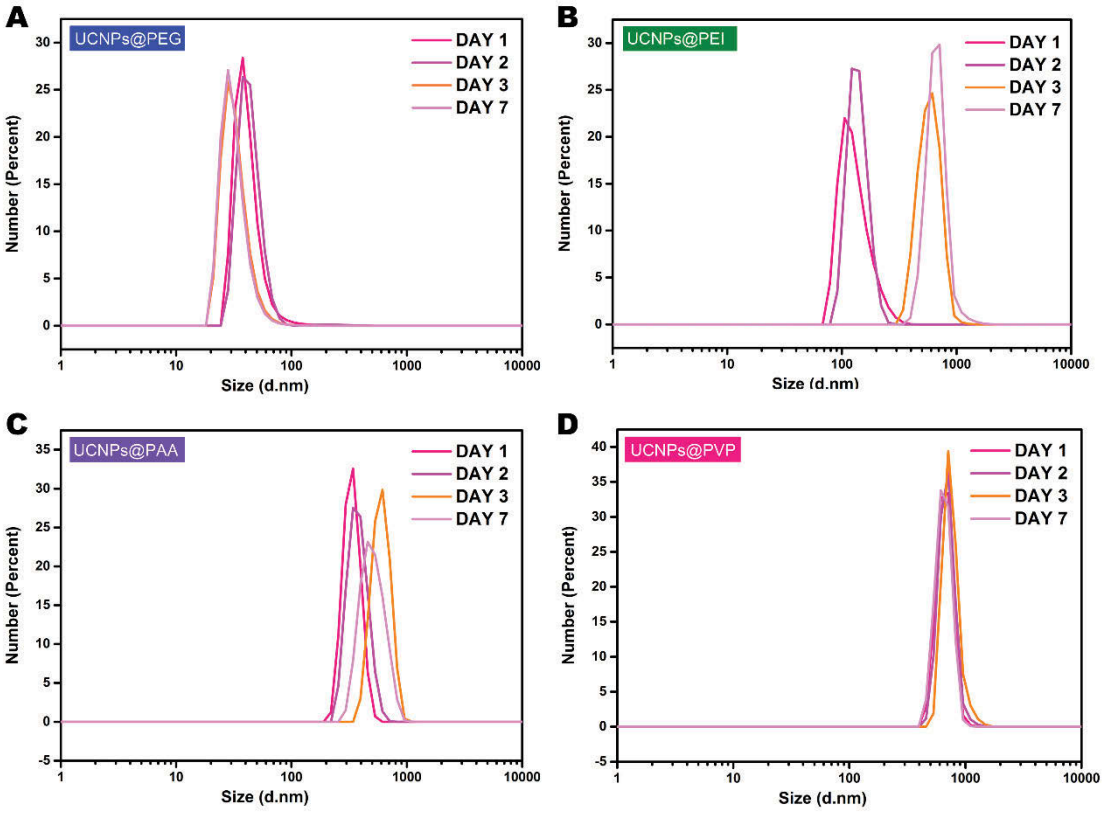

Figure III-7.Colloidal stability of (A)UCNPs@PEG, (B)UCNPs@PEI, (C) UCNPs@PAA, and (D)UCNPs@PVP over one-week storage in MES buffer measured by DLS.

Size distribution of UCNPs@polymers was tested over one week period in MES buffer (pH 5.1). The result (Figure III-7) shows that UCNPs@PEG has good dispensability of around 43.31 nm, and still keep the uniform hydraulic diameter of approximately 41.85 nm over one week. Although UCNPs@PVP stables at around 600 nm in one-week time, it heavily aggregated in MES buffer. Incomparable, UCNPs@PEI and UCNPs@PAA distribute both poor dispensability and stability, roughly varying sizes from 100 nm to 800 nm.

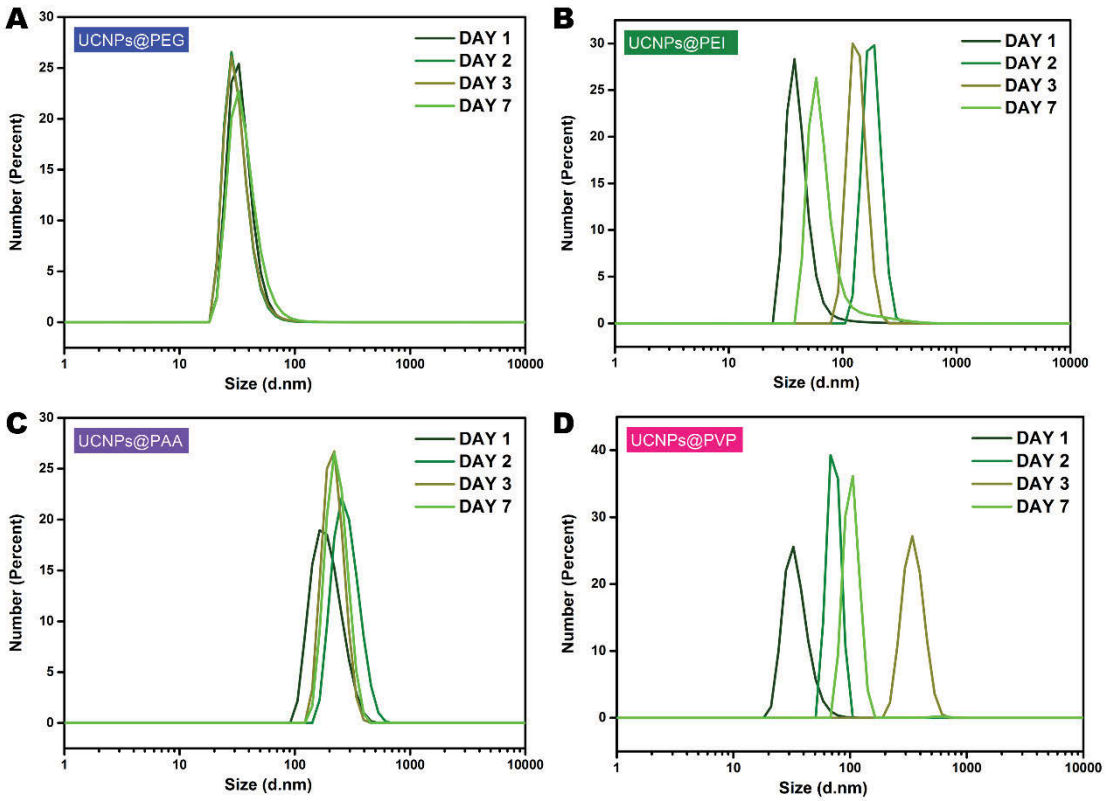

Figure III-8.Colloidal stability of (A)UCNPs@PEG, (B)UCNPs@PEI, (C)UCNPs@PAA, and (D)UCNPs@PVP over one-week storage in HEPES buffer measured by DLS.

Similar, UCNPs@polymers in HEPES buffer (pH 6.5, 0.1 M) were tested again over one week (Figure III-7). UCNPs@PEG again shows excellent dispensability of around 34.4 nm and good stability with a slight size increase to 36.78nm. UCNPs@PEI and UCNPs@PVP show good dispensability on the first-day testing, with the size of 42.35 nm, and 32.12 nm respectively, while both of them aggregate afterwards. In contrast, UCNPs@PAA aggregates in HEPES with poor stability while relatively stable over one week, which suggests UCNPs@PAA can be used when the stability is more critical than dispensability and PEI and PVP coated UCNPs should be freshly prepared prior to each experiment.

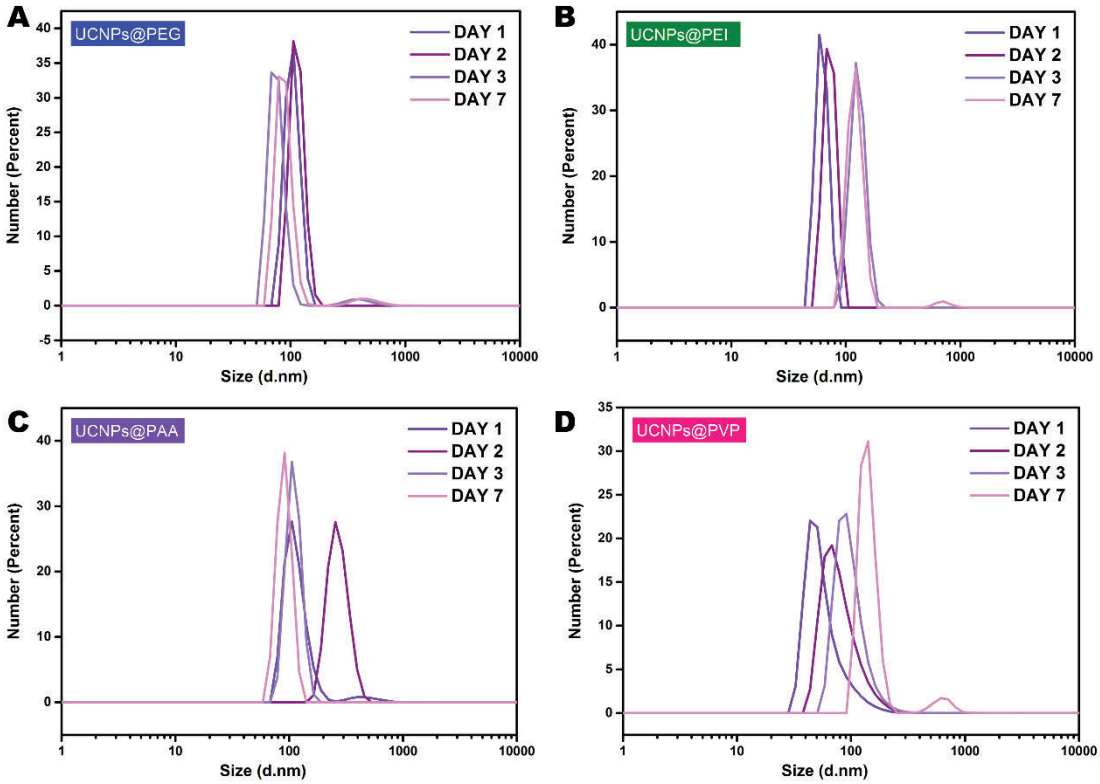

Figure III-9.Colloidal stability of (A)UCNPs@PEG, (B)UCNPs@PEI, (C)UCNPs@PAA, and (D)UCNPs@PVP over one-week storage in SSC buffer measured by DLS.

SSC buffer (pH 7.0) is generally used as a molecular hybridization buffer (Figure III-9). UCNPs@polymers size distribution was tested as well. According to the results, all samples were unstable from slightly to severely aggregation over long time storage. Besides, only the UCNPs@PVP well-dispensed on the first day, others UCNPs grafted by other polymers displayed relatively poor dispensability. The results suggest that when the analysed media is chosen to be SSC buffer, the freshly prepared UCNPs@polymers should be used to prevent aggregation.

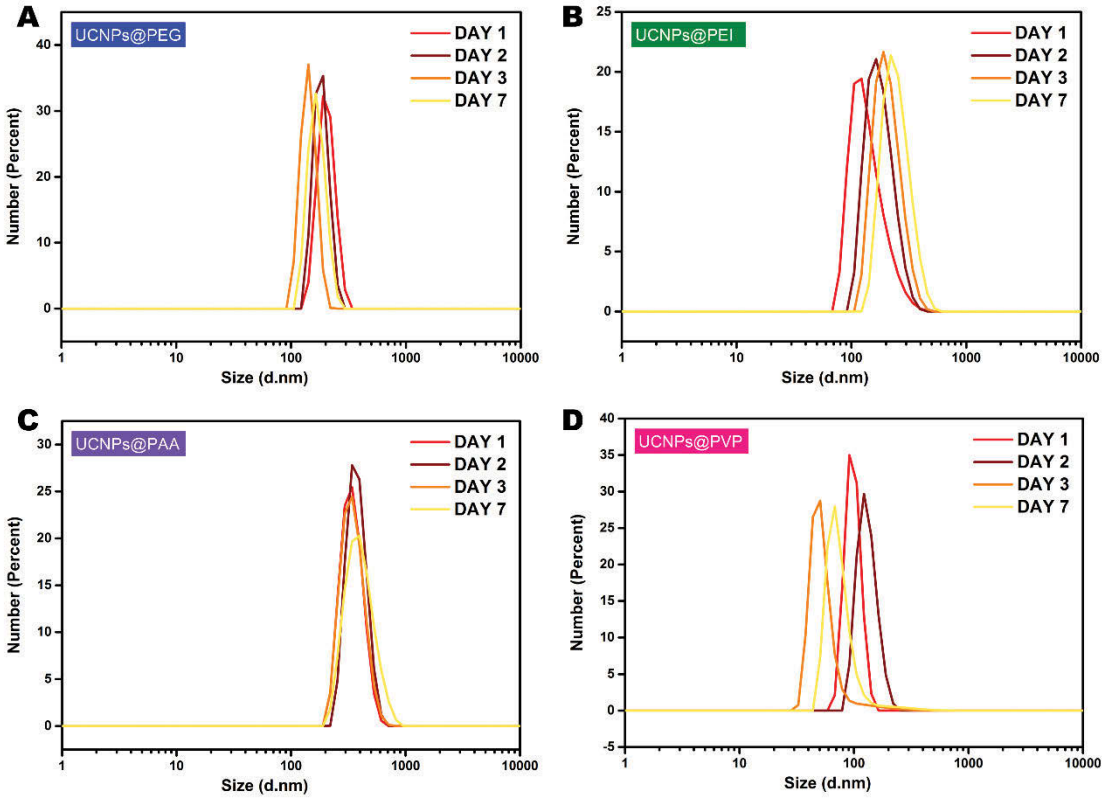

Figure III-10.Colloidal stability of (A)UCNPs@PEG, (B)UCNPs@PEI, (C)UCNPs@PAA, and (D)UCNPs@PVP over one-week storage in Tris buffer measured by DLS.

Tris Buffer (pH 7.6) is typical media choice for most biological systems, especially in DNA electrophoresis and western blotting, because it is an active and robust buffer in the range of pH 7-9. Therefore, similar DLS test was conducted based on four polymers coated UCNPs (Figure III-10). Over consecutive one week of testing, all of the UCNPs@polymers showed good stability without significant size variation except the UCNPs@PVP. However, only the UCNPs@PVP displayed relatively good dispensability while the rest of UCNPs@polymers tended to aggregate over 100 nm.

The size variation of UCNPs@polymers or colloidal stability is mostly associate with the surface charge, which can be analysed via a powerful technique, zeta potential. In the biological environment, charged cationic substance tends to absorb on proteins' surface and also quickly to occur precipitant(Honary and Zahir 2013). However, on the other hand, some studies also reported that the negative charged spherical particles could benefit in vitro uptake due to the nonspecific interactions(Ayala et al. 2013), and they

could also be recognized by cationic sites(Rigotti, Acton, and Krieger 1995). The positively charged surface has proven to possess many advantages such as it can prolong the drug release in internal tissue due to the electrostatic interaction. However, cationic charge is complained to exhibit cytotoxic in some cases(Liu et al. 2007). Therefore, a zeta potential value that combines electrostatic and steric stabilization is preferable. In contrast, UCNPs@PAA, UCNPs@PVP，and UCNPs@PEG were observed to have negatively charged surface and had different extent of stability in buffers. UCNPs@PAA with the most considerable absolute zeta potential value, -13.3 mA, was stable in more basic buffers. UCNPs@PVP could be well suspended in almost all kinds of buffers while hard to maintain its stability. Among all the test, UCNPs@PEG with the smallest absolute zeta potential value, -4.96 mV, exhibit the best dispersity in almost all buffers, as well as the colloidal stability

Table III-2 summarizes the surface charge of four polymers with different functional groups capped UCNPs. The results show that only the UCNPs@PEI, displayed a positive charge in water (pH 5.4) and was unstable in lower pH buffers.

In contrast, UCNPs@PAA, UCNPs@PVP，and UCNPs@PEG were observed to have negatively charged surface and had different extent of stability in buffers. UCNPs@PAA with the most considerable absolute zeta potential value, -13.3 mA, was stable in more basic buffers. UCNPs@PVP could be well suspended in almost all kinds of buffers while hard to maintain its stability. Among all the test, UCNPs@PEG with the smallest absolute zeta potential value, -4.96 mV, exhibit the best dispersity in almost all buffers, as well as the colloidal stability

Table III-2. Zeta Potential of UCNPs@PEG, UCNPs@PEI, UCNPs@PAA, and UCNPs@PVP

	Surface Ligands	Zeta Potential (mA)
UCNPs@PEG	Carboxyl	-4.96
UCNPs@PEI	Amino	+12.7
UCNPs@PAA	Carboxyl	-13.3
UCNPs@PVP	Amide	-9.34

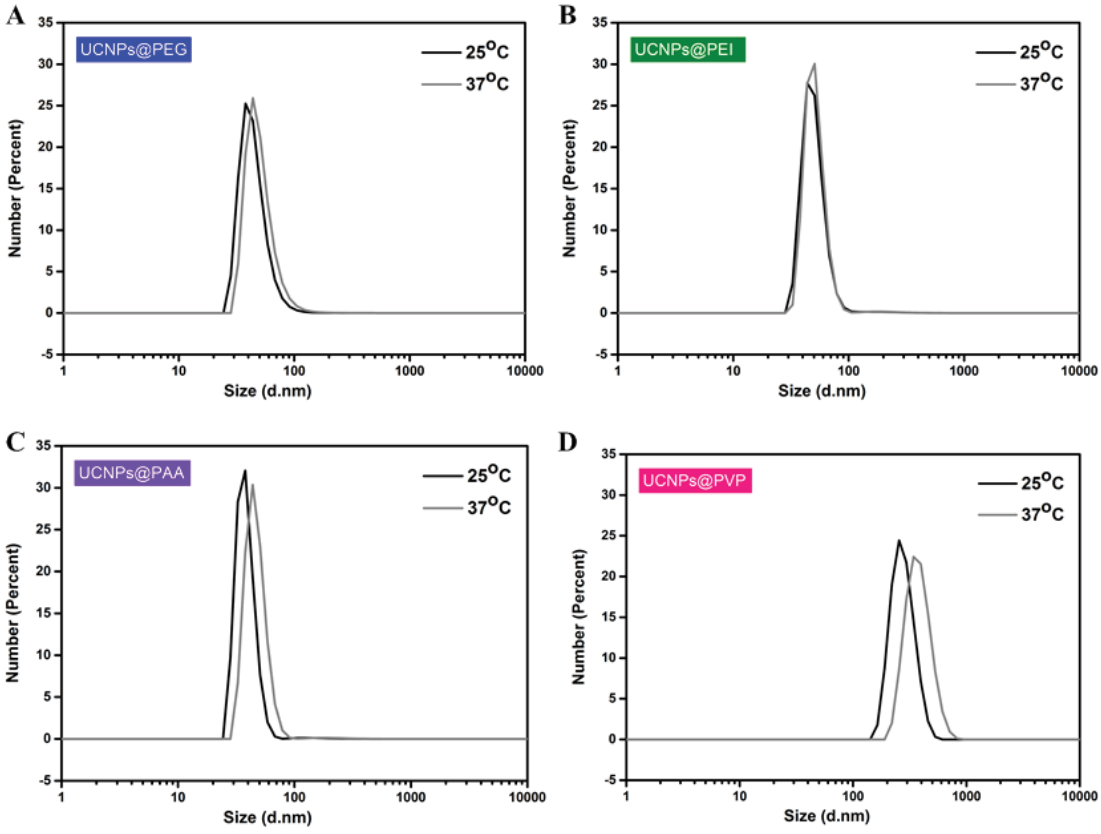

Figure III-11. Size distribution of UCNPs@polymers in different temperatures.

To further evaluate the performance of nanoparticles in vivo, the temperature dependence of size distribution was tested again in Figure III-11. Since the average temperature of the biological tissue is 37℃, the DLS data were measured both under room temperature 25℃ and 37℃. The results proved that the UCNPs@PEG, UCNPs@PEI, UCNPs@PAA were all acquired a stable and well dispense ability in both rooms and in vivo temperatures,

while UCNPs@PVP tended to create precipitate under 37℃. Therefore, both PEG, PEI and PAA polymers could be utilized in biological creatures internally, such as drug delivery, cell images, photodynamic therapy, etc.

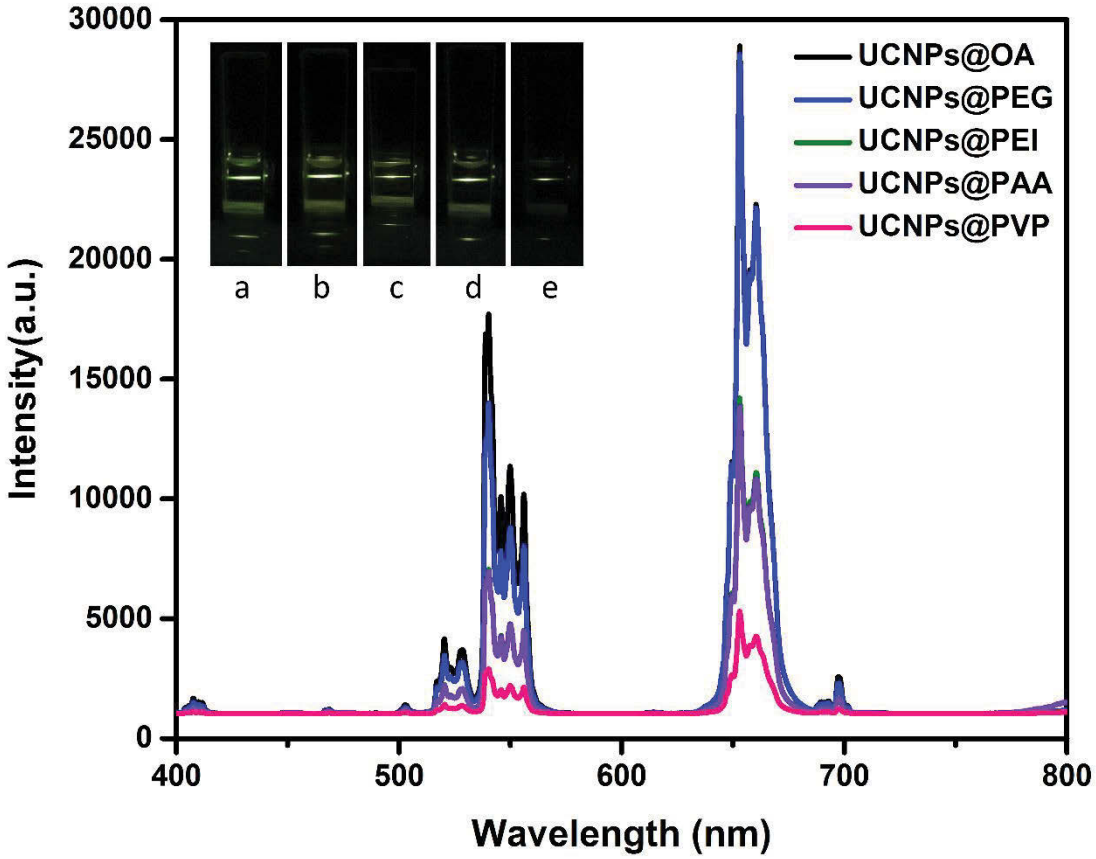

Figure III-12. Emission intensities of UCNPs before and after ligand exchange by polymers.

Emission intensities were tested before and after the polymers coatings. The $NaYF_4$: Er/Yb distributed two sharp peaks at around 550 nm and 650 nm. UCNPs@OA were tested in cyclohexane; the UCNPs@polymers were tested in water. All the tested samples were concentrated at 1 mg/ml. The results showed that only the PEG polymer did not inhibit the emission of UCNPs, while after PEI and PAA polymer coating, only half of the original intensity could be achieved. The PEI coated UCNPs quenching effect could be related with the tertiary amine groups on the PEI toward fluorophores(Qiao and Zheng 2016). PVP coated UCNPs largely reduced the intensity to one-sixth of uncoated one. This might due be the quenching effect of water and specific polymers, and loss during surface modification process could also be a reason.

3.4 Conclusion

Colloidal stability of nanoparticles in chemical, and especially the biological environment is always one of the biggest challenges in practical applications. Therefore, four most commonly used polymers, PEG, PEI, PAA and PVP, were studied systematically to analyse their behaviour in different buffers and environment. Table III-3 summarizes the performance of four different polymers coated UCNPs. Overall, UCNPs@PEG are stable, and well suspended in all buffers. Also, it is the one can retain the highest luminescence intensity after ligand exchange. HEPES buffer is a good choice that quite a lot of polymers can be stabilized in. Therefore, PEG is considered as the best UCNPs surface modification polymers in terms of the colloidal stability, water dispensability, bio-environment stability, and cell toxicity, which does not require careful choice of buffers and operating temperature.

Table III-3. Evaluation of UCNPs@polymers in different buffers.

	MES buffer		HEPES buffer		SSC buffer		Tris Buffer	
	dispensability	stability	dispensability	stability	dispensability	stability	dispensability	stability
UCNPs@PEG	√	√	√	√				√
UCNPs@PEI			√					√
UCNPs@PAA				√				√
UCNPs@PVP		√	√		√		√	

Chapter IV. Application of Hydrophilic UCNPs in DNA detection

4.1 Introduction of Molecular Beacon Structure

Molecule beacon is a single-stranded oligonucleotide twisted in a hairpin structure. It was first introduced in 1996 and developed to sensitively detect the specific complementary target oligonucleotides(Tyagi and Kramer 1996).

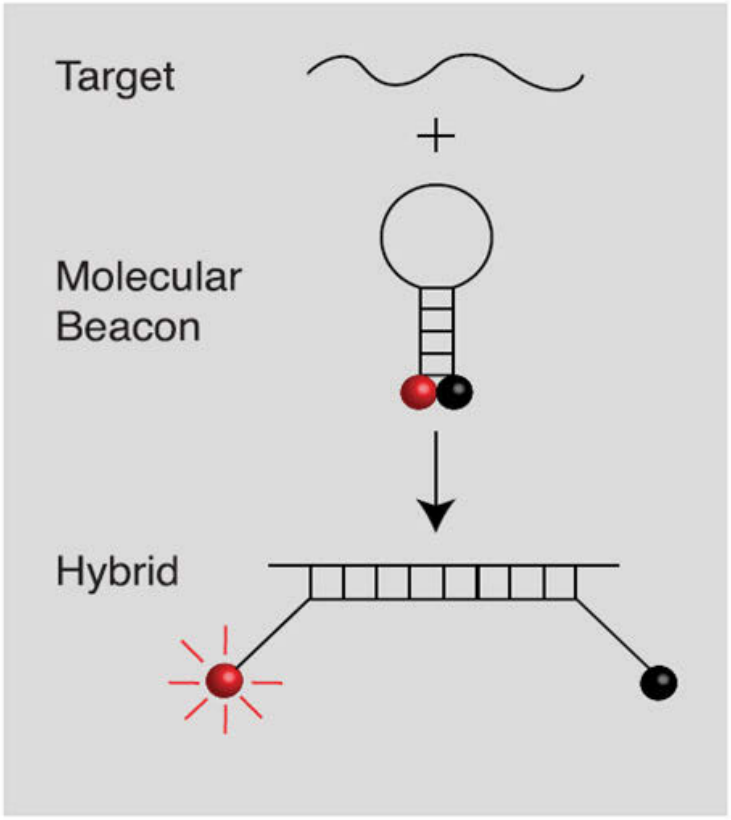

Figure IV-1. The schematic structure of molecular beacon and its function mechanisms.（Ref: http://www.genelink.com/newsite/products/amp&analysis.asp）

The basic structure of molecular beacon is shown in Figure IV-1. Overall, the molecular beacon consists of four parts:

1) Loop: The loop is an oligonucleotide sequence with 18-30 base pair which is complementary with the target sequence

2) Stem: The regular stem has 5-7 base pair long at each end of the loop, serving as the "arms" of the loop. They are complementary with each other to form a so-called "hairpin" structure

3) 5' fluorophore: At the 5' end of the single-stranded oligo, a fluorophore molecule attached will be quenched when the hairpin structure formed.

4) 3' quencher: At the 3' end of sequence, a non-fluorescent chromophore, quencher, is attached, which prevents the fluorescence of fluorophore in a well-formed molecular beacon.

In a homogeneous assay, the target sequence has a complementary designed loop with the molecular beacon. The as-designed probe is firstly formed by annealing and enclosed a hairpin structure that brings fluorophore and quencher in close proximity. The quencher absorbs the fluorescence from the nearby molecule and emits the energy in a form of heat, which results in fluorescence quenching. However, when target present in the solution, a sort of energy was "locked" inside the previous hairpin loop will be released by hybridization between two matched oligo sequences. Since the hybrid double-stranded oligo is longer than stem, it is more rigid and stable than a previous single loop. The straight double-stranded oligo pulls the fluorophore and quencher away from each other. Therefore, the fluorescence restores can be detected and implied the target oligo has successfully hybridized with the hairpin. Moreover, labelling the molecular beacons with different colored dyes can be used to simultaneously process multiple targets detection in a single assay(Tyagi and Kramer 2012).

4.2 Homogenous DNA Hybridization Assay Based on UCNPs and AuNPs

A Homogeneous DNA Assay by Recovering Inhibited Emission of Rare Earth Ions-Doped Upconversion Nanoparticles

Yingzhu Zhou[a], Yinghui Chen[a,b], Hao He[a,b], Jiayan Liao[a], Hien T.T. Duong[c], Maryam Parviz[a,b], Dayong Jin[a,b*]*

[a] Institute for Biomedical Materials and Devices, School of Mathematical and Physical Sciences, Faculty of Science, University of Technology Sydney, NSW 2007, Australia

[b] ARC Research Hub for Integrated Device for End-User Analysis at Low-levels, Faculty of Science, University of Technology Sydney, NSW, 2007, Australia

[c] The Faculty of Pharmacy, The University of Sydney, NSW 2006, Australia

*E-mail: maryam.parviz@uts.edu.au, *E-mail: dayong.jin@uts.edu.au

ABSTRACT: Robust and easy-to-use kits specific for a particular DNA sequence are desirable for early detection of diseases. However, the major challenge with these tests is often the background fluorescence artifacts arising from biological species due to employing UV and visible range of light. Here, we have reported a near-infrared (NIR) fluorescence "turn-on" kit based on rare earth ions doped nanoparticles, upconversion nanoparticles (UCNPs), and gold nanoparticles (AuNPs), which forms a fluorescence-quencher pair, brought together by a hairpin structure through the formation of double-stranded DNA (dsDNA), with quenched upconversion luminescence. In the presence of

analytes, the molecular beacon opens to push AuNPs away from UCNPs, with a distance longer than the efficient quenching distance, so that the inhibited upconversion emission will be restored. We demonstrated that this assay provides a homogeneous, facile, simple and highly selective HIV-1 based DNA detection system with restore efficiency up to 85%, and the detection limit of 5 *nM*.

Graphical Abstract:

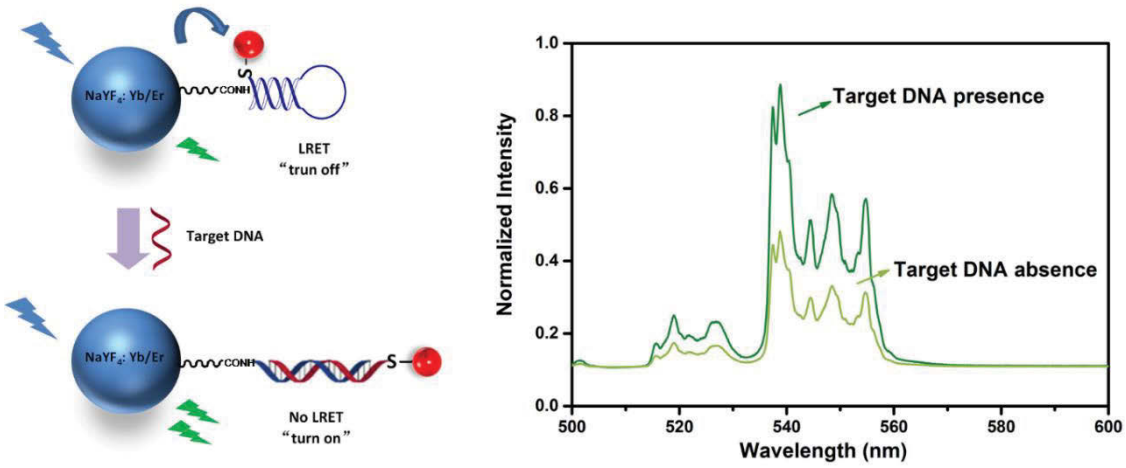

A representative illustration of DNA assay mechanism and simplified emission spectra of the probe.

KEYWORDS: upconversion, rare earth, molecular beacons, gold nanoparticles, luminescence quenching, fluorescence recovery, HIV-1, DNA.

1. Introduction

The human immunodeficiency virus (HIV-1) infection can result in acquired immunodeficiency syndrome (AIDS) with high mortality [1, 2]. Nucleic acid detection in blood can achieve early diagnosis of HIV even before the expression of retroviral proteins and lethal effects of live cells. Although HIV can be transmitted in many ways, reducing

the chance of infection through contaminated blood is the most critical and facile prevention strategy. Therefore, screening of donated blood is of great importance in preventing HIV transmission [3]. Currently, polymerase chain reaction (PCR) assay [4-6] is a promising and standard method to detect nucleic acids. However, PCR results are associated with false-positive signals since the primers can partly hybridize with each other [3]. Moreover, expensive equipment, sophisticated, and time-consuming procedure limit PCR clinical acceptance. Therefore, there are a lot of interests in developing cheaper and more user-friendly DNA hybridization detection platforms.

In recent decades, the fluorescence resonance energy transfer (FRET)-based techniques have been broadly applied in DNA detection due to its simplicity, compatibility with various systems, and high sensitivity [7, 8]. These assays require careful choice of fluorescence energy donor and acceptor pair. Fluorescent dyes with small sizes and large detectable optical signals are popular as donor candidates [9]. However, the narrow absorption spectra and broad emission band of most organic dyes limit their applications in FRET-based assays [10]. On the other hand, nanoparticles have tremendously contributed to ultrasensitive detection platforms [11-14]. Among them, fluorescent nanoparticles have attracted tremendous interests often due to their high quantum yield, high photobleaching threshold, and resistant to photo and chemical degradation [15-18]. For instance, quantum dots (QDs) were utilized as donors to detect nanomolar amounts of target DNA [19]. However, these nanoparticles usually require dealing with UV laser and, therefore, suffer from the typical limitations of intermittence emission,

autofluorescence, and high background signals [20]. This fuels the need for more advanced materials to overcome these challenges.

Lanthanide-doped upconversion nanoparticles (UCNPs) are emerging as a new generation of nanomaterials to minimize the background artifact in bioimaging [21-25] and biological assays [20, 26, 27]. UCNPs are excited under the irradiation in near-infrared (NIR) region, where the most biological and organic molecules, and, importantly, the water content are transparent [28, 29]. Moreover, by sequentially absorbing two or more photons from doped ions in host lattice, UCNPs display sharp f-f emission with long lifetime that enhances the luminescent signals. Besides, UCNPs also can be engineered to exhibit low toxicity and tunable emission which promise them to be an appropriate substitution as energy donors employed in lanthanide resonance energy transfer (LRET) [27, 30, 31]. Recently, many novel biosensors and platforms are designed based on UCNPs to detect specific nucleic acid sequences [32-35]. Gold nanoparticles (AuNPs) are superior to conventional quenchers, organic dyes, as energy acceptors due to their favourable biocompatibility and, high chemical stability [36-38]. Typically, AuNPs have a broad absorbance band, which largely overlaps with the emission of luminescent nanoparticles to process efficient quenching effect [39]. Recently, intensive studies have focused on UCNPs and AuNPs couple for bioassays and luminescence mechanisms studies, attribute to the interesting quenching or enhancement effect of UCNPs by AuNPs due to localized surface resonance. Normally, quenching effect dominates especially in the solution caused by LRET, which usually arises when UCNPs and AuNPs are in close

proximity (<15 *nm*) [28, 37, 40, 41]. Therefore, UCNPs and AuNPs are appropriate donor-acceptor pair in homogenous detections.

In this study, we report the design of a NIR fluorescence-quencher DNA assay platform. The system employs Er^{3+} doped UCNPs and AuNPs as the donor-acceptor pair. UCNPs were modified with a synthesized polyethylene glycol-like copolymer, which makes the nanoparticles water-dispersible and biocompatible. Hairpin shaped ssDNA structures, molecular beacons, that specifically hybridized with HIV-1 DNA target molecules were attached to polymer coated UCNPs. These molecules also bind to AuNPs to provide the required close proximity between donor and acceptor through formation of Au-S bonds. The introduction of target molecules resulted in the recovery of the subsequently quenched fluorescence, significantly. Here, the application of the developed simple platform for rapid detection of HIV-1 has been demonstrated in an amplification and enzyme-free manner.

2. Experimental

2.1 Chemicals and Materials

The chemicals required to synthesize the Er^{3+} doped UCNPs, and AuNPs with different sizes of 5 *nm*, 10 *nm*, and 20 *nm* (OD=1) stabilized in citrate buffer were purchased from Sigma-Aldrich (Sydney, Australia). Specifically, Yttrium (III) chloride hexahydrate ($YCl_3 \cdot 6H_2O$, 99.99%), ytterbium chloride hexahydrate ($YbCl_3 \cdot 6H_2O$, 99.99%), and erbium chloride hexahydrate ($ErCl_3 \cdot 6H_2O$, 99.99%) for UCNPs synthesis were from Sigma-Aldrich (Sydney, Australia). All oligonucleotides were purchased from Integrated

DNA Technologies (Singapore). The specific sequences are shown in Table S1. The HIV-I specific oligonucleotide sequence was designed according to Russell's work [3]. It was modified with an amine group (–NH2) on its 5' end and a thiol group (–SH) on its 3' end, respectively. There were six pairs of complementary bases on the stem part, and 33 bases on the loop part, which resulted in a so-called "hairpin structure". All materials were used as received without further purification except 2,2'azobisisbutyronitrile for polymer synthesis, which was purified through recrystallization from methanol.

2.2 Instrumentation and Apparatus

Powder X-ray diffraction (XRD) characterization was performed using D8 Discover diffractometer (Bruker Corporation) to confirm the β phase of UCNPs. Transmission electron microscopy (TEM) images were recorded on an FEI-Tecnai T20 instrument to analyze the size and morphology of nanoparticles. Fourier-transform infrared spectroscopy (FTIR) spectra tests were carried out using a Nicolet 6700 FT-IR spectrometer (Thermo Scientific) to determine the surface ligands. Dynamic light scattering (DLS) was run using Zetasizer nano series (Malvern Instrument) to test the hydrodynamic size of nanoparticles. Cary 60 UV-Vis spectrometer (Agilent Technologies) was generated to collect the absorbance of AuNPs. Nanodrop 2000 (Thermos Scientific) was utilized to test the DNA absorbance. Upconversion luminescence intensity spectra were measured by an iHR550 spectrometer (HORIBA Scientific Instruments Inc.) with a modified external 980*nm* laser. The excitation irradiance value was up to $1.36 \times 10^6\ W\,cm^{-2}$.

2.3 Synthesis of $NaYF_4$: Yb, Er UCNPs

UCNPs used in this project were doped by 20% Yb and 2% Er by traditional co-precipitation method [2]. Specifically, 1 *mmol* $LnCl_3$ (Ln=Y, Yb, Er) with the molar ratio of 78:20:2 were reacted with 6 *mL* of oleic acid (OA) and 15 *mL* 1-octadecene. Then, the solution was heated up to 160 ℃ under continuous argon gas for 30 *min*. The clear solution was obtained and cooled down to the room temperature, followed by the addition of 5 *mL* methanol solution of 4 mmol NH_4F and 2.5 *mmo*l NaOH. After continuous stirring for 30 *min*, methanol was evaporated under 100 ℃ for 20 *min*, and water was removed under 120 ℃ for another 20 *min*. The reaction was finalized by further heating the solution at 300 ℃ for 90 *min*. The nanocrystals were precipitated by centrifuge at 13,000 *rpm* and washed with cyclohexane, ethanol, and methanol, respectively. The synthesized products, dispersed in cyclohexane, were well-monodispersed.

2.4 Surface modification of UCNPs with polymer

$NaYF_4$: Yb, Er nanoparticles in this project required a hydrophilic amendment to replace the OA groups and make the structure proper for applications in aqueous biological environments. The hydrophilic modification was also designed to pose functional groups on the surface of UCNPs to be further conjugated with DNA hairpin structures. This surface modification was achieved by anchoring a copolymer containing phosphate and carboxyl groups onto the surface of UCNPs. The copolymer was synthesized by using poly(ethylene glycol) methyl ether acrylate as a macro-RAFT agent for chain development with mono(2-acryloyloxyethyl) phosphate (MAEP) to form a copolymer

namely POEGA-b-PMAEP as we have reported previously [42]. This polymer substitutes the total original ligands and therefore provide long-term stability. To coat POEGA-b-PMAEP copolymer on UCNPs, first, cyclohexane on UCNPs (10 *mg/ml*) was remove by centrifuging at 14,680 *rpm* followed by re-dispersing the precipitate in 500 *uL* THF. Next, UCNPs were mixed with 10 *mg* of the copolymer dissolved in 2 *mL* THF and stirred overnight. Then, the solution was rinsed three times with THF and water to completely remove excess polymer molecules and detached OA groups. The obtained product was polymer coated UCNPs (UCNPs@PEG) in water (10 *mg/mL*) and was stored at 4 ℃ for further usage.

2.5 Surface coating of hairpin probe

Designed HIV based oligonucleotide has amine group modified on its 5' end and thiol group modified on 3' end. After annealing molecular beacons at 90 ℃ and stabling at 72 ℃ for 20 *min*, the hairpin structure was formed [43]. For molecular beacons modification on UCNPs, the EDC coupling chemistry was used [44]. Briefly, UCNPs@PEG activated by EDC were mixed with DNA in MES buffer (pH 5.1) and gently stirring overnight under 37 ℃. Then, the solution was rinsed three times with sterilized water to remove the excess DNA and re-suspended in SSC buffer (pH 7.0). The $-NH_2$ group on DNA processed condensation reaction with –COOH on UCNPs@PEG surface through stable covalent binding to form UCNPs@PEG@DNA hybrids. The final product was stored at 4 ℃ for further use.

2.6 DNA target detection strategies

In order to introduce the target molecules to the sensing system, briefly, sample solutions containing 0.05 *mg/mL* UCNPs@PEG@DNA was hybridized with different concentrations of target ssDNA at 37 ℃ for 2 *h*. The negative control group with no target DNA was also incubated under the same conditions. Next, 15 μL stock solution of 5 *nm* AuNPs were added to each solution and gently shake for 100 minutes. Finally, luminescence intensity spectra measurements were done under 980 *nm* excitation. Each sample was loaded in a quartz cuvette, and spectra were collected by wavelength in the range of 400-800 *nm*.

3. Results and discussion

It is crucial to optimize the design to fabricate an efficient facile DNA hybridization assay platform based on hairpin ssDNA and UCNPs. Fig. 1 illustrates the basis and mechanisms of the probe function. Firstly, the synthesized OA capped UCNPs were modified with the prepared POEGA-b-PMAEP copolymer to produce water-dispersible UCNPs@PEG with long-term stability. The utilized copolymer poses phosphate and carboxyl groups. The phosphate group has a higher binding affinity with UCNPs than carboxyl acid of OA, and therefore, completely, substitutes the original ligands and formed UCNPs@PEG [45]. Secondly, hairpin HIV-1 based ssDNA structures with amine and thiol groups on their 5' end and 3' end, respectively, were attached to UCNPs@PEG. This bio-conjugation was achieved through a covalent bond between the amine and carboxyl groups to form the UCNPs@PEG@DNA nanosensor probe. AuNPs attached to probe's surface due to Au-

S bond formation between the gold and thiolated ssDNA resulting in luminescence quenching. However, when the target is available, the DNA hybridization leads to conformational changes of the hairpin molecules. This prolongs the distance between the UCNPs and AuNPs, and, restores the luminescence intensity as shown in Scheme 1.

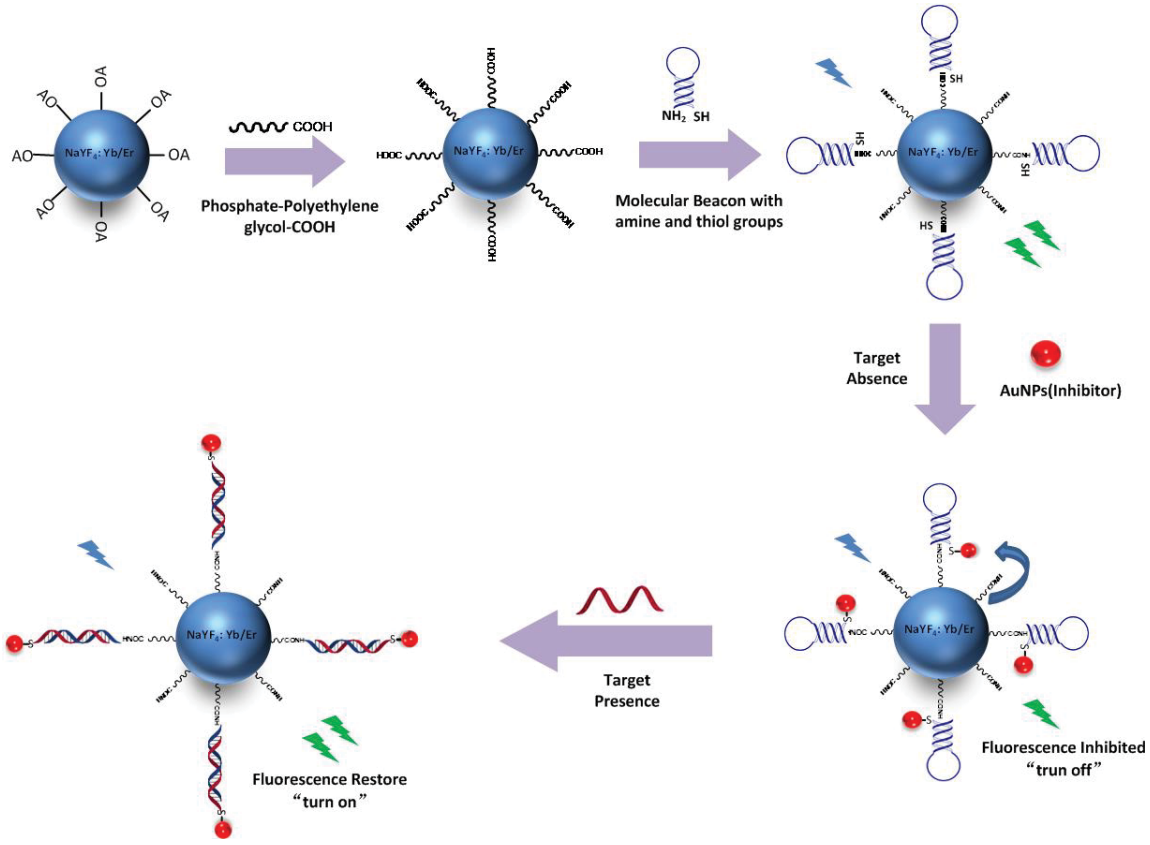

Scheme 1. Schematic illustration of HIV-1 detection based on restoring the inhibited emission of UCNPs.

Various techniques including TEM, DLS, FTIR spectroscopy, and XRD were employed to characterize each synthesis and surface modification step. TEM results (Fig. 1A) implied that original OA capped UCNPs had uniform structures with average diameter of around 25 *nm*. Fig. 1B-C confirmed that further modification of UCNPs with either the copolymer or DNA did not change the UCNPs morphology. XRD results confirmed a β phase for the synthesized UCNPs (Fig. 1D). Typical FTIR peaks of OA-UCNPs at 3005

cm^{-1} and 1548 cm^{-1} confirmed C=C bond and C-O bond vibration stretch, respectively, which are attributed to the primary functional groups of OA ligands. After surface modification using the POEGA-b-PMAEP copolymer, new peaks at 1729 cm^{-1} and 1099 cm^{-1} representing C=O and P=O vibration stretches appeared confirming successful ligand exchange (Fig. 1E). DLS was performed to confirm the formation of the polymer and DNA layers on UCNPs. UCNPs@OA were dispersed in cyclohexane and UCNPs@PEG and UCNPs@PEG@DNA were dispersed in water. The data showed a stepwise increase in the average size of UCNPs from 31.29 nm to 37.84 nm, and 58.77 *nm* after polymer and hairpin DNA modifications, respectively (Fig. 1F). In addition, the appearance of a typical absorbance peak at around 260 *nm* acquired using nanodrop test also confirmed the successful conjugation of molecular beacons to the nanoparticles (Fig. S1). The difference of nanoparticle diameters in TEM and DLS can be explained as the TEM only shows the UCNPs morphology on grid while the DLS displays the hydrodynamic diameter of nanoparticles in solution.

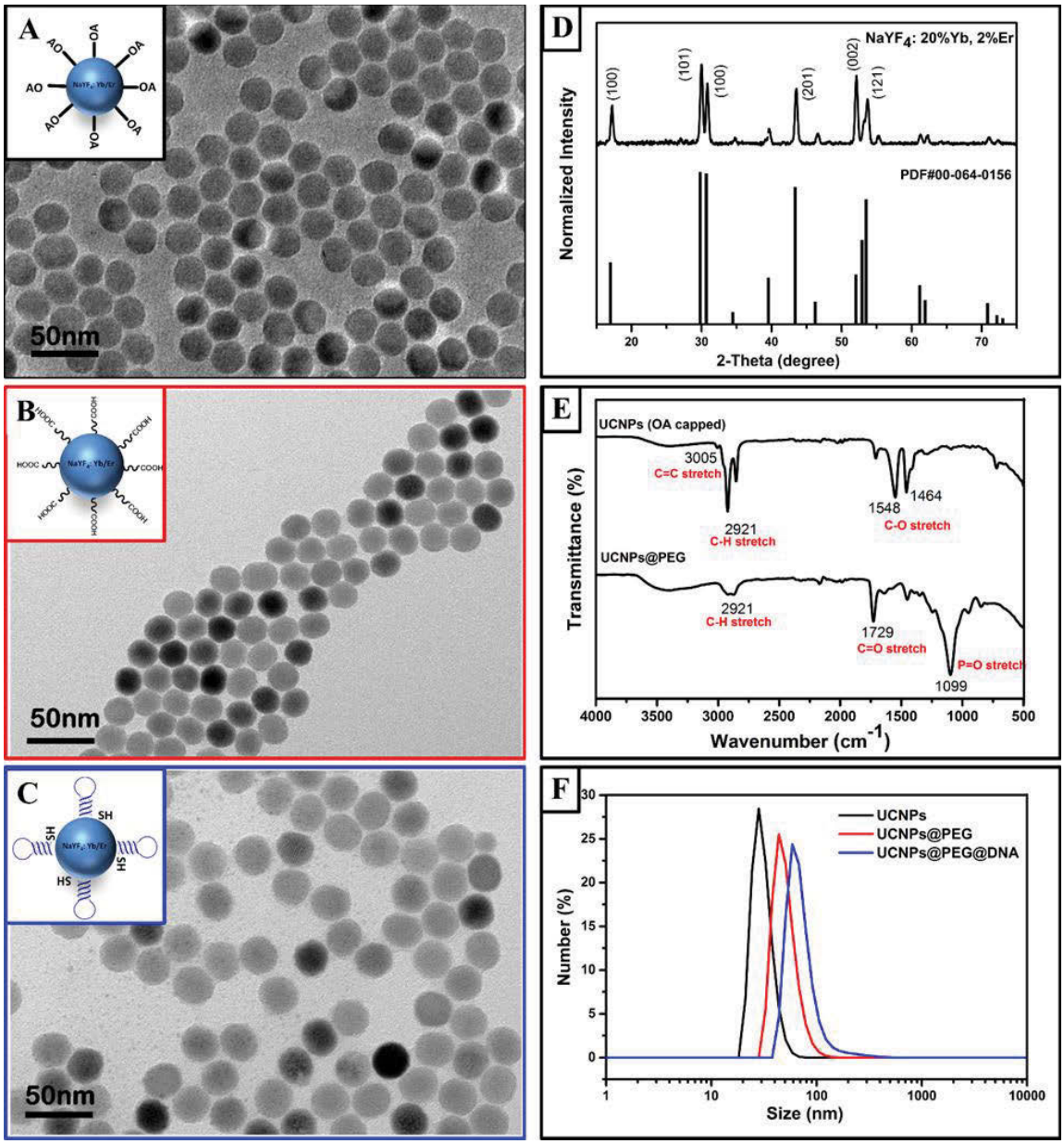

Fig. 1. TEM images of (A) UCNPs@OA in cyclohexane, (B) UCNP@PEG with the carboxyl groups, and (C) as-prepared UCNP@PEG@DNA. Inner graphs are simplified illustrations of tested nanoparticles. (D) XRD results of synthesized UCNPs. (E) FRIT spectra of UCNPs@OA and UCNPs@PEG. (F) Size distribution profile of UCNPs, UCNPs@PEG, and UCNPs@PEG@DNA.

Fluorescence spectroscopy results showed that under the NIR 980 *nm* excitation, Er/Yb doped UCNPs emitted two firm emission peaks centered approximately at 539 *nm* and 650 *nm* (Fig. 2A). The AuNPs displayed the plasmonic absorbance band centered at around 525 *nm*, which mainly overlaps with the emission of $NaYF_4$:Yb:Er UCNPs at

around 539 *nm* (Fig. 2B). This shows that AuNPs are the appropriate quencher candidates. The control test was performed to confirm the target itself did not change the optical properties in the absence of AuNPs (Fig. 2A). Therefore, the subsequent quenching in the assay is inferred to be the consequences of quencher, AuNPs.

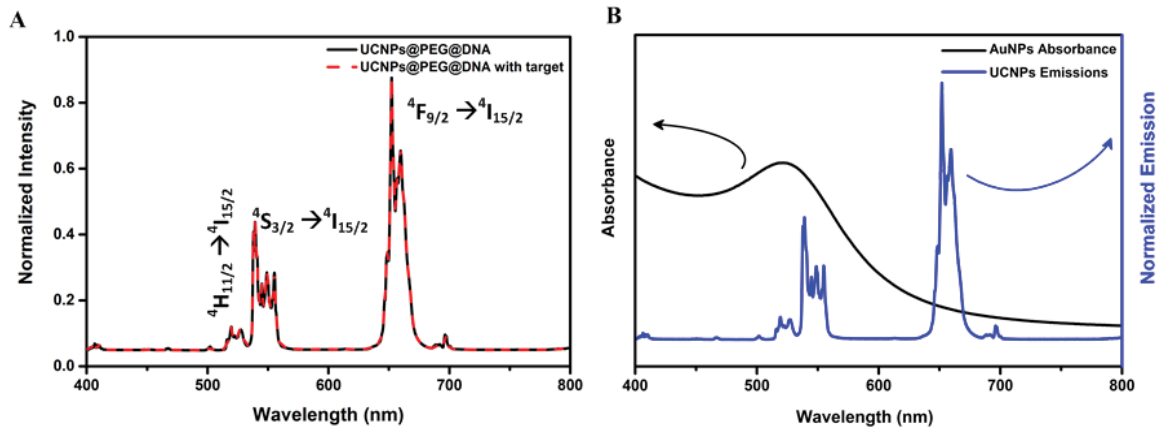

Fig. 2. (A) The luminescence spectra of UCNPs@PEG@DNA with and without target. (B)The absorbance of AuNPs (black line) and luminescence emission of $NaYF_4$:Yb:Er UCNPs (blue line). Normalized intensity values were calculated by dividing the raw data into the highest intensity of UNCPs@PEG@DNA in the absence of the target at 539 *nm*.

The molar ratio of UCNPs@PEG and hairpin ssDNA was optimized in order to bind sufficient AuNPs to UCNPs@PEG@DNA and tune quenching. For this purpose, 15 μL of 5 *nm* AuNPs (5.5×10^{13} *particles/ml*) were used and the amount of ssDNA was tuned. The quenching efficiency was calculated by dividing the initial luminescence of UCNPs@PEG@DNA at 539 *nm* (F_0) into the intensity of probe after AuNPs conjugation (F_1). Increasing molar ratio of UCNPs@PEG to hairpin ssDNA (1:1, 1:5, 1:10, 1:20, 1:40) resulted in gradually luminescence decrease, while the quenching phenomenon alleviated for samples with a molar ratio of 1:50 (Fig. 3A). The results implied the saturated molar ratio of UCNPs@PEG to ssDNA was 1:40, where the maximum amount of AuNPs could

be attached. The DNA addition with the molar ratio up to 1:50 blocked the UCNPs@PEG and shielded AuNPs away from the surface, thus, led to less quenching compared with 1:40 one. It is crucial to select the optimum size of AuNPs and utilize the adequate quantity (Fig. S3) to develop an efficient fluorescence-quenching platform. TEM images of three different AuNPs candidates were shown in Fig. S4. 15 *μL* of 5, 10, or 20 *nm* AuNPs were mixed with the same amount of UCNPs@PEG@DNA and gently stirred for 2 h, followed by examining the emission intensity of the probe (Fig. 3C). Among the tested sizes (5, 10, 20 *nm*), the 5 *nm* AuNPs gave the most efficient quenching results compared with the other dimensions of AuNPs. The phenomena may be due to two reasons: 1) the larger size of AuNPs face higher steric hindrance thus harder to access the thiolate ssDNA, and 2) the smaller AuNPs possessing more considerable overlap with UNCPs emission thus lead to the sufficient quenching. The results shown in Fig. 3B confirmed that 5 *nm* AuNPs had the broadest absorbance band centered at around 520 *nm*. In addition, the effects of reaction duration on quenching were examined. Fig. 3D displays the intensity of the probe exposed to different sizes of AuNPs at 539 *nm* versus the reaction time (0, 5, 10, 20, 40, 60, 80, 100, 120 *min*). The normalized intensity was firstly divided by the highest values of intensity of UCNPs@PEG@DNA at 539 *nm*, and then the calculated data for each sample was divided into the acquired value at the beginning of the reaction (0 *min*) to provide a systematic comparison over time. Quenching of UCNPs quickly appeared within 10 minutes after addition of AuNPs followed by a mild decrease after 40 minutes, and finally reached a stable level at around

100 minutes of reaction time. Overall, AuNPs of 5 *nm* size and the reaction time of 100 minutes were selected as the most appropriate quenching conditions.

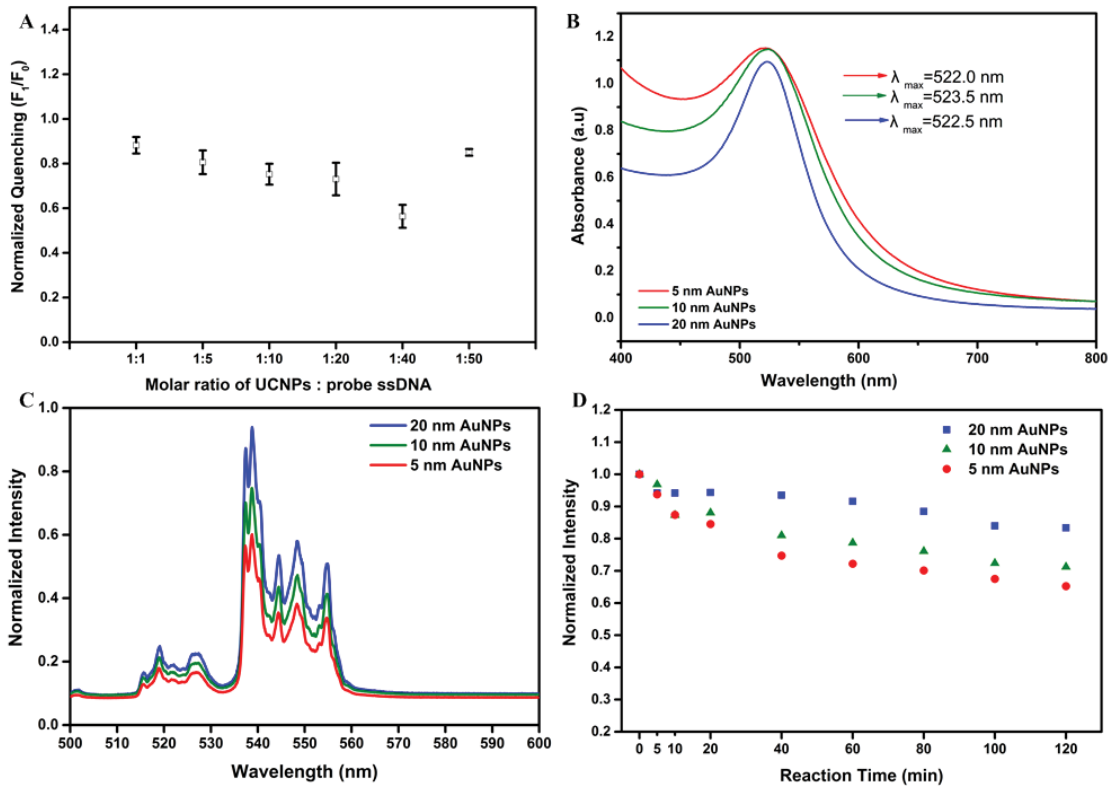

Fig. 3. Optimization of the molar ratio of UNCPs@PEG to hairpin ssDNA to achieve highest quenching efficiency by the same amount of gold. (A) Quenching efficiency of AuNPs to UCNPs@PEG as a function of the molar ratio of hairpin ssDNA exposed to 5 *nm* AuNPs. Optimization of AuNPs size selection to achieve the most efficient quenching. (B) The absorbance spectra of 5, 10, and 20 *nm* AuNPs. (C) Normalized luminescence spectra of UCNPs@PEG@DNA with different sizes of AuNPs after 100 *min* reaction (D) The normalized intensity of UCNPs@PEG@DNA after reaction with 5 *nm*, 10 *nm*, and 20 *nm* AuNPs with increasing reaction time from 0 *min* to 120 *min*.

Avoiding non-specific binding of AuNPs to UCNPs is essential in preventing false results in the developed sensing platform. To test this feature, luminescence spectra of UCNPs@PEG were compared with those of UCNPs@PEG and UCNPs@PEG@DNA reacted with the same amount of AuNPs. Compared with UCNPs@PEG, the luminescence intensity of UCNPs@PEG exposed to AuNPs displayed no observable difference, while UCNPs@PEG@DNA in the presence of AuNPs showed a significant

quenching. These results confirmed that the polymer coated UCNPs prevented the nonspecific absorbance of AuNPs. However, coating UCNPs@PEG with thiolated ssDNA led to efficient bonding to AuNPs, which pulled AuNPs into close proximity with UCNPs@PEG@DNA and thus attributed the significant quenching. It is worth mentioning that in addition to the primary quenching that occurred on green emission (539 *nm* emission), the red emission (650 *nm*) of UCNPs was also partially inhibited (Fig. S5). This might be related to the induction of the red emission by nonradioactive decay from green emission, and also to the shift of absorbance peak of aggregated AuNPs to higher wavelength [46].

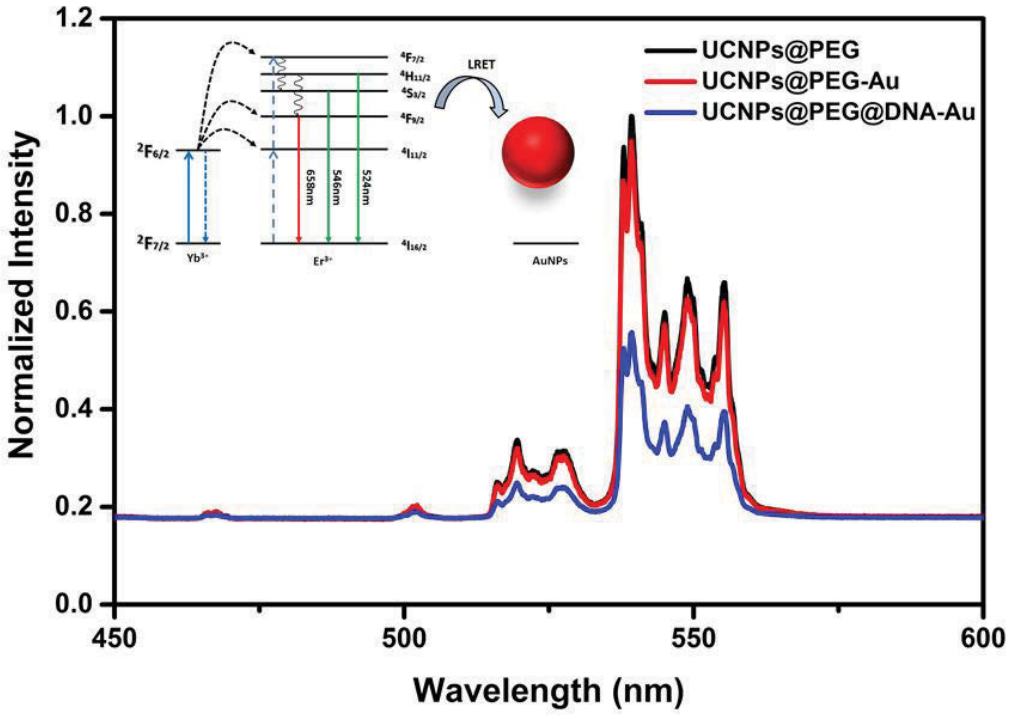

Fig. 4. The normalized luminescence intensity of UCNPs@PEG as the control group versus intensity of UCNPs@PEG and UCNPs@PEG@DNA after reaction with 5 *nm* AuNPs. The inner graph illustrates the energy transfer process that causes the luminescence quenching effect.

Molecular beacons have been used in ultrasensitive detection of diseases biomarkers [11]. The sensitivity of the current fluorescence-quencher probe was examined by applying

incremental target concentrations into the system until the sensing reached saturation in detecting the target DNA molecules. The designed hairpin ssDNA and complementary target sequences are listed in Table S1. Fig. 5B illustrates the normalized intensity of restored luminescence as the function of various concentrations of target molecules (5 *nM*-1000 *nM*). Hybridization process opens the hairpin loop, stretching the grafted AuNPs far away from the UCNPs surface, and, therefore, the luminescence intensity recovered. As displayed in Fig. 5A, increasing the concentration of HIV-1 target DNA up to 500 nM led to a steady rise in normalized recovered fluorescence intensities. The normalized values were calculated using $(F-F_1)/F_1$ equation, where F and F_1 stand for the fluorescence intensity of the probe at 539 *nm* before and after AuNPs conjugation, respectively. We did not observe any further recovery in the luminescence intensity of UCNPs by addition of higher concentrations than 500 *nM* of target DNA (Fig. 5B). The results indicate the application of the developed probe for detection of 5 *nM* to 500 *nM* DNA analytes.

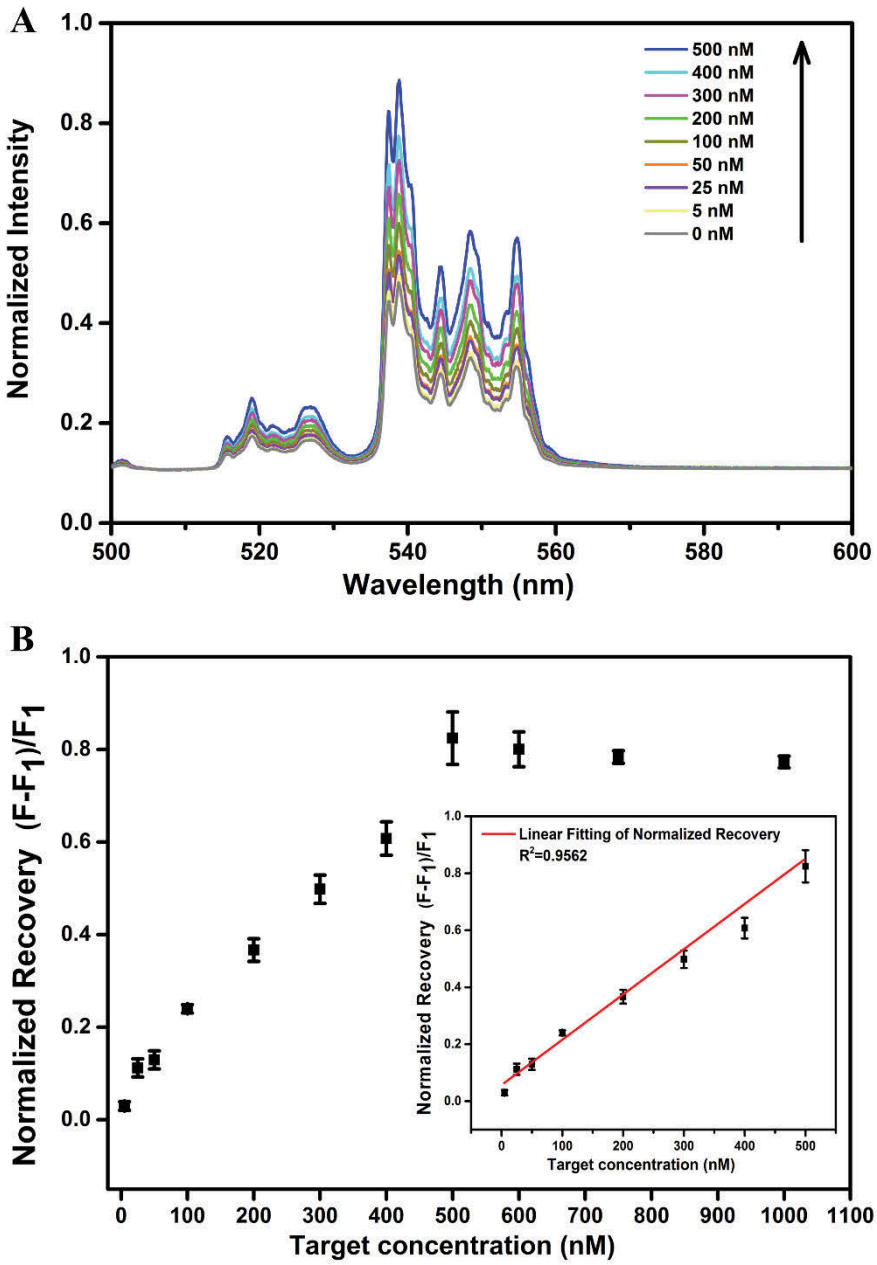

Fig. 5. (A) The fluorescence emission spectra of UCNP@PEG@DNA with incremental concentrations of target DNA from 0 *nM* to 500 *nM* in the presence of 15 *μL* of 5 *nm* AuNPs. (B) The fitting curve of the normalized fluorescence restore with increasing concentration of target within range of 0 nM to 1000 *nM*. The inner graph is the linear fitting of target concentration up to 500 *nM*.

The performance of the probe with the mismatched target and random sequences was tested to investigate the selectivity of the developed platform. The mismatched sequences are listed in Table S2. According to the results shown in Fig. 6, the probe intensity displayed the highest restore value after hybridization with the complementary target

sequence, while showed much lower response with 1 base and 3 base mismatches. In addition, the minimum fluorescence recovery was observed when the probe was hybridized with the random sequences. The results demonstrated that the designed sensing platform is a highly selective probe to detect the HIV-1 target DNA.

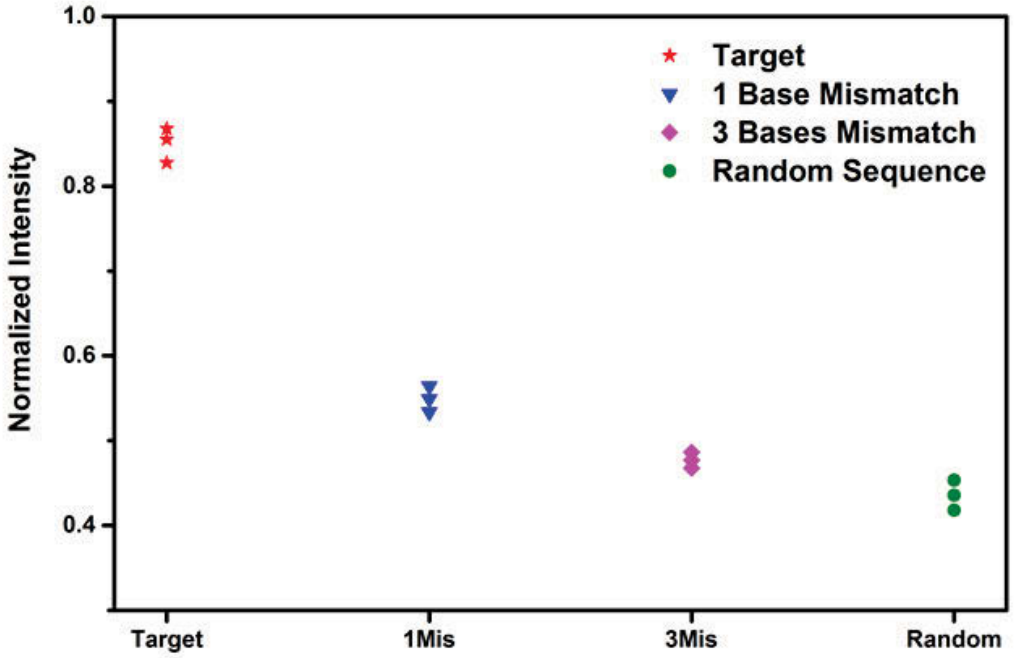

Fig. 6. Normalized intensity of UCNPs@PEG@DNA in the presence of complementary target and mismatched DNA strands.

4. Conclusions

In conclusion, it was demonstrated that the proposed homogenous hairpin coated UCNPs detects HIV-1 viral DNA with high sensitivity and selectivity in NIR region. This sensing platform is established based on quenching of UCNPs using AuNPs, while the quenched fluorescence recovers in the presence of target DNA. The future design of this nanosensor may consider employing smaller size of UCNPs and shortening the polymer coating or substitute the polymer coatings with small organic compounds to increase the quenching

efficiency of UCNPs. The developed platform offers to advance the field of early detection and disease prevention owing to its cost-effectiveness, selectivity, and amplification/enzyme-free nature and easy to set up. More importantly, the use of the rare earth lanthanide-doped nanoparticles provides the opportunity of dealing with 980 *nm* NIR excitation source which avoids the typical false results raising from autofluorescence of biological species at UV range.

5. Acknowledgements

The authors acknowledge the financial support from the Australian Research Council (ARC) Future Fellowship Scheme (D.J., FT 130100517) and ARC Industry Transformational Research Hub Scheme (IH150100028).

References

1. Navia, M.A., et al., *Three-dimensional structure of aspartyl protease from human immunodeficiency virus HIV-1.* Nature, 1989. **337**(6208): p. 615-620.
2. Wang, H., et al., *Estimates of global, regional, and national incidence, prevalence, and mortality of HIV, 1980-2015: the Global Burden of Disease Study 2015.* The lancet. HIV, 2016. **3**(8): p. e361-87.
3. Vet, J.A., et al., *Multiplex detection of four pathogenic retroviruses using molecular beacons.* PNAS, 1999. **96**(11): p. 6394-6399.
4. Saiki, R.K., et al., *Enzymatic amplification of b-globin genomic sequences and restriction site analysis for diagnosis of sickle cell anemia.* Science, 1985. **230**(4732): p. 1350-1354.
5. Mullis, K., et al. *Specific enzymatic amplification of DNA in vitro: the polymerase chain reaction*. in *Cold Spring Harbor symposia on quantitative biology*. 1986. Cold Spring Harbor Laboratory Press.
6. Mulder, J., et al., *Rapid and simple PCR assay for quantitation of human immunodeficiency virus type 1 RNA in plasma: application to acute retroviral infection.* JCM, 1994. **32**(2): p. 292-300.
7. Didenko, V.V., *DNA probes using fluorescence resonance energy transfer (FRET): designs and applications.* BIOTECHNIQUES, 2001. **31**(5): p. 1106.

8. Peng, X., D.R. Draney, and W.M. Volcheck. *Quenched near-infrared fluorescent peptide substrate for HIV-1 protease assay*. in *Proceedings of SPIE*. 2006.
9. DiNitto, J.P., L. Wang, and J.C. Wu, *Continuous fluorescence-based method for assessing dicer cleavage efficiency reveals 3′ overhang nucleotide preference.* BIOTECHNIQUES, 2010. **48**(4): p. 303-311.
10. Clapp, A.R., et al., *Fluorescence resonance energy transfer between quantum dot donors and dye-labeled protein acceptors.* JACS, 2004. **126**(1): p. 301-310.
11. Lu, L., et al., *Ultrasensitive detection of cancer biomarker microRNA by amplification of fluorescence of lanthanide nanoprobes.* JNanoR, 2018. **11**(1): p. 264-273.
12. Yuan, J., et al., *MnO2-nanosheet-modified upconversion nanosystem for sensitive turn-on fluorescence detection of H2O2 and glucose in blood.* ACS Appl Mater Interfaces, 2015. **7**(19): p. 10548-10555.
13. Wang, Z., et al., *An upconversion luminescence nanoprobe for the ultrasensitive detection of hyaluronidase. Am J Analyt Chem*, 2015. **87**(11): p. 5816-5823.
14. Nasiri, N., et al., *Ultraporous Electron-Depleted ZnO Nanoparticle Networks for Highly Sensitive Portable Visible-Blind UV Photodetectors. JAM*, 2015. **27**(29): p. 4336-4343.
15. Murray, C., D.J. Norris, and M.G. Bawendi, *Synthesis and characterization of nearly monodisperse CdE (E= sulfur, selenium, tellurium) semiconductor nanocrystallites.* JACS, 1993. **115**(19): p. 8706-8715.
16. Berlina, A.N., et al., *Quantum dot-based lateral flow immunoassay for detection of chloramphenicol in milk. Anal Bioanal Chem*, 2013. **405**(14): p. 4997-5000.
17. Clapp, A.R., I.L. Medintz, and H. Mattoussi, *Förster resonance energy transfer investigations using quantum-dot fluorophores.* ChemPhysChem, 2006. **7**(1): p. 47-57.
18. Parviz, M., et al., *Synthsis of CdSe/ZnS core shell quantum dots and in vitro evaluation of their emission effects on raji cells death.* 2009. **3**(1): p. 89-98.
19. Shamsipur, M., et al., *A highly sensitive quantum dots-DNA nanobiosensor based on fluorescence resonance energy transfer for rapid detection of nanomolar amounts of human papillomavirus 18. J PHARMACEUT BIOMED*, 2017. **136**: p. 140-147.
20. Wang, F., et al., *Upconversion nanoparticles in biological labeling, imaging, and therapy. ANALYST*, 2010. **135**(8): p. 1839-1854.
21. Nyk, M., et al., *High contrast in vitro and in vivo photoluminescence bioimaging using near infrared to near infrared up-conversion in Tm3+ and Yb3+ doped fluoride nanophosphors*. Nano Lett, 2008. **8**(11): p. 3834-3838.
22. Shi, Y., et al., *Stable Upconversion Nanohybrid Particles for Specific Prostate Cancer Cell Immunodetection. Sci Rep*, 2016. **6**.
23. Zhou, J., et al., *Upconversion luminescent materials: advances and applications. CHEM REV*, 2014. **115**(1): p. 395-465.
24. Yang, L., et al., *Synthesis, Characterization and Cell Imaging Properties of Rare Earth compounds Based on Hydroxamate Ligand. J RARE EARTH*, 2018.

25. Yang, D., et al., *Synthesis of NaYF4: Nd@ NaLuF4@ SiO2@ PS colloids for fluorescence imaging in the second biological window. J RARE EARTH*, 2017.
26. Hu, H., et al., *Facile epoxidation strategy for producing amphiphilic up-converting rare-earth nanophosphors as biological labels. CHEM MATER*, 2008. **20**(22): p. 7003-7009.
27. Wang, C., X. Li, and F. Zhang, *Bioapplications and biotechnologies of upconversion nanoparticle-based nanosensors.* ANALYST, 2016. **141**(12): p. 3601-3620.
28. Jesu Raj, J.G., et al., *Sensitive Detection of ssDNA Using an LRET-Based Upconverting Nanohybrid Material. ACS APPL MATER INTER*, 2015. **7**(33): p. 18257-18265.
29. Zhou, B., et al., *Controlling upconversion nanocrystals for emerging applications. Nat Nanotechnol*, 2015. **10**(11): p. 924.
30. Zhang, C., et al., *Rare earth upconversion nanophosphors: synthesis, functionalization and application as biolabels and energy transfer donors. J RARE EARTH*, 2010. **28**(6): p. 807-819.
31. Su, Q., et al., *Resonance energy transfer in upconversion nanoplatforms for selective biodetection. ACCOUNTS CHEM RES*, 2016. **50**(1): p. 32-40.
32. Alonso-Cristobal, P., et al., *Highly sensitive DNA sensor based on upconversion nanoparticles and graphene oxide. ACS APPL MATER INTER*, 2015. **7**(23): p. 12422-12429.
33. Huang, L.-J., R.-Q. Yu, and X. Chu, *DNA-functionalized upconversion nanoparticles as biosensors for rapid, sensitive, and selective detection of Hg 2+ in complex matrices.* ANALYST, 2015. **140**(15): p. 4987-4990.
34. Li, J., et al., *Detection of microRNA by fluorescence amplification based on cation-exchange in nanocrystals. Am J Analyt Chem*, 2009. **81**(23): p. 9723-9729.
35. Tang, Q., et al., *A novel AgNP/DNA/TPdye conjugate-based two-photon nanoprobe for GSH imaging in cell apoptosis of cancer tissue. ChemComm*, 2015. **51**(94): p. 16810-16812.
36. He, M., et al., *Portable upconversion nanoparticles-based paper device for field testing of drug abuse. Am J Analyt Chem*, 2016. **88**(3): p. 1530-1534.
37. Wu, S., et al., *Dual fluorescence resonance energy transfer assay between tunable upconversion nanoparticles and controlled gold nanoparticles for the simultaneous detection of Pb 2+ and Hg 2+. TALANTA*, 2014. **128**: p. 327-336.
38. Zhang, Y., et al., *Hairpin DNA switch for ultrasensitive spectrophotometric detection of DNA hybridization based on gold nanoparticles and enzyme signal amplification. Am J Analyt Chem*, 2010. **82**(15): p. 6440-6446.
39. Chan, M.-H., et al., *Single 808 nm Laser Treatment Comprising Photothermal and Photodynamic Therapies by Using Gold Nanorods Hybrid Upconversion Particles. JPC C*, 2018. **4**(122): p. 2402–2412.
40. Emrani, A.S., et al., *A novel fluorescent aptasensor based on hairpin structure of complementary strand of aptamer and nanoparticles as a signal amplification*

approach for ultrasensitive detection of cocaine. Biosens Bioelectron, 2016. **79**: p. 288-293.

41. Ye, W.W., et al., *Upconversion Luminescence Resonance Energy Transfer (LRET)-Based Biosensor for Rapid and Ultrasensitive Detection of Avian Influenza Virus H7 Subtype.* SMALL, 2014. **10**(12): p. 2390-2397.
42. Hien Duong, Y.C., Sherif Tawfik,, Maryam Parviz, Olga Shimoni, Mike Ford, Shihui Wen, Dayong Jin, *Systematic Investigation of Functional Ligands for Colloidal Stable Upconversion Nanoparticles.* Submitted, 2018. **8**(9): p. 4842-4849.
43. Wang, P., et al., *Ligase-assisted signal-amplifiable DNA detection using upconversion nanoparticles. RSC ADV*, 2013. **3**(37): p. 16326-16329.
44. Chen, D., et al., *ZnS nano-architectures: photocatalysis, deactivation and regeneration.* Nanoscale, 2010. **2**(10): p. 2062-2064.
45. Chen, Y., et al., *Exonuclease III-assisted Upconversion Resonance Energy Transfer in a Wash-Free Suspension DNA Assay. Am J Analyt Chem*, 2017. **90**(1): p. 663-668.
46. Zhang, S.-Z., et al., *Reversible luminescence switching of NaYF 4: Yb, Er nanoparticles with controlled assembly of gold nanoparticles. ChemComm*, 2009(18): p. 2547-2549.

Supporting Information

A Homogeneous DNA Assay by Recovering Inhibited Emission of Rare Earth Ions-Doped Upconversion Nanoparticles

Yingzhu Zhou[a], Yinghui Chen[a,b], Hao He[a,b], Jiayan Liao[a], Hien T.T. Duong[c], Maryam Parviz[a,b*], Dayong Jin[a,b*]

[a] Institute for Biomedical Materials and Devices, School of Mathematical and Physical Sciences, Faculty of Science, University of Technology, Sydney, NSW 2007, Australia

[b] ARC Research Hub for Integrated Device for End-user Analysis at Low-levels (IDEAL), Faculty of Science, University of Technology Sydney, NSW, 2007, Australia

[c] The Faculty of Pharmacy, The University of Sydney, NSW 2006, Australia

*E-mail coressponding authors: Dayong.Jin@uts.edu.au (D. Jin), Maryam.Parviz@uts.edu.au (M. Parviz)

The original synthesized upconversion nanoparticles (UCNPs) were capped by oleic acid (OA). In order to render the UCNPs a hydrophilic surface, phosphate-polyethylene glycol (PEG) with a carboxyl group were applied to substitute the OA. The formed UCNPs@PEG are water soluble and stable. The polymer structure and simple surface modification process is illustrated in Figure S1.

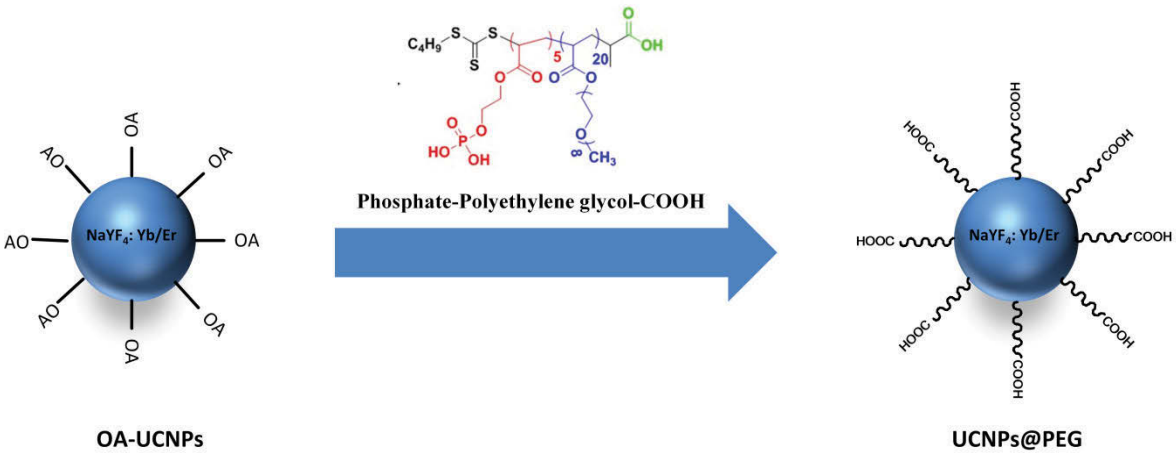

Figure S1: Polymer structure and surface modification illustration of OA-UCNPs to UCNPs@PEG

To functionalize the UCNPs@PEG, hairpin shaped ssDNA were coated on nanoparticle surface to form UCNPs@PEG@DNA by classical EDC-catalyzed method. After

modification of the DNA, a typical absorbance peak appeared at around 260 nm(Yeates et al. 1998), which is a common DNA absorbance band. The result confirms the DNA has successfully attached on UCNPs@PEG.

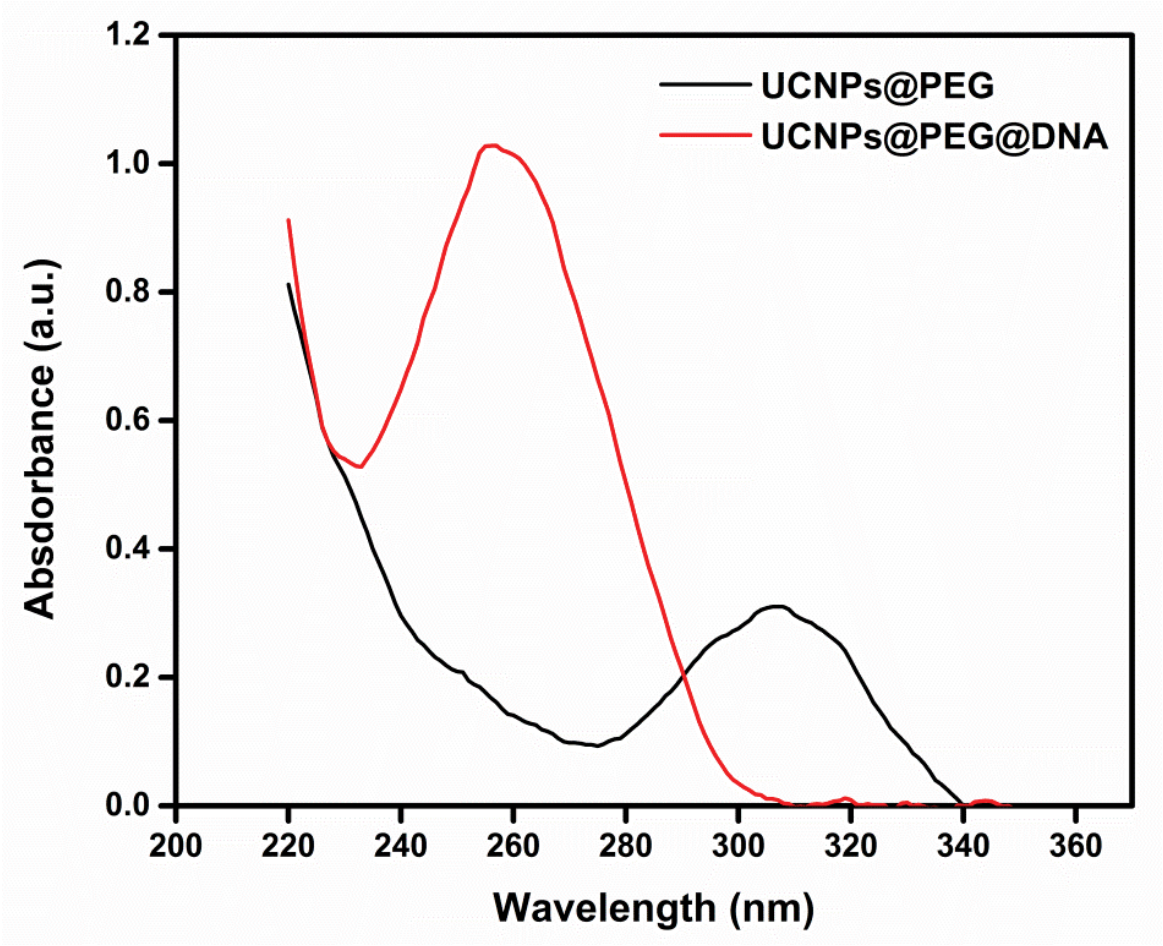

Figure S2: Nanodrop results of UCNPs@PEG (black line) and UCNPs@PEG@DNA (red line) that confirm the DNA has successfully attached on UCNPs.

The normalized intensity of increasing volume ratio of UCNPs@PEG@DNA to AuNPs were measures. The higher volume ratio, in the other words, the higher mass of AuNPs additions achieved higher quenching efficiency.

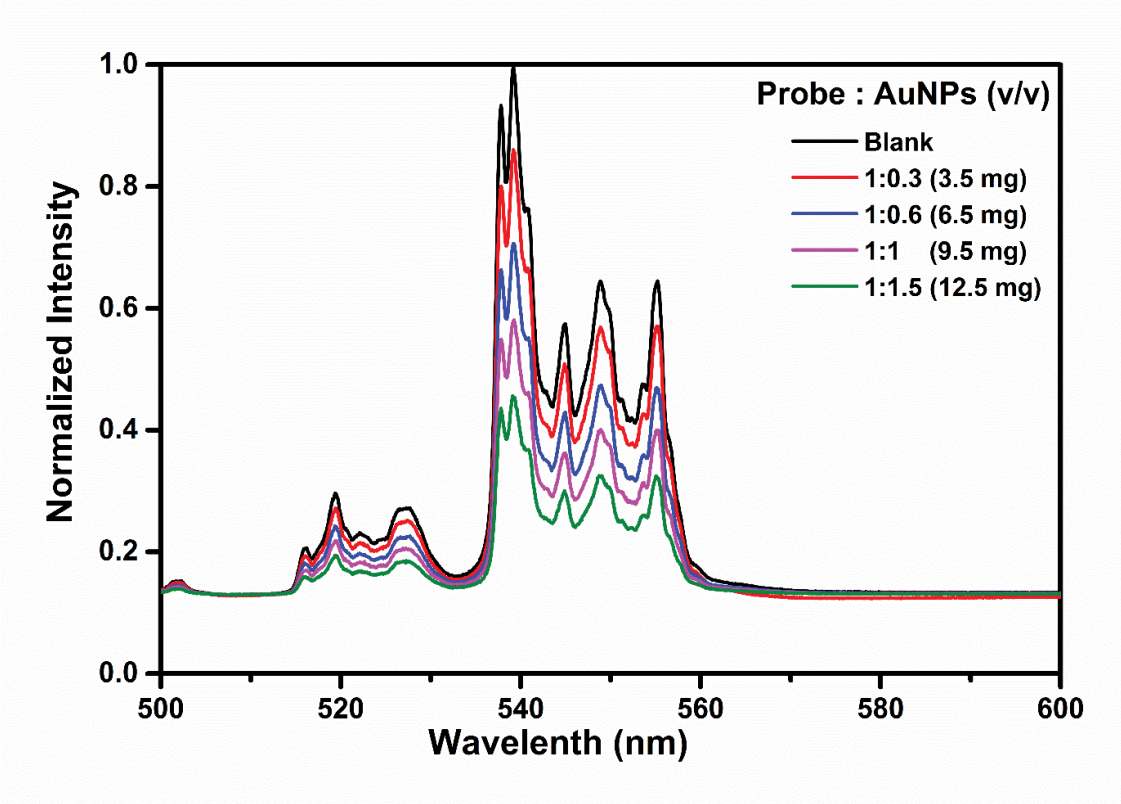

Figure S3: The normalized intensity of probe (UCNPs@PEG@DNA) exposed to different volume ratio (increasing mass of AuNPs).

The commercial AuNPs with diameters of 5 nm, 10 nm, and 20 nm were selected quenchers in detection experiment. The TEM images show the different AuNPs candidates in stock solution (OD=1).

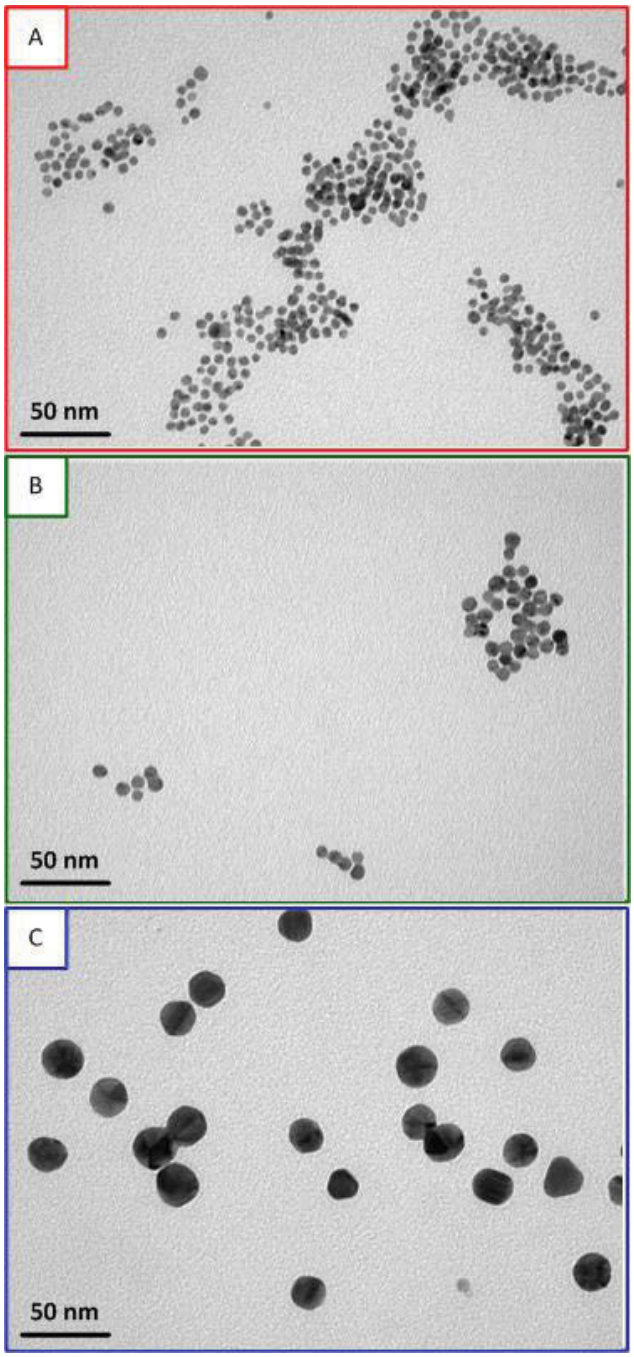

Figure S4. TEM images of 5, 10 and 20 nm AuNPs stabilized in citrate buffer (OD=1).

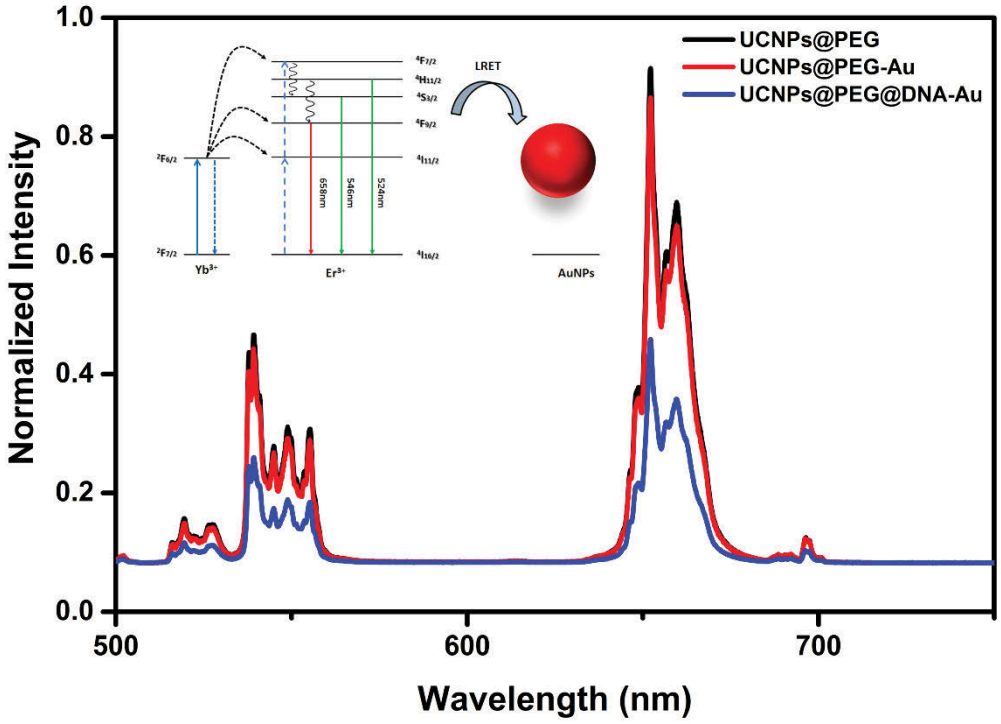

Figure S5: Full emission range of normalized luminescence intensity of UCNPs@PEG as the control group versus intensity of UCNPs@PEG and UCNPs@PEG@DNA after reaction with 5 nm AuNPs. The inner graph illustrates the energy transfer process that causes the luminescence quenching effect. The intensity values were divided by the highest amount of intensity of bare UCNPs at 539 nm to obtain the normalized values.

The HIV based hairpin ssDNA and complementary target sequences are listed in Table S1. The designed mismatched sequences with 1 base mismatch, 3 bases mismatch and random sequences are listed in Table S2.

Table S1: Designed hairpin and target sequences.

Hairpin Sequence	5AmMC6/GCG AGC CTG GGA TTA AAT AAA ATA GTA AGA ATG TAT AGC GCT CGC/3ThioMC3-D/
Target sequence	5'-GCT ATA CAT TCT TAC TAT TTT ATT TAA TCC CAG -3'

Table S2. Designed mismatched sequences

1-mismatch	GCT ATA CAT TCT TAC TTT TTT ATT TAA TCC CAG
1-mismatch	GCT ATA CAT TCT TAC TAA TTTATTTAATCCCAG
3-mismatch	GCT ATA CAT TCT TAC ATA TTT ATT TAA TCC CAG
3-mismatch	GCT ATA CAT TCT TAC CGA TTT ATT TAA TCC CAG
Random	TGT GTG TGT GTG TGT GTG TGT TGT GTG TGT GTG

The red underline represents the mismatched bases.

Chapter V. Conclusion and Outlook

5.1 Concluding Remarks

In this thesis, I introduced a DNA homogenous detection platform, based on a systematic study of polymer surface modifications via one-step ligand exchange. The core material employed in this thesis, UCNPs, have been such a favourite selection in numerous applications, owing to its excellent properties including biocompatible, low cytotoxicity to live cells, resistant to photobleaching and photoblinking, minimal autofluorescence, and their profound penetration ability in tissues. Here, UNCPs regarding of architecture, synthesis method, characteristics, and surface modification methods are reviewed, followed by two significant parts of research outputs, which are highlighted as below:

1) Four polymers, including three most commercially available polymers, were applied to generate a hydrophilic surface of UCNPs via one-step ligand exchange. According to a series investigation, POEGA-b-PMAEP polymer coated UCNPs are proved to show the best water solubility, dispensability, colloidal stability, and they adapted in varies buffers with different pH and temperature. Furthermore, HEPES buffer is the one that can stabilize different polymers coated UCNPs in solution and also maintain relatively good mono-dispensability over an extended period.
2) UCNPs and AuNPs were joined together by the molecular beacon and acted as the LRET energy donor-acceptor pairs. This developed LRET platform was used to and quickly achieve single target DNA molecule detection. Luminescence quenching could tell the target absence while luminescence recovery indicated the presence of target. This system produced high selectivity and satisfactory sensitive results (5nM) without the enzyme assistance and amplification process.

5.2 Future Works

In this thesis, significant efforts have put in investigating a simple hydrophilic surface modification of UCNPs and developing a user-friendly DNA assay. However, the existing works remains potential for further improvement.

1) To meet the strict clinical acceptance, or being more competitive compared with other developed HIV-DNA based detection platform (some of them already achieve the detection limit up to 15 Pm(Y. Chen et al. 2018)), limit of detection should be pushed lower and matched higher sensitivity. Therefore, multiple ways can be considered. (a) A relatively smaller size of UCNP can be selected to achieve larger surface-to-volume ratio, and tuning the UCNPs-AuNPs molar ratio for higher efficient quenching. (b) The more advanced surface modification can be even improved, either by using shorter polymers or small organic compounds to produce an evenly hydrophilic surface of UCNPs. In this way, making a better water dispensability of UCNPs possible, and bringing a closer distance between two nanoparticles for the sake of more efficient LRET quenching. These approaches expect the platform to reach the lowest luminescence intensity before the target addition, which makes the signal difference as large as possible.
2) The works demonstrated in this thesis only present a single-stranded DNA sequence detection. However, in practical applications, more types of biomarkers are used in disease detections. Therefore, the designed platform can be extended to broader molecular recognition, such as proteins, enzymes, and even metal ions detections.
3) The DNA assay reported in this thesis is an in vitro test. To move into in vivo applications, more cellular relative works should be done. For example, a facile surface modification of UCNPs which enhances the cellular uptake efficiency should be explored first. Then the detection platform can be designed to achieve the specific target recognition in vivo.

REFERENCES

Abolhasani, Jafar, Javad Hassanzadeh, Ebrahim Ghorbani-kalhor, and Zohreh Saeedi. 2015. "Fluorescence Quenching of CdS Quantum Dots and Its Application to Determination of Copper and Nickel Contamination in Well and Dam Water." *Journal of Chemical Health Risks* 5: 145–54.

Alonso-Cristobal, P., P. Vilela, A. El-Sagheer, E. Lopez-Cabarcos, T. Brown, O. L. Muskens, J. Rubio-Retama, and A. G. Kanaras. 2015a. "Highly Sensitive DNA Sensor Based on Upconversion Nanoparticles and Graphene Oxide." *ACS Applied Materials and Interfaces*. doi:10.1021/am507591u.

———. 2015b. "Highly Sensitive DNA Sensor Based on Upconversion Nanoparticles and Graphene Oxide." *ACS Applied Materials and Interfaces* 7 (23): 12422–29. doi:10.1021/am507591u.

Auzel, François. 2004. "Upconversion and Anti-Stokes Processes with f and d Ions in Solids." *Chemical Reviews*. doi:10.1021/cr020357g.

Ayala, Vanessa, Adriana P. Herrera, Magda Latorre-Esteves, Madeline Torres-Lugo, and Carlos Rinaldi. 2013. "Effect of Surface Charge on the Colloidal Stability and in Vitro Uptake of Carboxymethyl Dextran-Coated Iron Oxide Nanoparticles." *Journal of Nanoparticle Research* 15 (8): 1–24. doi:10.1007/s11051-013-1874-0.

Bagheri, Ali, Hamidreza Arandiyan, Cyrille Boyer, and May Lim. 2016. "Lanthanide-Doped Upconversion Nanoparticles: Emerging Intelligent Light-Activated Drug Delivery Systems." *Advanced Science*. doi:10.1002/advs.201500437.

Baicu, Simona C., and Michael J. Taylor. 2002. "Acid-Base Buffering in Organ Preservation Solutions as a Function of Temperature: New Parameters for Comparing Buffer Capacity and Efficiency." *Cryobiology* 45 (1): 33–48. doi:10.1016/S0011-2240(02)00104-9.

Baker, Sheila N., and Gary A. Baker. 2010. "Luminescent Carbon Nanodots: Emergent Nanolights." *Angewandte Chemie - International Edition* 49 (38): 6726–44. doi:10.1002/anie.200906623.

Baride, A., J. M. Meruga, C. Douma, D. Langerman, G. Crawford, J. J. Kellar, W. M. Cross, and P. S. May. 2015. "A NIR-to-NIR Upconversion Luminescence System for Security Printing Applications." *RSC Advances* 5 (123). Royal Society of Chemistry: 101338–46. doi:10.1039/c5ra20785a.

Bogdan, Nicoleta, Fiorenzo Vetrone, Geoffrey A. Ozin, and John A. Capobianco. 2011. "Synthesis of Ligand-Free Colloidally Stable Water Dispersible Brightly Luminescent Lanthanide-Doped Upconverting Nanoparticles." *Nano Letters* 11 (2): 835–40. doi:10.1021/nl1041929.

Boyer, John-Christopher, Louis A Cuccia, and John A Capobianco. 2007. "Synthesis of Colloidal Upconverting NaYF4: Er3+/Yb3+ and Tm3+/Yb3+ Monodisperse Nanocrystals." *Nano*

Lett. 7 (3): 847–52. doi:10.1021/nl070235+.

Chen, Guanying, Hailong Qiu, Paras N. Prasad, and Xiaoyuan Chen. 2014. "Upconversion Nanoparticles: Design, Nanochemistry, and Applications in Theranostics." *Chemical Reviews* 114 (10): 5161–5214. doi:10.1021/cr400425h.

Chen, Hongqi, Fei Yuan, Shaozhen Wang, Juan Xu, Yi Yan Zhang, and Lun Wang. 2013. "Aptamer-Based Sensing for Thrombin in Red Region via Fluorescence Resonant Energy Transfer between NaYF4: Yb,Er Upconversion Nanoparticles and Gold Nanorods." *Biosensors and Bioelectronics* 48. Elsevier: 19–25. doi:10.1016/j.bios.2013.03.083.

Chen, Jiao, and Julia Xiaojun Zhao. 2012. "Upconversion Nanomaterials: Synthesis, Mechanism, and Applications in Sensing." *Sensors* 12 (3): 2414–35. doi:10.3390/s120302414.

Chen, Y., H.T.T. Duong, S. Wen, C. Mi, Y. Zhou, O. Shimoni, S.M. Valenzuela, and D. Jin. 2018. "Exonuclease III-Assisted Upconversion Resonance Energy Transfer in a Wash-Free Suspension DNA Assay." *Analytical Chemistry* 90 (1). doi:10.1021/acs.analchem.7b04240.

Chen, Yinghui, Hien T.T. Duong, Shihui Wen, Chao Mi, Yingzhu Zhou, Olga Shimoni, Stella M. Valenzuela, and Dayong Jin. 2018. "Exonuclease III-Assisted Upconversion Resonance Energy Transfer in a Wash-Free Suspension DNA Assay." *Analytical Chemistry* 90 (1): 663–68. doi:10.1021/acs.analchem.7b04240.

Chen, Zhigang, Huili Chen, He Hu, Mengxiao Yu, Fuyou Li, Qiang Zhang, Zhiguo Zhou, Tao Yi, and Chunhui Huang. 2008. "Versatile Synthesis Strategy for Carboxylic Acid-Functionalized Upconverting Nanophosphors as Biological Labels." *Journal of the American Chemical Society* 130 (10): 3023–29. doi:10.1021/ja076151k.

Clapp, Aaron R., Igor L. Medintz, and Hedi Mattoussi. 2006. "F??Rster Resonance Energy Transfer Investigations Using Quantum-Dot Fluorophores." *ChemPhysChem* 7 (1): 47–57. doi:10.1002/cphc.200500217.

Clapp, Aaron R., Igor L. Medintz, J. Matthew Mauro, Brent R. Fisher, Moungi G. Bawendi, and Hedi Mattoussi. 2004. "Fluorescence Resonance Energy Transfer Between Quantum Dot Donors and Dye-Labeled Protein Acceptors." *Journal of the American Chemical Society* 126 (1): 301–10. doi:10.1021/ja037088b.

Dąbrowski, Janusz M., and Luis G. Arnaut. 2015. "Photodynamic Therapy (PDT) of Cancer: From Local to Systemic Treatment." *Photochem. Photobiol. Sci.* 14 (10): 1765–80. doi:10.1039/C5PP00132C.

Dong, Hao, Ling-Dong Sun, and Chun-Hua Yan. 2015. "Energy Transfer in Lanthanide Upconversion Studies for Extended Optical Applications." *Chem. Soc. Rev.* 44 (6). Royal Society of Chemistry: 1608–34. doi:10.1039/C4CS00188E.

Dong, Hao, Ling Dong Sun, and Chun Hua Yan. 2013. "Basic Understanding of the Lanthanide Related Upconversion Emissions." *Nanoscale* 5 (13): 5703–14. doi:10.1039/c3nr34069d.

Duong, Hien T. T., Yinghui Chen, Sherif Abdulkader Tawfik, Shihui Wen, Maryam Parviz, Olga

Shimoni, and Dayong Jin. 2018. “Systematic Investigation of Functional Ligands for Colloidal Stable Upconversion Nanoparticles.” *RSC Advances* 8 (9): 4842–49. doi:10.1039/C7RA13765F.

Ehlert, Oliver, Ralf Thomann, Masih Darbandi, and Thomas Nann. 2007. “A Four-Color Colloidal Multiplexing” 2 (1): 3–7.

Ferguson, Wilfred J., K. I. Braunschweiger, W. R. Braunschweiger, James R. Smith, J. Justin McCormick, Cathy C. Wasmann, Nancy P. Jarvis, Duncan H. Bell, and Norman E. Good. 1980. “Hydrogen Ion Buffers for Biological Research.” *Analytical Biochemistry* 104 (2): 300–310. doi:10.1016/0003-2697(80)90079-2.

Forster, Th. 1946. “Energiewanderung Und Fluoreszenz.” *Die Naturwissenschaften* 33 (6): 166–75. doi:10.1007/BF00585226.

Git, Anna, Heidi Dvinge, Anna Git, Heidi Dvinge, Michelle Osborne, and Claudia Kutter. 2010. “Next-Generation Sequencing Technologies for Measuring Differential MicroRNA Expression Systematic Comparison of Microarray Profiling , Real-Time PCR , and next-Generation Sequencing Technologies for Measuring Differential MicroRNA Expression,” 991–1006. doi:10.1261/rna.1947110.

Held, Paul. 2012. “An Introduction to Fluorescence Resonance Energy Transfer (FRET) Technology and Its Application in Bioscience.” *Biotek Instruments White Paper*, 1–6.

Hines, Margaret A., and Philippe Guyot-Sionnest. 1996. “Synthesis and Characterization of Strongly Luminescing ZnS-Capped CdSe Nanocrystals.” *The Journal of Physical Chemistry* 100 (2): 468–71. doi:10.1021/jp9530562.

Honary, Soheyla, and Foruhe Zahir. 2013. “Effect of Zeta Potential on the Properties of Nano - Drug Delivery Systems - A Review (Part 2).” *Tropical Journal of Pharmaceutic Al Research* 12 (2): 265–73. doi:10.4314/tjpr.v12i2.19.

Hu, He, Mengxiao Yu, Fuyou Li, Zhigang Chen, Xia Gao, Liqin Xiong, and Chunhui Huang. 2008. “Facile Epoxidation Strategy for Producing Amphiphilic Up-Converting Rare-Earth Nanophosphors as Biological Labels.” *Chemistry of Materials* 20 (22): 7003–9. doi:10.1021/cm801215t.

Huang, Li-Jiao, Ru-Qin Yu, and Xia Chu. 2015. “DNA-Functionalized Upconversion Nanoparticles as Biosensors for Rapid, Sensitive, and Selective Detection of Hg2+ in Complex Matrices.” *Analyst* 140 (15). Royal Society of Chemistry: 4987–90. doi:10.1039/C5AN00635J.

Huang, Xiaohua, and Mostafa A. El-Sayed. 2010. “Gold Nanoparticles: Optical Properties and Implementations in Cancer Diagnosis and Photothermal Therapy.” *Journal of Advanced Research* 1 (1): 13–28. doi:10.1016/j.jare.2010.02.002.

Jain, Prashant K., Kyeong Seok Lee, Ivan H. El-Sayed, and Mostafa A. El-Sayed. 2006. “Calculated Absorption and Scattering Properties of Gold Nanoparticles of Different Size,

Shape, and Composition: Applications in Biological Imaging and Biomedicine." *Journal of Physical Chemistry B* 110 (14): 7238–48. doi:10.1021/jp057170o.

König, K., A. Ehlers, F. Stracke, and I. Riemann. 2006. "In Vivo Drug Screening in Human Skin Using Femtosecond Laser Multiphoton Tomography." *Skin Pharmacology and Physiology* 19 (2): 78–88. doi:10.1159/000091974.

Kuningas, Katri, Terhi Rantanen, Telle Ukonaho, Timo Lövgren, and Tero Soukka. 2005. "Homogeneous Assay Technology Based on Upconverting Phosphors." *Analytical Chemistry* 77 (22): 7348–55. doi:10.1021/ac0510944.

Li, Zhenhua, Hang Yuan, Wei Yuan, Qianqian Su, and Fuyou Li. 2017. "Upconversion Nanoprobes for Biodetections." *Coordination Chemistry Reviews* 354. Elsevier B.V.: 155–68. doi:10.1016/j.ccr.2017.06.025.

Liu, Jie, Wen Hu, Huabing Chen, Qian Ni, Huibi Xu, and Xiangliang Yang. 2007. "Isotretinoin-Loaded Solid Lipid Nanoparticles with Skin Targeting for Topical Delivery." *International Journal of Pharmaceutics* 328 (2): 191–95. doi:10.1016/j.ijpharm.2006.08.007.

Lu, Huachang, Guangshun Yi, Shuying Zhao, Depu Chen, Liang Hong Guo, and Jing Cheng. 2004. "Synthesis and Characterization of Multi-Functional Nanoparticles Possessing Magnetic, up-Conversion Fluorescence and Bio-Affinity Properties." *Journal of Materials Chemistry* 14 (8): 1336–41. doi:10.1039/b315103d.

Mai, Hao Xin, Ya Wen Zhang, Rui Si, Zheng Guang Yan, Ling Dong Sun, Li Ping You, and Chun Hua Yan. 2006. "High-Quality Sodium Rare-Earth Fluoride Nanocrystals: Controlled Synthesis and Optical Properties." *Journal of the American Chemical Society* 128 (19): 6426–36. doi:10.1021/ja060212h.

Mejia-Ariza, Raquel, Laura Graña-Suárez, Willem Verboom, and Jurriaan Huskens. 2017. "Cyclodextrin-Based Supramolecular Nanoparticles for Biomedical Applications." *J. Mater. Chem. B* 5 (1): 36–52. doi:10.1039/C6TB02776H.

Meyer, Tobias, and Mary N. Teruel. 2003. "Fluorescence Imaging of Signaling Networks." *Trends in Cell Biology* 13 (2): 101–6. doi:10.1016/S0962-8924(02)00040-5.

Murray, C. B., D. J. Norris, and M. G. Bawendi. 1993. "Synthesis and Characterization of Nearly Monodisperse CdE (E = S, Se, Te) Semiconductor Nanocrystallites." *Journal of the American Chemical Society* 115 (19): 8706–15. doi:10.1021/ja00072a025.

Ni, Jingkai, Chongxin Shan, Bin Li, Liming Zhang, Heping Ma, Yongshi Luo, and Hang Song. 2015. "Assembling of a Functional Cyclodextrin-Decorated Upconversion Luminescence Nanoplatform For." *Chemical Communications* 51. Royal Society of Chemistry: 14054–56. doi:10.1039/C5CC04750A.

Phan, Tri Giang, and Andrew Bullen. 2010. "Practical Intravital Two-Photon Microscopy for Immunological Research: Faster, Brighter, Deeper." *Immunology and Cell Biology* 88 (4): 438–44. doi:10.1038/icb.2009.116.

Pollok, Brian A., and Roger Heim. 1999. “Using GFP in FRET-Based Applications.” *Trends in Cell Biology* 9 (2): 57–60. doi:10.1016/S0962-8924(98)01434-2.

Qiao, Yali, and Xingwang Zheng. 2016. “Investigation of the Fluorescence Quenching Behavior of PEI-Doped Silica Nanoparticles and Its Applications.” *RSC Advances* 6 (99). Royal Society of Chemistry: 97187–93. doi:10.1039/c6ra21543b.

Resch-Genger, Ute, Markus Grabolle, Sara Cavaliere-Jaricot, Roland Nitschke, and Thomas Nann. 2008. “Quantum Dots versus Organic Dyes as Fluorescent Labels.” *Nature Methods* 5 (9): 763–75. doi:10.1038/nmeth.1248.

Rigotti, A., S. L. Acton, and M. Krieger. 1995. “The Class B Scavenger Receptors SR-BI and CD36 Are Receptors for Anionic Phospholipids.” *Journal of Biological Chemistry*. doi:10.1074/jbc.270.27.16221.

Seidel, Claus A. M., Andreas Schulz, and Markus H. M. Sauer. 1996. “Nucleobase-Specific Quenching of Fluorescent Dyes. 1. Nucleobase One-Electron Redox Potentials and Their Correlation with Static and Dynamic Quenching Efficiencies.” *The Journal of Physical Chemistry* 100 (13): 5541–53. doi:10.1021/jp951507c.

Sekar, Rajesh Babu, and Ammasi Periasamy. 2003. “Fluorescence Resonance Energy Transfer (FRET) Microscopy Imaging of Live Cell Protein Localizations.” *Journal of Cell Biology* 160 (5): 629–33. doi:10.1083/jcb.200210140.

Selvin, Paul R., Tariq M. Rana, and John E. Hearst. 1994. “Luminescence Resonance Energy Transfer.” *Journal of the American Chemical Society* 116 (13): 6029–30. doi:10.1021/ja00092a088.

Shamsipur, Mojtaba, Vahid Nasirian, Kamran Mansouri, Ali Barati, Asad Veisi-Raygani, and Soheila Kashanian. 2017. “A Highly Sensitive Quantum Dots-DNA Nanobiosensor Based on Fluorescence Resonance Energy Transfer for Rapid Detection of Nanomolar Amounts of Human Papillomavirus 18.” *Journal of Pharmaceutical and Biomedical Analysis* 136. Elsevier B.V.: 140–47. doi:10.1016/j.jpba.2017.01.002.

Shen, Jie, Liang Zhao, and Gang Han. 2013. “Lanthanide-Doped Upconverting Luminescent Nanoparticle Platforms for Optical Imaging-Guided Drug Delivery and Therapy.” *Advanced Drug Delivery Reviews* 65 (5). Elsevier B.V.: 744–55. doi:10.1016/j.addr.2012.05.007.

Song, Kai, Xianggui Kong, Xiaomin Liu, Youlin Zhang, Qinghui Zeng, Langping Tu, Zhan Shi, and Hong Zhang. 2012. “Aptamer Optical Biosensor without Bio-Breakage Using Upconversion Nanoparticles as Donors.” *Chem. Commun.* 48 (8): 1156–58. doi:10.1039/C2CC16817K.

Song, Zhen, Yuri G. Anissimov, Jiangbo Zhao, Andrei V. Nechaev, Annemarie Nadort, Dayong Jin, Tarl W. Prow, Michael S. Roberts, and Andrei V. Zvyagin. 2012. “Background Free Imaging of Upconversion Nanoparticle Distribution in Human Skin.” *Journal of Biomedical Optics* 18 (6): 061215. doi:10.1117/1.JBO.18.6.061215.

Sun, Yulong, Wenjing Zhang, Baoming Wang, Xiaoxue Xu, Joshua Chou, Olga Shimoni, Alison T. Ung, and Dayong Jin. 2018. "A Supramolecular Self-Assembly Strategy for Upconversion Nanoparticle Bioconjugation." *Chemical Communications* 54 (31). Royal Society of Chemistry: 3851–54. doi:10.1039/c8cc00708j.

Tong, Lemuel, Elsa Lu, Jothirmayanantham Pichaandi, Pengpeng Cao, Mark Nitz, and Mitchell A. Winnik. 2015. "Quantification of Surface Ligands on $NaYF_4$ Nanoparticles by Three Independent Analytical Techniques." *Chemistry of Materials* 27 (13): 4899–4910. doi:10.1021/acs.chemmater.5b02190.

Tyagi, Sanjay, and Fred Russell Kramer. 1996. "Molecular Beacons: Probes That Fluoresce upon Hybridization." *Nature Biotechnology* 14 (3): 303–8. doi:10.1038/nbt0396-303.

———. 2012. "Molecular Beacons in Diagnostics." *F1000 Medicine Reports* 4 (October). doi:10.3410/M4-10.

Walling, Maureen A., Jennifer A. Novak, and Jason R E Shepard. 2009. "Quantum Dots for Live Cell and in Vivo Imaging." *International Journal of Molecular Sciences* 10 (2): 441–91. doi:10.3390/ijms10020441.

Wang, Chengli, Xiaomin Li, and Fan Zhang. 2016. "Bioapplications and Biotechnologies of Upconversion Nanoparticle-Based Nanosensors." *The Analyst* 141 (12). Royal Society of Chemistry: 3601–20. doi:10.1039/C6AN00150E.

Wang, Feng, Debapriya Banerjee, Yongsheng Liu, Xueyuan Chen, and Xiaogang Liu. 2010. "Upconversion Nanoparticles in Biological Labeling, Imaging, and Therapy." *The Analyst* 135 (8): 1839. doi:10.1039/c0an00144a.

Wang, Leyu, and Yadong Li. 2007. "Controlled Synthesis and Luminescence of Lanthanide Doped NaYF4 Nanocrystals." *Chemistry of Materials* 19 (4): 727–34. doi:10.1021/cm061887m.

Wang, Leyu, Ruoxue Yan, Ziyang Huo, Lun Wang, Jinghui Zeng, Jie Bao, Xun Wang, Qing Peng, and Yadong Li. 2005. "Fluorescence Resonant Energy Transfer Biosensor Based on Upconversion-Luminescent Nanoparticles." *Angewandte Chemie - International Edition* 44 (37): 6054–57. doi:10.1002/anie.200501907.

Wang, Meng, Cong Cong Mi, Jin Ling Liu, Xian Long Wu, Yi Xin Zhang, Wei Hou, Feng Li, and Shu Kun Xu. 2009. "One-Step Synthesis and Characterization of Water-Soluble NaYF4:Yb,Er/Polymer Nanoparticles with Efficient up-Conversion Fluorescence." *Journal of Alloys and Compounds* 485 (1–2): 24–27. doi:10.1016/j.jallcom.2009.05.138.

Wang, Y, P Shen, C Li, Y Wang, and Z Liu. 2012. "Upconversion Fluorescence Resonance Energy Transfer Based Biosensor for Ultrasensitive Detection of Matrix Metalloproteinase-2 in Blood." *Anal Chem* 84 (3): 1466–73. doi:10.1021/ac202627b.

Xie, Jin, Seulki Lee, and Xiaoyuan Chen. 2010. "Nanoparticle-Based Theranostic Agents." *Advanced Drug Delivery Reviews* 62 (11). Elsevier B.V.: 1064–79.

doi:10.1016/j.addr.2010.07.009.

Yang, Fan, Tingting Zhang, Shan-Shan Li, Pei Song, Kai Zhang, Qi-Yuan Guan, Bin Kang, Jing-Juan Xu, and Hong-Yuan Chen. 2017. "Endogenous MicroRNA-Triggered and Real-Time Monitored Drug Release via Cascaded Energy Transfer Payloads." *Analytical Chemistry*. doi:10.1021/acs.analchem.7b01582.

Yeates, C., M. R. Gillings, A. D. Davison, N. Altavilla, and D. A. Veal. 1998. "Methods for Microbial DNA Extraction from Soil for PCR Amplification." *Biological Procedures Online* 1 (1): 40–47. doi:10.1251/bpo6.

Yi, Guang-Shun, and Gan-Moog Chow. 2005. "Colloidal LaF3:Yb,Er, LaF3:Yb,Ho and LaF3:Yb,Tm Nanocrystals with Multicolor Upconversion Fluorescence." *Journal of Materials Chemistry* 15 (41): 4460. doi:10.1039/b508240d.

Zadran, Sohila, Steve Standley, Kaylee Wong, Erick Otiniano, Arash Amighi, and Michel Baudry. 2012. "Fluorescence Resonance Energy Transfer (FRET)-Based Biosensors: Visualizing Cellular Dynamics and Bioenergetics." *Applied Microbiology and Biotechnology* 96 (4): 895–902. doi:10.1007/s00253-012-4449-6.

Zako, Tamotsu, Hiroshi Hyodo, Kosuke Tsuji, Kimikazu Tokuzen, Hidehiro Kishimoto, Masaaki Ito, Kazuhiro Kaneko, Mizuo Maeda, and Kohei Soga. 2010. "Development of near Infrared-Fluorescent Nanophosphors and Applications for Cancer Diagnosis and Therapy." *Journal of Nanomaterials* 2010 (April). doi:10.1155/2010/491471.

Zhang, Chao, Lingdong Sun, Yawen Zhang, and Chunhua Yan. 2010. "Rare Earth Upconversion Nanophosphors: Synthesis, Functionalization and Application as Biolabels and Energy Transfer Donors." *Journal of Rare Earths* 28 (6). The Chinese Society of Rare Earths: 807–19. doi:10.1016/S1002-0721(09)60206-4.

Zhou, Bo, Bingyang Shi, Dayong Jin, and Xiaogang Liu. 2015. "Controlling Upconversion Nanocrystals for Emerging Applications." *Nature Nanotechnology* 10 (11): 924–36. doi:10.1038/nnano.2015.251.

Zhou, Feng, M. Omair Noor, and Ulrich J. Krull. 2014. "Luminescence Resonance Energy Transfer-Based Nucleic Acid Hybridization Assay on Cellulose Paper with Upconverting Phosphor as Donors." *Analytical Chemistry* 86 (5): 2719–26. doi:10.1021/ac404129t.

Zhou, Huan Ping, Chun Hu Xu, Wei Sun, and Chun Hua Yan. 2009. "Clean and Flexible Modification Strategy for Carboxyl/ Aldehyde- Functionalized Upconversion Nanoparticles and Their Optical Applications." *Advanced Functional Materials* 19 (24): 3892–3900. doi:10.1002/adfm.200901458.

Zhou, Jing, Qian Liu, Wei Feng, Yun Sun, and Fuyou Li. 2015. "Upconversion Luminescent Materials: Advances and Applications." *Chemical Reviews* 115 (1): 395–465. doi:10.1021/cr400478f.

Zhou, Jing, Zhuang Liu, and Fuyou Li. 2012. "Upconversion Nanophosphors for Small-Animal

Imaging.” *Chem. Soc. Rev.* 41 (3): 1323–49. doi:10.1039/C1CS15187H.